TRANSIENT RESPONSE OF A SILICON pn JUNCTION SOLAR CELL

A Thesis
Submitted in partial fulfilment of the
requirements of the degree of
DOCTOR OF PHILOSOPHY

by
SURYA KUMAR SHARMA

PHYSICS GROUP
BIRLA INSTITUTE OF TECHNOLOGY AND SCIENCE
PILANI (Rajasthan) INDIA
OCTOBER, 1981

BIRLA INSTITUTE OF TECHNOLOGY AND SCIENCE
PILANI (RAJASTHAN)

C E R T I F I C A T E

This is to certify that the thesis entitled "TRANSIENT RESPONSE OF A SILICON pn JUNCTION SOLAR CELL" and submitted by Mr. Surya Kumar Sharma ID No. 78S85513 for award of Ph.D. degree of the Institute, embodies original work done by him under my supervision.

V.K. Tewary

V.K. TEWARY
PROFESSOR OF PHYSICS AND
DEAN OF RESEARCH AND CONSULTANCY DIVISION

Date: October 31, 1981.

ACKNOWLEDGEMENT

It gives me great pleasure to place on record my deep sense of gratitude towards my supervisor Dr. V.K.Tewary, Professor of Physics and Dean of Research and Consultancy Division, B.I.T.S., Pilani who not only guided and encouraged but also helped me in all possible ways during the course of this work. I am indeed grateful to him.

I am thankful to the staff of Research and Consultancy Division, Physics Group, Mathematics Group, Information Processing Centre and Library of B.I.T.S. Pilani for their kind help during the course of this work. I also thank Dean, Faculty Division III and Director of B.I.T.S. Pilani for providing necessary facilities.

My sincere thanks are due to Prof. T.N.R.K. Kurup, Dr. V.P. Mainra, Dr. C.S. Shastri, Dr.(Mrs.) Amita Agrawala, Mr. M.K. Madan and Dr. R. Mehrotra who helped me a lot in the research work. I am highly thankful to Dr. A.Subramanian for reading the manuscript. I also thank Dr. V.S. Kulhar, Dr.(Mrs.) Anita Dube, Dr. N.K. Swami, Dr. G.S. Tyagi, Dr. Murlidhar and Mr. D. Sahani who made my stay at Pilani a lively experience.

I am grateful to the Indian National Science Academy for awarding a research fellowship and Allahabad Bank of Lucknow for granting a loan in the time of need.

I am thankful to Mr. G.R. Verma for typing the manuscript accurately and efficiently, Mr. B.D. Sukheeja for tracing the diagrams and Mr. S.N. Vyas for Xeroxing the diagrams.

I am highly thankful to Dr. Chaman Mehrotra of Lucknow University for advising me to join research under Prof. V.K. Tewary. I owe my sincere and heartfelt thanks to Mr. and Mrs. K.C. Misra, Mr. and Mrs. R.N. Tewary, Mr. Rajiv Misra, Mr. Rishi Kant Tewary and Mr. Gyanendra Singh of Lucknow who took a very personal interest in my academic growth.

I affectionately thank my family members who took every trouble to bring me to this level.

Lastly, the thesis to whatever it is worth is dedicated to my grandfather Shri Indra Pal Sharma who could not live long to see his dream being fulfilled.

October, 1981.

(SURYA KUMAR SHARMA)

C O N T E N T S

			Page
CHAPTER 1 :	GENERAL INTRODUCTION	..	
	1.1 Introduction	..	1
	1.2 Solar Cell	..	6
	1.3 Importance of the Transient Studies	..	7
	1.4 pn Coupling	..	11
	1.5 Heavy Doping Effects	..	16
	1.6 Surface Boundary Condition - Effect of Surface Generation of Carriers	..	22
	1.7 Summary of the Work Presented in the Thesis	..	26
	References	..	35
CHAPTER 2 :	TRANSIENT RESPONSE OF A FINITE BASE SOLAR CELL WITH BUILT-IN-ELECTRIC FIELD	..	
	2.1 Introduction	..	40
	2.2 Normal Mode Analysis of Base	..	45
	2.2.1 Steady-State Analysis	..	48
	2.2.2 Transient State Analysis - Open Circuit Photo-voltage Decay		49
	2.3 Excess Minority Carrier Profile in the Open Circuit Configuration	..	55
	2.4 Effect of Base Thickness on PVD	..	57

2.5 Effect of Built-in-Electric Field on PVD .. 63

2.6 Spectral Dependence of PVD .. 67

2.7 Effect of Back Surface Recombination on PVD .. 70

2.8 Interpretation of Experimental Results on PVD .. 70

2.9 Conclusions .. 74

References .. 76

Tables .. 78

Captions for Figures .. 80

CHAPTER 3 : EFFECT OF pn COUPLING ON STEADY-STATE RESPONSE OF A SOLAR CELL ..

3.1 Introduction .. 109

3.2 Theory .. 111

3.2.1 Steady-State Short-Circuit Current .. 117

3.2.2 Steady-State Open Circuit Photovoltage .. 120

3.2.3 Steady-State Carrier Profile in the Base .. 121

3.2.4 Steady-State Carrier Profile in the Diffused Layer .. 124

3.3 Conclusions .. 125

References .. 127

Figure Captions .. 128

CHAPTER 4 : EFFECT OF pn COUPLING ON THE TRANSIENT RESPONSE OF A SOLAR CELL ..

4.1 Introduction .. 134

4.2 Theory .. 136

4.3 PVD by Assuming Uniform Absorption of Incident Radiation .. 143

4.4 Low Time Behaviour of PVD - Exponential Absorption of Incident Radiation .. 151

4.5 Tricomi Method - Its Applications in Inverting the Laplace Transform .. 156

4.6 Results and Discussions .. 160

4.6.1 Effect of Relative Dark Saturation Current of the Diffused Layer on PVD .. 168

4.6.2 Effect of Absorption Coefficient of Light on PVD .. 169

4.6.3 Effect of Surface Generation Coefficient on PVD .. 172

4.6.4 Effect of Surface Recombination Velocity on PVD .. 172

4.6.5 Effect of Relative Excess Minority Carrier Life Time in the Diffused Layer on PVD .. 173

4.6.6 Effect of Diffused Layer Thickness on PVD .. 173

4.7 Convergence of the Series for Open Circuit Photovoltage Decay .. 175

4.8 Conclusions .. 177

References .. 179

Table .. 182

Captions for Figures .. 183

CHAPTER 1

GENERAL INTRODUCTION

1.1 Introduction

The existence of energy crisis has become all too clear during the last two decades. A frequently mentioned solution to the problem of obtaining an alternate source of energy for the future is the use of photovoltaic conversion of the energy contained in the sun light with the help of solar cells.

Photovoltaic effects were first noticed more than a century ago. In 1839, E. Becquerel observed a photovoltage (a voltage that depends on light) when sun light was allowed to shine on one electrode in an electrolytic solution. The first scientific paper to report on photovoltage was published in 1877 and concerned selenium. In 1954, an RCA group demonstrated practical conversion of radiation into electrical energy by a silicon pn junction cell, and shortly thereafter Chapin, Fuller and Pearson (1954) reported on a 6% efficient solar cell.

Because of their relatively high efficiency and optical sensitivity over a wide range of wave lengths

modern solar cells are also useful as optical switching devices and radiation detectors. It is important to develop the testing methods for use of solar cells as the solar energy conversion devices as well as for switching applications.

It is well known that the transient photoconducting response of a semiconductor provides a powerful method for testing, particularly for measurement of carrier life time, surface recombination velocity etc. It is expected therefore that the transient response of a solar cell should also provide a method for the determination of excess carrier life time and other material parameters of a finished solar cell.

In order to develop suitable testing methods it is important to study the basic physical processes which determine the response of solar cells. Inspite of a substantial effort, these physical processes have not yet been fully analysed. One of the usual approximation is to neglect the effect of diffused layer and consider only the base of the solar cell which amounts to the approximation that solar cell is a uniform semiconductor. Whereas this approximation may be valid in several realistic situations, in certain devices the diffused layer does make an important contribution - in the steady-state as

well as transient state. Diffused layer and its coupling with the base in accordance with certain boundary conditions is referred to as pn coupling (see section 1.4). Even if the effect of pn coupling is negligible it is important to study the effect of finite thickness of the base as well as built-in-electric (drift) field caused by non-uniform doping in the base. In the calculations which have been published so far by other authors these effects have not been included in the transient response of solar cells.

The objective of the present thesis is to study the transient response of a solar cell taking into account the aforementioned effects which have not been included in the work published by other authors so far. It is hoped that the thesis fills up this important gap in the literature.

The transient response of a solar cell is determined by either of the two main characteristics - decay of open circuit photovoltage (PVD) or short-circuit current after abrupt termination of the exciting radiation. The short-circuit current depends upon the series resistance of the solar cell which introduces some uncertainties in the analysis of the experimental data. It is therefore more convenient to study the open circuit photovoltage decay which is an important characteristic of the transient

response of a solar cell. In view of this in the present thesis we confine our studies to the open circuit photovoltage decay.

In particular the thesis attempts the following:

(i) To develop a theory of open circuit photovoltage decay in a solar cell with a view to apply it for measurement of various material parameters of solar cell by analysing the experimental data on photovoltage decay.

(ii) To study the effect of built-in-electric field and thickness of the base on open circuit photovoltage decay.

(iii) To study the effect of pn coupling on the transient response of a solar cell and also steady-state response in as much as it affects the transient response.

Where the pn coupling makes substantial contribution the PVD will obviously be sensitive to the bulk and surface-material parameters of the diffused layer. Hence the work presented here would also include the effect of surface recombination velocity, surface generation of carriers as introduced by Tewary and Jain (1980) in the solar cell surface boundary condition, excess carrier life time in the diffused layer and the dark saturation current of the diffused layer. As will be discussed in this chapter in section 1.4, the dark saturation current

response of a solar cell. In view of this in the present thesis we confine our studies to the open circuit photovoltage decay.

In particular the thesis attempts the following:

(i) To develop a theory of open circuit photovoltage decay in a solar cell with a view to apply it for measurement of various material parameters of solar cell by analysing the experimental data on photovoltage decay.

(ii) To study the effect of built-in-electric field and thickness of the base on open circuit photovoltage decay.

(iii) To study the effect of pn coupling on the transient response of a solar cell and also steady-state response in as much as it affects the transient response.

Where the pn coupling makes substantial contribution the PVD will obviously be sensitive to the bulk and surface-material parameters of the diffused layer. Hence the work presented here would also include the effect of surface recombination velocity, surface generation of carriers as introduced by Tewary and Jain (1980) in the solar cell surface boundary condition, excess carrier life time in the diffused layer and the dark saturation current of the diffused layer. As will be discussed in this chapter in section 1.4, the dark saturation current

depends upon the band gap narrowing caused by heavy doping in the diffused layer which is thus indirectly included in the present analysis.

(iv) To study the spectral dependence of PVD because the relative contribution of various material parameters modify the spectral dependence of PVD.

First in this chapter we shall give a brief review of a solar cell and the basic concepts needed for the development of the theory in the text of the thesis. In section 1.2 a brief introduction to solar cell and its working is given. The importance of transient studies in pn junction devices (solar cells and diodes) is discussed in section 1.3. In section 1.4 the importance of the diffused layer and its coupling with the base viz. pn coupling in the solar cell response is discussed. Heavy doping effect in the modern solar cells are discussed in section 1.5. Tewary and Jain (1980) boundary condition for solar cells which accounts for the recombination as well as generation of carriers at the front (illuminated) surface is discussed in section 1.6. In section 1.7 a chapterwise summary of the work presented in this thesis is given.

1.2 Solar Cell

The modern solar cell is an electronic device, fabricated from semiconductors that converts a fraction of the energy contained in the incident sunlight directly into electrical energy.

The conversion of light into electricity in a solar cell is caused by the photovoltaic effect at a boundary layer. When photons with an energy greater than the band gap are incident on a solar cell, the absorption of the photons creates free electron-hole pairs. These excess minority carriers may diffuse to the space charge region, cross the junction and give rise to photocurrent, photovoltage, and power into a load.

The number of electron-hole pairs generated per unit time in an unit volume of the cell is proportional to the optical energy absorbed in that time in the unit volume of the cell. If the cell is exposed to the incident optical radiation for sufficiently long time(of the order of the excess minority carrier life time) a steady-state is reached: a state of a dynamical system is called steady if all the variables describing its behaviour do not vary with time or are a periodic function of time (within a defined time interval)(Gardner and Barnes 1942). Now, if the incident radiation is switched off abruptly, the created

electrons and holes start recombining and after some time once again a steady-state will be reached. The rapid transition of the cell from one steady-state to the other is accompanied by a transient process: the state of a dynamical system which cannot be described by time-independent values of its parameters is called a transient state. The finite life time of the excess carriers enables this state to last for a time which is roughtly equal to their life time.

1.3 Importance of the Transient Studies

The existence of a transient state between two steady-states is of immense importance in the measurement of the solar cell parameters and in this respect transient measurements supplement the steady-state measurements. A very important parameter which plays the key role in deciding the quality of the cell is the excess minority carrier life time. It is defined as the time required for the concentration of the excess charges to decay by recombination to 1/e of its initial value. Since the semiconductor crystal undergoes several temperature treatments during the preparation of the cell, life time of the excess minority carriers in the finished device is quite different as compared to its value in the as grown crystal.

The transient response of the solar cell can be

explored to measure this important parameter. There are various methods of doing this. The best and most widely used method, however, is the open circuit photovoltage decay method. The advantages of this method over the other methods for transient measurements can be summarised as follows:

(i) Since no current flows in the external circuit in the open circuit case, it is purely a junction property.

(ii) The effect of shunt resistance is significant at low voltages only (Bassett 1969).

(iii) Since no current flows through the device, the uncertainties associated with the series resistance are avoided.

(iv) When studied at high injection levels, this method yields the value of the diffusion potential (Gossik 1955 and Tkhorik 1966).

(v) Since the total current through the device is zero, the problem of its heating is almost eliminated.

The PVD in a solar cell involves following two steps:

(i) Creation of excess carriers by incident photons which cause a photovoltage to appear across the junction. Since the solar cell in illuminated mode is in open circuit configuration, this voltage is also equal to the open circuit photovoltage.

(ii) Subsequent observation of the photovoltage decay pattern on a CRO following an abrupt termination of light.

The slope of the best straight line in the PVD pattern then gives the life time of the excess minority carriers (Mohan et. al. 1979 and Jain 1981).

The conventional theories for the transient processes in solar cells neglect the contribution of the diffused layer. However, recently it has been shown that the heavy doping in the diffused layer of modern solar cells causes band gap narrowing in this part of the cell (Lindholm and Sah 1977, Sah and Lindholm 1977, Hauser and Dunbar 1977, Slatboom and Degraff 1976, Lindholm et.al. 1977, Fossum et. al. 1979, Shibib et. al. 1979a and Shihib et. al. 1979b) because of which the contribution of the diffused layer to cell response can no more be neglected. Detailed discussions on the contribution of the diffused layer (pn coupling) and the effects of heavy doping will be presented in next two sections.

Transient response of the solar cell can also be explored for the measurements of the heavy doping effects as is done by Lindholm and Sah (1977). These authors have attempted to measure the band gap narrowing through transient measurements.

The importance of the transient response in diodes was realized much earlier than in solar cells. Many authors including Ledderhander et. al. (1955), Gosaik (1955), Lindholm and Sah (1976) and Tewary and Jain (1981) have used FCVD method for the determination of excess minority carrier life time in a diode. Madan and Tewary (1981) have employed this method for the measurement of series resistance of a diode. The decay of open circuit voltage following an abrupt termination of forward current is called FCVD.

Further studies in diodes by Kingston (1954), Kennedy (1962), Muto and Wang (1962) and Moll et. al. (1962) showed that when a diode was switched from the forward to the reverse direction, an 'anomalously' large reverse current flowed for some time. This phenomenon is known as reverse recovery. Reverse recovery in the case of solar cells has been attempted by Dhariwal (1980). In view of the importance of the reverse recovery in the efforts to reduce the response time of the pulsed circuits, many investigations of the phenomena were carried out (see, for example, Nosov 1969).

The theory of transient processes has stimulated to development of new devices as charge storage diodes (Moll et. al. 1962).

To conclude, it can be said that the development of the theory of transient processes has made it possible considerably to extend investigations of relaxations processes in semiconductor devices, in particular, the recombination of excess carriers.

1.4 pn Coupling

In the usual calculations of the solar cell characteristics the contribution of the diffused layer is neglected. It has, however, been shown by Hauser and Dunbar (1977) that the diffused layer can represent an important limitation to efficiency, specially in the low resistivity base solar cells. Short-circuit current losses occur in the diffused layer due to surface recombination and the bulk carrier recombination. The diffused layer contributes to the dark saturation current through carrier injection and recombination either in the bulk or at the surface. It has been observed by Fossum et. al. (1979) that the diffused layer can make an important contribution to the dark saturation current of the solar cell and hence limit the open circuit photovoltage. The presence of the band gap narrowing (to be discussed in the next section) further deteriorates the cell performance. Fossum et. al. (1979) find that the contribution of the diffused layer to the dark saturation current in the presence of band gap narrowing can be as large as 30 times the contribution to it from the base.

Fossum et. al. (1979) further show that the inclusion of the effects of band gap narrowing, modified by the Fermi-Dirac statistics, in the diffused layer in the analysis can be used to explain the inconsistency observed in the open circuit photovoltage of low base resistivity silicon solar cells. Open circuit photovoltage in such cells is smaller than that predicted by conventional theory which neglects diffused layer in the calculation of cell response (Brandhorst Jr. 1975 and Shibib et. al. 1979a).

Diffused layer and its coupling with the base in accordance with certain boundary conditions (to be discussed next) is referred to as pn coupling.

Mathematically, pn coupling in a solar cell (or diode) arises from the following considerations which are imposed as boundary conditions on time dependent diffusion equations for the excess minority carrier concentrations in the diffused and the base layers of the cell:

(1) The excess minority carrier concentrations at the junction on both sides are related to the junction voltage by the Boltzmann law in accordance with the Shockley boundary condition as follows:

$$\frac{n(0,t)}{n_{po}} = \frac{p(0,t)}{p_{no}} = \exp(qV/kT) - 1 \qquad .. (1.1)$$

where n and p denote the excess minority carrier concentrations at the junction at time t. n_{po} and p_{no} denote their thermal equilibrium values respectively. V is the voltage across the junction and q denotes the electronic charge. kT represents the thermal energy at temperature T.

It can be shown that the ratio of the two concentrations $n(0,t)$ and $p(0,t)$ remains constant during the decay (Nosov 1969).

(2) The total current through the junction is the sum of the minority carrier currents from the diffused layer and the base. The expression for the same can be written as follows (see, for example, McKelvey 1966).

$$I = q D_n \left(\frac{dn}{dx}\right)_o + q D_p \left(\frac{dp}{dx}\right)_o \qquad .. (1.2)$$

where D_n and D_p denote the diffusion coefficients of n and p type carriers respectively.

In the open circuit total current through the device has to be zero and not necessarily the base and diffused layer currents individually.

In the transient case the origin of the pn coupling can be explained as follows. The minority carrier concentrations at the junction are related to the voltage across the junction. As mentioned in (1) in the preceding

discussions the ratio of their concentrations at the junction on its either side remains constant i.e. does not depend upon time during the decay (at low injection levels). The minority carriers on either side of the junction cannot therefore decay independently. The minority carriers on the diffused layer side of the junction will be anihilated more rapidly than those in the base because the life time of the excess minority carriers on this side is much smaller than that of the excess minority carriers on the base side. The base therefore has to supply some carriers to the diffused layer in order to keep aforementioned ratio constant. Thus the minority carrier concentration on the base side would reduce at a faster rate than required by their own life time. The voltage decay across the junction in the presence of pn coupling would therefore be faster than that determined by the base alone.

To include pn coupling in the analysis of the cell we have to solve a coupled set of two continuity equations subject to appropriate boundary conditions. The amount of pn coupling can be expressed in terms of a parameter $J \equiv J_d/J_b$, where J_d and J_b denote the contributions to the dark saturation current from the diffused layer and the base respectively. If $J = 0$, we return to usual

calculations which neglect pn coupling. If $J < 1$, the usual approximation that the diffused layer contribution to the cell response is negligible is valid. But if $J > 1$ as is the case with modern solar cells, this approximation is not valid and the theory must account for the contribution of the diffused layer.

The effect of pn coupling in steady-state, as mentioned earlier in this section, has been analysed by Hauser and Dunbar (1977), Wolf (1963) and Fossum et. al. (1979). Expression for I-V characteristics of a solar cell with pn coupling is available in the literature (see, for example, Mckelvey 1966). Wolf (1963) has considered the most general case which also includes the drift fields in both the regions. We find that pn coupling in steady-state shifts the position of the excess minority carrier profile maximum in the base (in open circuit configuration) away from the junction which in the absence of pn coupling always occurs right at the junction.

Effect of pn coupling on PVD in a solar cell has been investigated by us and will be presented in chapter 4. PCVD with coupling in a diode has been investigated by North (1955), Gossik (1955), Lindholm and Sah (1976) and Tewary and Jain (1981). Lindholm and Sah (1976) analysed the normal modes of the diode and gave an expression for

the dominant (natural) mode. Their theory predicts a linear decay of open circuit voltage with time. However, the experimental results reported by Neugroschel et. al. (1978) and Mehan et. al. (1979) exhibit nonlinear behaviour of FCVD in the initial stages of the transient. Measurements made on germanium diodes at Solid State Physics Laboratory, Delhi (India) show that FCVD plot for small values of time is not linear even if the space charge layer effects are negligible. Space charge layer effects are negligible provided voltage level considered is above 0.4 volts (Moll et. al. 1962).

Recently Tewary and Jain (1981) have given a theory which explains the nonlinear behaviour of FCVD in the initial stages of the transient. These authors show that coupling between the diffused and base increases the curvature of the FCVD plot in the beginning of the transient. Similar results for PVD in a solar cell have been obtained by us and will be presented in chapter 4.

1.5 Heavy Doping Effects

Shockley (1949) theory for current voltage characteristics of a pn junction diode based on diffusion of minority carriers in the neutral regions on either side of the junction is applicable only at low doping levels; when the thermal equilibrium density of minority carriers is inversely

proportional to the doping level. However, above a doping level of 10^{18} cm^{-3} the minority carrier concentration exceeds that predicted by this law. Early in 1970's it became obvious that large deviations from Shockley's(1949) theory were occuring in solar cells which had a heavily doped diffused layer on low resistivity base layers, resulting in discrepancies of upto 100 mV between the open circuit photovoltage observed in such cells and that expected theoretically (Brandhorst Jr. 1975 and Shibib et. al. 1979a). Two principal mechanisms were proposed to account for these discrepancies: Band Gap Narrowing and Auger Recombination (Redfield 1978, 1981). The dominant effect in the heavily doped diffused layer, however, is the modification by band gap narrowing of the electric fields which are present because of the doping gradient (Fossum et. al. 1979, Shibib et. al. 1979b and Lanyon 1981). This reduces the effective width of the diffused layer by an order of magnitude so that the surface recombination velocity is a significant factor in determining the dark saturation current through the device (Lanyon 1981). Below we briefly summarise the physics underlying the band gap narrowing effect based on the model presented by Lanyon and Tuft (1979).

The basic concept which leads to the idea of band gap narrowing is that the charge of minority carrier

attracts to it majority carriers of the opposite polarity, producing a screened Coulomb potential

$$\phi(r) = \frac{q}{4\pi\varepsilon r} \exp(-r/a_s) \qquad .. \quad (1.3)$$

where q denotes the electronic charge and ε the permitivity of the medium. a_s, the Debye radius is a function of free carrier concentration. One unit of free carrier surrounds each central charge. Because of the electrostatic force between the charges, work must be done to separate them since the paired charges have a lower energy than when each is isolated. This reduction in energy can be shown to be $3q^2/16\pi\varepsilon a_s$ and thus a function of free carrier concentration. It must be substracted from the band gap energy at infinite dilution to determine the activation energy for pair production with a finite density of majority carriers, causing a reduction in the effective band gap for both thermal and optical processes.

The model employed by Lanyon and Tuft (1979) for the band gap narrowing is the rigid band model. According to this model, the shape of the conduction band is unchanged by the incorporation of a large density of donars. Although the single donar level is broadened into a band by interactions between neighbouring sites (Morgan 1965), the dominant effect is the shift of donor level into the conduction band by a sufficiently large distance that it lies

above the Fermi level which also lies in the band for degenerate materials. This essentially means that the band gap narrowing occurs without changing the parabolic dependence on energy of the density of states in the conduction and valence bands.

The other effects of heavy doping which also tend to produce a narrowing in the band gap and are known to us since a long time are as follows:

(i) At high doping levels the energy band edges are no longer sharp. Electronic energy levels can extend beyond the energy positions of perfect single crystal material, forming thereby so called band tails (Lifshitz 1942).

(ii) A spatial variation of energy gap can result from macroscopic lattice strain introduced by high concentration of diffused impurity and structural imperfections in the lattice (see, for example, Fistul 1969).

Another modification in the presence of heavy doping which arises as a natural consequence of the Pauli's exclusion principle is that one must use Fermi-Dirac statistics instead of the conventional Maxwell-Baltzmann statistics. The band gap narrowing and Fermi-Dirac statistics affect the minority carrier concentration in opposite ways. For any given position of the Fermi level

relative to the band edges, band gap narrowing tends to increase the minority carrier concentration, whereas inclusion of the Fermi-Dirac statistics tends to decrease the minority carrier concentration below the value calculated by using Maxwell-Baltazmann statistics. The dominance of the either of the two effects, at any specific impurity level, depends upon the model of the band gap narrowing adopted.

For the model adopted by us the combined effects of band gap narrowing and Fermi-Dirac statistics can be represented through a single parameter called effective doping density (Hauser 1969 and Shibib et. al. 1979a). It is defined as the doping level that would produce the same minority carrier concentration as the actual doping if the heavy doping effects were not present.

It is straight forward to show that the heavy doping effects (band gap narrowing and Fermi-Dirac statistics) degrade n^+p cell performance more than that of p^+n cell because the effective mass of electrons in silicon is greater than the effective mass of holes. The resulting different effective densities of states in the conduction and valence bands (effective density of states in valence band is smaller than in conduction band) cause the on set of degeneracy to occur at lower impurity concentrations in

p-type material than in n-type material (Dunbar and Hauser 1977), if both p and n type materials have the same band gap narrowing. Thus the net effect of the band gap narrowing and Fermi-Dirac statistics is to degrade the n-type heavily doped region more than the p-type region with the same impurity concentration.

To examine qualitatively the effect of band gap narrowing on the conduction processes and the recombination generation-rates, one must distinguish whether the electronic states in the presence of heavy doping are localized or delocalized. For delocalized states, conduction can occur by drift and diffusion of carriers. For localized states, conduction can occur by carrier hoping between the neighbouring states due to thermally activated transfer of the trapped charge (Sah et. al. 1970 and Ryvkin 1964). However, for the ordinary temperatures encountered in solar cell operations only the delocalized or band states will have high carrier mobility and dominate the conduction processes (Lindholm and Sah 1977).

Regarding the effect of doping in the base which is moderate, it is usually assumed that the distribution of impurities in the base is uniform. However in the case of diffused solar cells (or diodes) this condition is not satisfied and the non-uniform distribution of impurities

in such devices causes a built-in-electric (drift)field to appear in the base. Effect of built-in-electric field on the solar cell response will be analysed in chapter 2.

To conclude we can say that the net effect of heavy doping in the diffused layer of modern solar cells (or diodes) is to reduce the band gap width below its actual value. Band gap narrowing in turn reduces the effective width of the diffused layer so that the front (illuminated) surface parameters play an important role in the conduction processes. In the conventional theories the front surface of the cell is characterised only by the surface recombination velocity incorporated in the usual surface boundary condition (see, for example, McKelvey 1966). Recently, however, Tewary and Jain (1980) have modified this boundary condition for solar cells to account for the surface generation of carriers. The resulting surface boundary condition is known as the Tewary and Jain (1980) boundary condition. The next section discusses the importance of the surface generation of carriers as included by Tewary and Jain (1980) in their surface boundary condition for solar cells.

1.6 Surface Boundary Condition - Effect of Surface Generation of Carriers

The usual surface boundary condition for the solar cell diffusion equations specifies that the diffusion current of the excess minority carriers is equal to their

recombination current. Mathematically the same for a p-type semiconductor can be expressed as follows (see, for example, McKelvey 1966):

$$D_n\left(\frac{dn}{dx}\right)_d = sn(d) \qquad .. (1.4)$$

where D_n and n denote the diffusion coefficient and the concentration of the excess minority carriers respectively. s denotes the surface recombination velocity and d is the distance between the junction and the illuminated surface.

Experiments (Mahan et. al. 1979 and Fabre et. al. 1975) show that the life time of excess minority carriers increases substantially (by a factor of 18) in the presence of light. Other advantage of the injection of minority carriers by light over the electrical injection is that the total current through the cell is zero. This is because the solar cell in the illuminated mode is in the open circuit configuration. The fact that the total current through the solar cell in the illuminated mode is zero allows us to neglect the electric field term in the continuity equation provided the excess carrier concentration is not too large in which case the Dember field which arises due to difference in the mobilities of electrons and holes will have to be considered. In addition to this,

when total current through the cell is zero, the Joule heating of the cell is eliminated and it is thus easier to make measurements at high injection levels. Another advantage of light injection of carriers is that this case more closely simulates the actual operation of the solar cell.

Referring back to the increase of excess minority carrier life time in the presence of light, there are two plausible explanations for this (Tewary and Jain 1980): (i) the traps may become saturated and therefore ineffective as recombination centres or (ii) the photons may depopulate the traps by ionizing them which increases the concentration of excess minority carriers and therefore their apparent life time. The second explanation is supported by the experiments on photoconductivity and Luminescence (Rube 1967) and by direct observations on photoionization of filled traps (Dekeersmaecker et. al. 1978 and Feigel et. al. 1976).

The rate of photoionization of filled traps is found to be proportional to the product of photon flux (or light intensity) and density of trap levels (Dekeersmaecker et. al. 1978). The photon flux will be much higher at the surface than in the bulk because of exponential absorption of light. Moreover, the density of trap levels will also be much higher

at the surface as compared to the bulk because of the various discontinuities and impurities at the surface (which results into a finite surface recombination velocity). It is therefore reasonable to postulate that the photo-generation of carriers near the surface will be quite appreciable.

Tewary and Jain (1980) incorporated this effect into the surface boundary condition forsolar cells (equation 1.4) in a manner similar to the surface recombination of excess minority carriers. The new surface boundary condition derived by these authors can be written as follows:

$$D_n\left(\frac{dn}{dx}\right)_d = sn(d) - \eta N_o \qquad .. (1.5)$$

wher e η is the surface generation coefficient. N_o is the incident photon flux. η is a material parameter which depends upon the nature of the surface treatment of the solar cell and also on the wavelength of light.

The second term on the right hand side of equation (1.5) viz. ηN_o accounts for the photogeneration of carriers at the surface. If $\eta = 0$, equation (1.5) reduces to the usual surface boundary condition (equation 1.4).

We see from equation (1.5) that the effect of η is to negate the effect of s. A surface treatment corresponding to a higher value of η will therefore yield a higher efficiency of the solar cell.

η can be measured by methods similar to those for measuring s viz. by effectively measuring $n(d)$ as a function of N_o or by measuring the transient response of solar cell to a pulse of light. Present measurements in which η is not separately identified, presumably yield an effective value of s in which the effect of η is partly included. However, η contributes in different ways to steady-state and transient response of solar cells. The effective value of s as determined by the two methods will therefore be inconsistent. Simfarly the value of s as derived from a measurement of dark characteristic of solar cell (for example when used as a diode $N_o = 0$) will not be applicable to the illuminated solar cell. The inconsistencies observed by Mahan et. al. (1979) between the dark and illuminated transient response may be partly due to this effect. Further, η will be larger for shorter wavelengths which is consistent with the observed increase of photocurrent at shorter wavelengths by Fabre et. al. (1975)

1.7 Summary of the Work Presented in the Thesis

The objective of the thesis is to study the transient response of a solar cell. It is determined by the following two characteristics:

(i) the short-circuit current decay.

(ii) the open circuit photovoltage decay (PVD).

The short-circuit current decay as mentioned in section 1.1 depends upon the series resistance of the solar cell which introduces some uncertainties in the analysis of the experimental data. The open circuit photovoltage decay on the other hand as mentioned in section 1.3 is free from such uncertainties and therefore is more reliable for the measurement of solar cell parameters. In view of this in this thesis we have confined our studies to the open circuit photovoltage decay following abrupt termination of incident radiation. In particular the thesis attempts to develop a theory of PVD with a view to apply it for the measurement of various material parameters of the solar cell by analysing the experimental data on PVD.

The work presented in this thesis analyses the effect of finite thickness of the base, built-in-electric field in the base and pn coupling on the transient response of a solar cell. In chapter 2 the effect of finite thickness of base and built-in-electric field on the transient response of a cell have been analysed by assuming that the effect of pn coupling is negligible. Effect of pn coupling on PVD is analysed in chapter 4. Since transient calculations require a prior knowledge of steady-state calculations, in chapter 3 we analysed the effect of pn

coupling on the steady-state resp onse of the solar cell.

An n on p silicon pn junction solar cell with an abrupt junction has been considered throughout the work presented in the thesis. We have neglected the space charge layer effects and also assumed the Shockley boundary condition at the junction. Thus the results reported in this thesis are valid only at moderate injection level i.e. when the excess minority carrier concentration is much less than the corresponding thermal equilibrium concentration and at the same time the junction voltage is high enough for space charge layer effects to be negligible.

The chapterwise summary is given below.

Chapter 1 - the present chapter: In this chapter the objective and the importance of the present work are defined and a brief introduction to the pn junction solar cell is given. The role of transient studies in the measurement of the parameters of a pn junction device is discussed. The importance of pn coupling in modern solar cells is discussed and a brief review of the relevant heavy doping effects is given. As remarked by Lanyon(1981) the heavy doping in the diffused layer decreases its effective width so that the front surface parameters play an important role in deciding the solar cell response. In view of this the importance of surface generation (along

with the absorption) of carriers as introduced by Tewary and Jain (1980) in the surface boundary condition for solar cells is discussed.

Chapter 2 - This chapter deals with the normal mode analysis of the solar cell base. A solar cell having a base with arbitrary thickness, a back contact which can account for an ohmic contact ($s = \infty$) as well as the back surface field (BSF) ($s = 0$) and a constant built-in-electric (drift) field has been considered. Both accelerating as well retarding fields have been treated and their effect on the transient response of the cell has been studied. The theory is quite rigorous and is based on the powerful mathematical technique of the Sturm Liouville R-transform (Sneddon 1972 and Kennedy 1962).

It has been shown that the infinite base approximation for solar cells as used by Jain (1981) and Dhariwal and Vasu (1981) is valid provided the thickness of the base layer is greater than three times the diffusion length of the excess minority carriers in the base. For very thin cells ($d/L_n << 1$; d-thickness and L_n diffusion length), the decay of open circuit photovoltage is very fast and linear. For $d/L_n >> 1$, the decay curve exhibits a kink in the beginning of the transient which is more pronounced for larger values of the absorption coefficient of light.

An accelerating field enhances the decay rate whereas a retarding field shows the opposite effect. Effect of an accelerating field on PVD increases as d/L_n increases. Effect of a retarding field on PVD also increases with d/L_n but only upto moderate value of d/L_n ($d/L_n \sim 1$). For large values of d/L_n ($>> 1$) the effect of field on the motion of carriers is exactly offset by their diffusive motion (because field and diffusion act in the opposite directions) and PVD is determined only by the bulk recombination of the carriers which yields unit slope of the PVD curve.

Lastly, the theory has been used to interpret the experimental results of Madan and Tewary (1981) on PVD. Spectral response of PVD has been fitted with the experimental data by using a least square fitting computer programme and the values of the life time of excess minority carriers, their diffusion length, thickness of the base and the magnitude of the built-in-electric field in the base have been obtained.

Chapter 3 - In this chapter it is shown that the diffused layer and its coupling with the base (pn coupling) make an important contribution to the steady-state response of a solar cell due to the band gap narrowing caused by the heavy doping in the diffused layer. The steady-state short circuit current, open circuit photo-

voltage and the excess minority carrier profile in the base in the open circuit configuration have been calculated for different values of the front surface parameters and the absorption coefficient of light. The front surface of the solar cell is modelled by using the Tewary and Jain (1980) boundary condition for solar cells which accounts for the surface generation of carriers as well as their absorption.

We find that pn coupling shifts the position of the maxima of the excess minority carrier profile in the base (in the open circuit configuration) away from the junction. The same in the absence of pn coupling as required by the open circuit condition always occurs at the junction.

Effect of surface generation of carriers is found to be more pronounced for low values of the absorption coefficient of light. This as remarked by Tewary and Jain (1980) increases the short-circuit current and hence also the open circuit photovoltage.

Surface absorption of carriers increases the dark saturation current of the cell and hence decreases the open circuit photovoltage.

Chapter 4 - In this chapter the effect of pn coupling on the transient response of a solar cell has been analysed. The theory is quite rigorous and is based

upon the powerful technique of Laplace transform (Sneddon 1972). Importance and applications of Tricomi method (Sneddon 1972 and Ward 1954) in inverting the Laplace transform have been discussed.

It is shown that the leading term in the low time expansion of PVD series is linear in t and is independent of the detailed nature of the source of excitation (optical). In addition to this, we also find that

(i) effect of pn coupling on PVD is substantial only in its initial stages.

(ii) an increase in the value of the relative dark saturation current (J) increases the curvature of the PVD plot in its initial stages

(iii) an increase in the value of the absorption coefficient of light (α) enhances the decay rate

(iv) surface generation coefficient (η) as introduced by Tewary and Jain (1980) in the solar cell surface boundary condition affects PVD more for lower values of the absorption coefficient of light

(v) surface absorption of carriers increases the decay rate

(vi) an increase in the value of the relative excess minority carrier life time (T) slows down the decay

(vii) an increase in the diffused layer thickness (d) increases the decay rate which is more pronounced for larger values of J and α.

From the analysis presented in this chapter we arrive at the conclusion that the measurement of PVD in its initial stages would yield useful information about the following:

(i) excess minority carrier life time in the diffused layer.

(ii) diffused layer thickness and

(iii) the front surface parameters i.e. s and η.

Measurement of PVD at larger times on the other hand would yield the excess carrier life time and other parameters of the base.

Literature references have been given at the end of each chapter. We have followed the system used by the Institute of Physics (U.K.) viz. authors' name and year of publication in the text and the whole reference given at the end of the chapter in the alphabatical order. The figures for each chapter have been given at the end of the chapter in the order of the figure numbers. The captions for all figures referred in the text of the chapter are given after the references in each chapter.

The work presented in this thesis is published/ to be published in the following papers:

1. S.K. Sharma, A. Agrawala and V.K. Tewary, "Effect of pn coupling on steady-stage and transient characteristics of a pn junction solar cell", J. Phys. D: Appl. Phys. 14 1115-1124, 1981.

2. S.K. Sharma and V.K. Tewary, "Photovoltage decay in a finite base solar cell with a drift field", accepted for presentation at the International Workshop on the Physics of Semiconductor Devices, to be held at Solid State Physics Laboratory, Delhi, India from Nov.23-28, 1981.

3. S.K. Sharma and V.K. Tewary, "Theory of open circuit photovoltage decay in a finite base solar cell with drift field", communicated to J. Phys. D: Appl. Phys.

4. S.K. Sharma and V.K. Tewary, "Effect of pn coupling on photovoltage decay in a solar cell", to be communicated.

References

1. Bassett R.J. (1969) Solid State Electronics 12 385.

2. Brandhorst Jr. H.W. (1975) Int. Electron Device Meeting, Tech. Dig. N.Y: 331.

3. Bube R.H. (1967) Photoconductivity of Solids (N.Y: John Willy) pp 275.

4. Chapin D.M., Fuller C.S. and Pearson G.L. (1954) J. Appl. Phys. 25 676-77.

5. Dekeersmaecker R.F., DiMeria D.J. and Pantelides S.T. (1978) Physics of SiO_2 and its Interfaces; pp 189-194; Editor - S.T. Pantelides (N.Y: Pergamon).

6. Dhariwal S.R. (1980) IEE Proc. (I) (G.B.) 127 20-24.

7. Dhariwal S.R. and Vasu N.K. (1981) IEEE Electron Device Letters EDL-2 53-55.

8. Dunbar P.M. and Hauser J.R. (1977) Solid State Electronics 20 697-701.

9. Fabre E., Mautref M. and Mircea A. (1975) Appl. Phys. Letters 27 239-41.

10. Feigl F.J., Butler S.R., DiMeria D.J. and Kapoor V.J. (1976) Thermal and Photoinduced Currents in Insulators, pp 118, Editor - D.J. Smyth (Princeton: The Electrochemical Society).

11. Fistul V. (1969) Heavily Doped Semiconductors (N.Y: Plenum Press).

12. Fossum J.G., Lindholm F.A. and Shibib M.A. (1979) IEEE Trans. on Electron Devices ED-26 1294-98.

13. Gardner M.F. and Barnes J.L. (1942) Transients in Linear Systems Studied by the Laplace Transformation Vol. 1 (N.Y: John Willy).

14. Gossik B.R. (1955) J. Appl. Phys. 26 1356.

15. Hauser J.R. (1969) Final Report (National Science Foundation Grant GK - 1615).

16. Hauser J.R. and Dunbar P.M. (1977) IEEE Trans. on Electron Devices ED-24 305-21.

17. Jain S.C. (1981) Solid State Electronics 179-83.

18. Kennedy D.P. (1962) IRE Trans. on Electron Devices ED-9 174-82.

19. Kingston R.H. (1954) Proc. IRE 42 829-34.

20. Lanyon H.P.D. and Tuft R.A. (1979) IEEE Trans. on Electron Devices ED-26 1014.

21. Lanyon H.P.D. (1981) Solar Cells 3 289-311.

22. Lederhandler S.R. and Giacoletto L.J. (1955) Proc. IRE 43 478-83.

23. Lifshitz I.M. (1942) J. Exp. Theor. Phys. 2 117, 137, 156.

24. Lindholm F.A. and Sah C.T. (1976) J. Appl. Phys. 47 4203-05.

25. Lindholm F.A. and Sah C.T. (1977) IEEE Trans. on Electron Devices ED-24 299-304.

26. Lindholm F.A., Neugroschel A., Sah C.T., Godlewski M.P. and Brandhorst Jr. H.W. (1977) IEEE Trans. on Electron Devices ED-24 402-10.

27. Madan M.K. and Tewary V.K. (1981) Submitted to J. Phys. D. Appl. Phys.

28. Madan M.K. and Tewary V.K. (1981) Submitted to Int. J. Electronics.

29. Mahan J.E., Ekstedt T.W., Frank R.I. and Kaplow R. (1979) IEEE Trans. on Electron Devices ED-26 733-39.

30. McKelvey J.P. (1966) Solid State and Semiconductor Physics (N.Y: Harper and Row).

31. Moll J.L., Krakauer S. and Shen R. (1962) Proc. IRE 50 43-53.

32. Morgan N. (1965) Phys. Rev. 139A A343-A348.

33. Muto S.Y. and Wang S. (1962) IRE Trans. on Electron Devices ED-9 183-87.

34. Neugroschel A., Chen P.J., Pao S.C. and Lindholm F.A. (1978) IEEE Trans. on Electron Devices ED-25 485.

35. North (1955) See the appendix of Reference 22.

36. Nosov Y.R. (1969) Switching in Semiconductor Diodes (N.Y: Plenum Press).

37. Redfield D. (1978) Appl. Phys. Letters 33 531-33.

38. Redfield D. (1981) Solar Cells 3 313-26.

39. Ryvkin S.M. (1964) Photoelectric Effects in Semiconductors (N.Y: Consultant Bureau).

40. Sah C.T., Forbes L., Rosier L.L. and Tasch Jr. A.F. (1970) Solid State Electronics 13 759-88.

41. Sah. C.T. and Lindholm F.A. (1977) IEEE Trans. on Electron Devices ED-24 358-62.

42. Shibib M.A., Lindholm F.A. and Therez F. (1979a) IEEE Trans. on Electron Devices ED-26 959-65.

43. Shibib M.A., Lindholm F.A. and Fossum J.G. (1979b) IEEE Trans. on Electron Devices ED-26 1104-06.

44. Shockley W. (1949) Bell Syst. Tech. J. 28 435.

45. Slatboom J.W. and Degraff H.C. (1976) Solid State Electronics 19 857-62.

46. Sheddon I.N. (1972) The Use of Integral Transforms (N.Y: McGraw-Hill).

47. Tewary V.K. and Jain S.C. (1980) J. Phys. D: Appl. Phys. 13 835-37.

48. Tewary V.K. and Jain S.C. (1981) Technical Report Solid State Physics Laboratory Delhi, India.

49. Tkhorik Yu. A. (1968) Transients in Pulsed Semiconductor Diodes (Jerusalem: Israel Programme for Scientific Translation).

50. Ward E.E. (1954) Proc. Cambridge Phylosphical Soc. 50 49-59.

51. Wolf M. (1963) Proc. IEEE 51 674-93.

****

CHAPTER 2

TRANSIENT RESPONSE OF A FINITE BASE SOLAR CELL WITH BUILT-IN-ELECTRIC FIELD

2.1 Introduction

In this chapter we shall study the transient response of a solar cell in the approximation that the effect of diffused layer vis. pn coupling is negligible. As discussed in chapter 1 section 1.4 this is a valid approximation in certain devices of practical interest under certain situations. The effect of pn coupling will be taken up in later chapters.

The transient response of a solar cell can be studied by measuring the decay of open circuit photovoltage (PVD) or the short-circuit current. As discussed in chapter 1 section 1.1 the open circuit photovoltage decay is a more reliable method in view of dependence of short-circuit current on the series resistance. In this and the following chapters, therefore, only the decay of open circuit photovoltage has been discussed. As is well known the decay of open circuit photovoltage

is determined by the carrier concentration profile, in this chapter we have also examined the time dependence of the carrier concentration profile.

The decay of open circuit photovoltage following abrupt termination of light can be used to determine the excess minority carrier life time and possibly the other parameters of a pn junction solar cell (Mahan et. al.1979). Experimental results of Mahan et. al. (1979) show that the life time of excess minority carriers in the presence of light increases by a factor of about 18 as compared to its value obtained by forward current voltage decay method. Consequently, the photovoltage persists for longer time.

Theories of photoinduced open circuit voltage decay in a solar cell have been given by Jain (1981) and Dhariwal and Vasu (1981). These theories, however, are based on the assumptions that (i) the base of the solar cell is infinitely thick and (ii) the distribution of impurities as well as resistivity in the base is uniform.

In solar cells (or diodes), however, a parallel ohmic contact is usually located in the immediate vicinity of the junction and the base resistance is decreased by decreasing base thickness. In such cases when the distance between the pn junction and the contact is comparable with the diffusion length of excess minority carriers, the

presence of an ohmic contact alters the process of accumulation and dispersal of excess carriers and consequently, the accompanying transient process.

The assumption (ii) amounts to saying that the solar cell base is uniform in its electrical properties. But there are devices like diffused solar cells and diodes where this assumption is not satisfied. All types of non-uniform distributions of impurity (acceptors for p-type semiconductor) concentration (N_a) can be divided into two categories: an increasing value of N_a away from the junction in the direction of the body of the base; and a decreasing value of N_a along the same direction (see, for example, Nosov 1969).

It is known that electric field always exists in the body of the semiconductor solar cell (or diode) with a non-uniform distribution of acceptor or donor impurities. The expression for the electric field in the base of an np solar cell (or diode) is given below (Nosov 1969).

$$E(x) = \frac{kT}{q} \frac{1}{N_a(x)} \frac{dN_a(x)}{dx} \qquad .. (2.1)$$

Thus, the presence of an acceptor concentration gradient in the base of an np solar cell produces an electric field pointing in the direction of increasing impurity concentration. Such a field is called Built-in-Electric

field since it is not associated with the flow of an electric current through the semiconductor but is established during the preparation of the cell. Built-in-Electric field or drift field, in general, is a function of x (equation 2.1). However, to a good approximation (Moll et. al. 1962 and Wolf 1963), we can replace it by an uniform field extending throughout the base.

An electric field in a base with a non-uniformly distributed accepter densities alters the equilibrium distribution and the rate of establishment of the equilibrium of excess minority carriers.

This field is called accelerating or retarding depending upon its action on the motion of the minority carriers. If it enhances minority carrier movement towards the back contact, it is called accelerating. On the other hand if it retards their motion towards the back contact, it is called retarding field.

It should be mentioned that equation (2.1) is valid only when low injection condition is satisfied. When the injection level is increased so that excess minority carrier concentration exceeds the equilibrium majority carrier concentration, the field produced by a non-uniform distribution of impurities becomes weaker and eventually ceases to have any effect altogether. Therefore, all processes involving built-in-electric field in solar cells (or diodes) are of interest only in the low injection case (Nosov 1969).

Effect of the finite size of base on the transient response of a solar cell has been studied by Tada (1966) and Dhariwal et. al. (1976, 1977). Toda (1966) measured excess minority carrier life time by measuring the decay constant of short-circuit current. His results show a great dependence of short-circuit current decay constant on the thickness of the base. Dhariwal et. al. (1977) have carried out a theoretical analysis of the transient photocurrent, photovoltage and photoconductivity of the solar cell. Their results support the findings of Tada (1966) and show that the decay constant of photocurrent for a very thin cell is independent of the carrier life time.

Effect of built-in-electric field on the steady-state response of the solar cell has been studied by Wolf (1963). Wolf (1963) has shown that the presence of built-in-electric field in the base of the solar cell increases its resistance to radiation damage. Its effect on the transient response of a solar cell has not been investigated in any of the published calculations so far.

In this chapter we present a theory of PVD in a solar cell which accounts for the finite size of the base as well as built-in-electric field in the base. An n on p silicon pn junction solar cell with a base of arbitrary thickness and a back contact with arbitrary surface recombination velocity has been considered. An uniform electric

field is assumed to exist in the base of the solar cell at low injection level. Both accelerating as well as retarding fields have been considered and their effect on the transient response of the solar cell has been analysed. The theory is quite rigorous and is based upon the powerful mathematical technique of Sturm Liouville R - transform (Sneddon 1972) as used by Kennedy (1962) for studying the reverse recovery transient in a pn junction diode. We have also used our theory to interpret the experimental results of Madan and Tewary (1981) on PVD.

In section 2.2 and its subsections the normal mode analysis of solar cell base as obtained by applying the Sturm Liouville R-transform is given. In section 2.3 the time dependence of the excess minority carrier concentration has been calculated. The effect of base thickness and built-in-electric field on PVD have been calculated in sections 2.4 and 2.5 respectively. Spectral dependence of PVD is analysed in section 2.6. Effect of back surface recombination on PVD is calculated in section 2.7. Finally in section 2.8 the theory is used to interpret the experimental results of Madan and Tewary (1981) on PVD.

2.2 Normal Mode Analysis of Base

The one dimensional distribution of excess minority carriers (electrons) in the base of an np solar cell is

governed by the following continuity equation (see, for example, McKelvey 1966).

$$D_n \frac{\partial^2 n}{\partial x^2} + f D_n \frac{\partial n}{\partial x} + \alpha N_o \exp[-\alpha(x+d_1)] - \frac{n}{\tau_n} = \frac{\partial n}{\partial t} \quad .. (2.2)$$

where $f = qE/kT$. q is the electronic charge and kT represents the thermal energy. E denotes the magnitude of built-in-electric or drift field (uniform) in the base. D_n and τ_n respectively denote the diffusion coefficient and the life time of excess minority carriers. α is the absorption coefficient of light (assumed to be monochromatic). N_o is the number of photons per unit area per unit time in the incident light. The cell under consideration has an abrupt junction at $x = 0$ and back surface at $x = d$. d_1 denotes the thickness of the diffused layer.

Equation (2.2) has to be solved subject to following boundary conditions:

(i) at $x = 0$: Usual Schockley boundary condition gives

$$\frac{n(0,t)}{n_{po}} = \exp(qV/kT) - 1 \quad .. (2.3)$$

While writing this boundary condition we assume that Boltzmann law is valid in the transient case also (Nosov 1969, Lindholm and Sah 1976, Neugroschel et. al 1977, Lindholm et. al. 1977 and Neugroschel et. al. 1978).

(ii) at $x = d$: We have the surface boundary condition

$$\left(\frac{dn}{dx}\right)_d + (f + s/D_n)\, n(d) = 0 \qquad .. (2.4)$$

where s denotes the surface recombination velocity.

The open circuit condition at $x = 0$ requires

$$\left(\frac{dn}{dx}\right)_o + fn(0) = 0 \qquad .. (2.5)$$

In transient case, in addition to above, we also impose the initial condition that $n(x,t)$ for $t = 0$, returns to its steady-state value. While imposing this condition we assume that the cell has been exposed to light such that steady-state is reached for $t \leq 0$ and light is switched off at $t = 0$.

To solve equation (2.2), we carry out the transformation $n(x,t) = y(x,t) \exp(-fx/2)$. The transformed equation (2.2) can be written as follows:

$$D_n \frac{\partial^2 y}{\partial x^2} - \left(\frac{f^2 D_n}{4} + \frac{1}{\tau_n}\right) y + \alpha N_o \exp[-\alpha(x + d_1)] = \frac{\partial y}{\partial t} \qquad .. (2.6)$$

Boundary conditions (equations 2.3 - 2.5) subject to above transformation can be written as follows:

(iii) at $x = 0$: $\dfrac{y(0)}{n_{po}} = \exp(qV/kT) - 1$ .. (2.7)

(iv) at $x = d$: $\left(\dfrac{dy}{dx}\right)_d + (f/2 + s/D_n)\, y(d) = 0$ .. (2.8)

and (v) $\left(\frac{dy}{dx}\right)_o + \frac{f}{2} y(0) = 0$ .. (2.9)

respectively.

2.2.1 Steady-State Analysis

To solve equation (2.6) in steady-state, we replace its right hand side by zero. The expression for the relative value $y(x)/y(0)$, where $y(0)$ denotes the value of y at the junction as given by equation (2.7), can be written as follows:

$$\frac{y(x)}{y(0)} = A_1 \exp(G_n x) + A_2 \exp(-G_n x) - W \exp[(F_n - \alpha)x] \quad .. (2.10)$$

where:

$$F_n = \frac{f}{2} \quad .. (2.11)$$

$$G_n = \left(F_n^2 + \frac{1}{L_n^2}\right)^{1/2} \quad .. (2.12)$$

$$L_n^2 = D_n \tau_n \quad .. (2.13)$$

The constants A_1 and A_2 in equation (2.10) can be evaluated by applying boundary conditions (iii) and (iv) (equations 2.7 and 2.8). The results are

$$A_1 = \frac{X_4 + (1 + W)X_2}{X_2 - X_1} \quad .. (2.14)$$

$$A_2 = \frac{X_4 + (1 + W)X_1}{X_1 - X_2} \quad .. (2.15)$$

$$X_4 = WX_3 \quad .. (2.16)$$

$$W = R/R' \qquad .. (2.17)$$

$$R = \frac{2G_n X_1}{X_1 - X_2} - (F_n + G_n) \qquad .. (2.18)$$

$$R' = (G_n - F_n + \alpha) - \frac{2G_n(X_3 + X_1)}{X_1 - X_2} \qquad .. (2.19)$$

$$X_1 = (F_n + G_n + s/D_n)\exp(G_n d) \qquad .. (2.20)$$

$$X_2 = (F_n - G_n + s/D_n)\exp(-G_n d) \qquad .. (2.21)$$

$$X_3 = (\alpha - 2F_n - s/D_n)X_5 \qquad .. (2.22)$$

$$X_5 = \exp[(F_n - \alpha)d] \qquad .. (2.23)$$

2.2.2 Transient State Analysis - Open Circuit Photovoltage Decay

Equation (2.6) without the generation term is the desired equation which governs the transient behaviour of the cell. It is given below

$$D_n \frac{\partial^2 y}{\partial x^2} - \left(\frac{f^2 D_n}{4} + \frac{1}{\tau_n}\right)y = \frac{\partial y}{\partial t} \qquad .. (2.24)$$

A general solution of this equation is obtained by assuming that the excess minority carrier distribution function, $y(x,t)$, can be expressed in the form (see, for example, Carslaw and Jaeger 1959).

$$y(x,t) = X(x).T(t) \qquad .. (2.25)$$

Upon substituting equation (2.25) into ecuation (2.24), we obtain the separated equations

$$\frac{\partial^2 X}{\partial x^2} - \frac{1}{D_n}\left(\frac{f^2 D_n}{4} + \frac{1}{\tau_n} - \varrho_r^2\right)X = 0 \qquad .. (2.26)$$

$$\frac{\partial T}{\partial t} + \varrho_r^2 t = 0 \qquad .. (2.27)$$

Solution of equation (2.26) can be obtained by applying Sturm Liouville R-transform technique (Sneddon 1972 and Kennedy 1962). From the solutions of equations (2.26) and (2.27), we can write relative $\frac{y(x,s)}{y(0)}$ as follows:

$$\frac{y(x,s)}{y(0)} = \sum_r A_r\left(\frac{\mu_r}{d}\cosh \mu_r \frac{x}{d} - \frac{f}{2}\sinh \mu_r \frac{x}{d}\right)\exp(-\varrho_r^2 s\tau_n) \qquad .. (2.28)$$

where $s = t/\tau_n$.

Back substitution of equation (2.28) into equation (2.24) yields

$$\varrho_r^2 = [1 + (fL_n/2)^2 - (\frac{\mu_r}{d/L_n})^2]/\tau_n \qquad .. (2.29)$$

Surface boundary condition equation (2.8) can be applied to evaluate μ_r. The result is

$$\frac{\mu_r}{dD_n} + [(\frac{\mu_r}{d})^2 - \frac{f}{2}(\frac{f}{2} + \frac{a}{D_n})]\tanh \mu_r = 0 \qquad .. (2.30)$$

The summation of equation (2.28) is conducted over ascending positive roots - both real and imaginary of equation (2.30). For each set of physical constants within equation (2.30), there is an infinite set of roots μ_r on the positive imaginary axis; in some physical situations it will also exhibit a root on the real axis. These independent roots give the normal modes of equation (2.30).

For $s = 0$, the positive imaginary roots of equation (2.30) are given by $n\pi$ where n is an integer. For $s = \infty$, equation (2.30) reduces to

$$\tanh \mu_r = \frac{2\mu_r}{i\delta} \qquad .. (2.31)$$

For $f = 0$, the positive imaginary roots of (2.31) are given by $(n+1/2)\pi$, where n is an integer. In this case it does not exhibit any finite real root.

The coefficients A_r can be evaluated by satisfying the initial condition

$$[y(x,t)]_{t=0} = y(x) \qquad .. (2.32)$$

where $y(x)$ denotes the steady-state value of y as given by equation (2.10). Upon substituting the values of $y(x,t)$ and $y(x)$ in equation (2.32), we get

$$\sum_r A_r \left(\frac{\mu_r}{d} \cosh \mu_r \frac{x}{d} - \frac{f}{2} \sinh \mu_r \frac{x}{d}\right)$$

$$= A_1 \exp(G_n x) + A_2 \exp(-G_n x) - W \exp[(F_n - \alpha)x] \quad .. (2.33)$$

The left hand side of equation (2.33) is a set of orthogonal functions and therefore by conventional methods we obtain

$$\int_0^d \{[A_1 \exp(G_n x) + A_2 \exp(-G_n x) - W \exp[(F_n - \alpha)x]] \times \left(\frac{\mu_r}{d} \cosh \mu_r \frac{x}{d} - \frac{f}{2} \sinh \mu_r \frac{x}{d}\right)] dx$$

$$A_r = \frac{}{I_{mm}} \quad .. (2.34)$$

where

$$\{d[\left(\frac{\mu_r}{d}\right)^2 - \left(\frac{f}{2}\right)^2][\left(\frac{\mu_r}{d}\right)^2 - \left(\frac{f}{2} + \frac{s}{D_n}\right)^2 - \frac{1}{d}\left(\frac{f}{2} + \frac{s}{D_n}\right)] + \frac{f}{2}[\left(\frac{\mu_r}{d}\right)^2 - \left(\frac{f}{2} + \frac{s}{D_n}\right)^2]\}$$

$$I_{mm} = \frac{}{2[\left(\frac{\mu_r}{d}\right)^2 - \left(\frac{f}{2} + \frac{s}{D_n}\right)^2]} \quad .. (2.35)$$

The integral in equation (2.34) can be easily evaluated and the resulting expression for A_r can be put in the following form

$$A_r = \frac{[A_1(\frac{\mu_r}{d} I_1 - F_n I_a) + A_2(\frac{\mu_r}{d} I_2 - F_n I_b) - W(\frac{\mu_r}{d} I_3 - F_n I_c)]}{I_{mm}} \quad ..(2.36)$$

where

$$I_1 = \left\{\frac{\sinh \mu_r}{\mu_r/d} \exp(G_n d) - \frac{G_n}{(\mu_r/d)^2}[\cosh \mu_r \exp(G_n d) - 1]\right\}/I \quad .. (2.37)$$

$$I_2 = \left\{\frac{\sinh \mu_r}{\mu_r/d} \exp(-G_n d) + \frac{G_n}{(\mu_r/d)^2}[\cosh \mu_r \exp(-G_n d) - 1]\right\}/I \quad .. (2.38)$$

$$I = 1 - \left(\frac{G_n}{\mu_r/d}\right)^2 \quad .. (2.39)$$

$$I_3 = \left\{\frac{\sinh \mu_r}{\mu_r/d} \exp[(F_n - \alpha)d] - \frac{(F_n - \alpha)}{(\mu_r/d)^2}[\cosh \mu_r \exp[(F_n - \alpha)d] - 1]\right\}/I' \quad .. (2.40)$$

$$I' = 1 - \left(\frac{F_n - \alpha}{\mu_r/d}\right)^2 \quad .. (2.41)$$

$$I_a = \left\{\frac{\cosh \mu_r \exp(G_n d) - 1}{\mu_r/d} - \frac{G_n}{(\mu_r/d)^2} \sinh \mu_r \exp(G_n d)\right\}/I \quad .. (2.42)$$

$$I_b = \left\{\frac{\cosh \mu_r \exp(-G_n d) - 1}{\mu_r/d} + \frac{G_n}{(\mu_r/d)^2} \sinh \mu_r \exp(-G_n d)\right\}/I \quad .. (2.43)$$

$$I_c = \left\{\frac{\cosh \mu_r \exp[(F_n - \alpha)d] - 1}{\mu_r/d} - \frac{(F_n - \alpha)}{(\mu_r/d)^2} \sinh \mu_r \exp[(F_n - \alpha)d]\right\}/I' \quad .. (2.44)$$

To find the coefficients A_r corresponding to imaginary roots, we only need to replace μ_r by $i\mu_r$ in equation (2.36).

Transendential equation (2.30), except for cases (i) $s = 0$ and (ii) $s = \infty$ and $f = 0$, has to be solved numerically for μ_r. Roots of this equation corresponding to these two cases have already been discussed earlier in this section.

Having calculated μ_r and A_r, the right hand side of equation (2.28) can be summed over ascending positive roots to find $y(x,z)/y(0)$. $y(x,z)/y(0)$ when multiplied by $\exp(-F_n x)$ gives the desired value of relative excess carrier concentration $n(x,z)/n(0)$ where $n(0)$ is equal to $y(0)$.

For $x = 0$, equation (2.28) reduces to

$$\frac{y(0,z)}{y(0)} = \sum_r A_r \frac{\mu_r}{d} \exp(-\mu_r^2 s\tau_n) \qquad .. (2.45)$$

It can be shown that the equation (2.45) is nothing but $\Delta V(s)$ which is related with V and V_o by the following relationship

$$\Delta V(s) = (V - V_o)q/kT \qquad .. (2.46)$$

From equations (2.46) and (2.45) we can write the following expression for PVD in a solar cell

$$\Delta V(s) = \ln\left[\sum_r A_r \frac{\mu_r}{d} \exp(-e_r^2 s\tau_n)\right] \qquad .. (2.47)$$

In writing equation (2.47) in this form we have made the two usual assumptions viz. (i) the space charge layer effects are negligible and (ii) the effect of pn coupling is negligible. Assumption (i) is valid for silicon solar cells at room temperature provided $V(t) > 0.4$ Volts (Moll et. al. 1962, Neugroschel et. al. 1977, Lindholm et.al. 1977 and Jain 1981). Regarding assumption (ii) as will be discussed in the following chapters the effect of pn coupling is important only in those devices in which the dark saturation current in the diffused layer is comparable to that in the base. In such devices, pn coupling affects the decay mainly in the initial stages during an interval which is of the order of the excess carrier life time in the diffused layer and will be discussed in the later chapters.

2.3 Excess Minority Carrier Profile in the Open Circuit Configuration

The effect of built-in-electric field on the nature of the excess minority carrier profile in the open circuit configuration has been shown in figures 2.1, 2.2 and 2.3 for $fL_n = -5, 0,$ and $+5$ respectively. In these figures relative $n(x,t)/n(0)$, where $n(0)$ denotes the number of carriers at the junction in steady-state, has been plotted

as a function of x/d. The values of fL_n which we have taken are the same as used by Kennedy (1962) for studying the reverse transient characteristics of a pn junction diode. The main observations of these figures are summarised below:

(i) For $fL_n = -5$, which corresponds to an accelerating field, $n(x,t)/n(0)$ increases with x/d.

(ii) For $fL_n = 0$, $n(x,t)/n(0)$ decreases monotonically with x/d.

(iii) For $fL_n = +5$, which corresponds to a retarding field, $n(x,t)/n(0)$ decreases much faster than that in case (ii).

The above observations can be explained with the help of equations (2.8) and (2.9). From equation (2.9) it is obvious that for negative f, dy/dx at the junction will be positive. At the surface, however, there is a competetion between $f/2$ and S/D_n (equation 2.8). If $f/2$ is negative and greater than s/D_n, dy/dx at the surface will also be positive. In our caloulations $f/2 = -250\ cm^{-1}$ and $s/D_n = 100\ cm^{-1}$. This, therefore, explains observation (i).

For $fL_n = 0$, $dy/dx = 0$ at the junction and negative at the surface. This explains monotonic fall of the relative carrier density with x/d in figure 2.2.

For $fL_n = +5$, dy/dx is negative at the junction as well as at the surface. Magnitude of dy/dx at the surface and the junction in this case, however, is much larger than their corresponding values in the case with $fL_n = 0$. This explains the rapid decrease of relative carrier density with x/d in figure 2.3.

It may be mentioned here that field does not create carriers; it only redistributes them. An accelerating field drags the minority carriers away from the junction and thus decreases the number of excess minority carriers at the junction. Consequently, the steady-state open circuit photovoltage (V_o) which depends upon the number of carriers at the junction, is reduced below its field-free value. A retarding field, on the other hand, pushes the minority carriers towards the junction and hence increases V_o above its field-free value. The degree to which V_o is changed depends upon the intensity of the field.

2.4 Effect of Base Thickness on PVD

To study the effect of base thickness on PVD and find a value of d/L_n which corresponds to the infinite base approximation as used by Jain (1981) for solar cells, we calculated PVD by using equation (2.47) for many different values of d/L_n. For the purpose of illustration, we have shown the calculated PVD for $d/L_n = 1$ and 5 in

figure 2.4. Since the decay of voltage for $d/L_n \ll 1$ is very fast, it was not found convenient to draw PVD curves corresponding to $d/L_n = 0.1$ on figure 2.4. The same however, have been shown separately in figure 2.5.

Figure 2.4 also shows the PVD curves as obtained by using Jain's (1981) theory based upon the infinite base approxd ation. The expression for PVD in a solar cell with infinitely thick base as derived by Jain (1981) is given below.

$$\Delta V(z) = -z + \ln \left[\frac{\sigma s(z) - s(\sigma^2 z)}{\sigma - 1} \right] \quad .. (2.48)$$

where

$$\sigma = \alpha L_n \quad .. (2.49)$$

$$s(z) = \exp(z)\ \mathrm{Erfc}\ (z)^{1/2} \quad .. (2.50)$$

The main observations of these figures are summarised below:

(i) For $d/L_n = 0.1$ the decay of $\Delta V(z)$ with z is linear and very fast.

(ii) For $d/L_n = 1$ the decay is linear but slower than in case (i).

(iii) For $d/L_n = 3$ the PVD plot exhibits curvature in the beginning of the transient and then becomes linear. For small values of z, results of the two theories match

but deviate as z increases. For large values of z, the theory presented in this chapter predicts a faster decay without altering the nature of the decay curve.

Above observations can be physically interpreted as follows. The moment we switch off light, junction loses carriers by diffusion and recombination. For $d/L_n \ll 1$ ($= 0.1$), diffusion effects predominate (Choo and Mazur 1980 and Bassett et. al. 1975) and the presence of an ideal ohmic contact very near to the junction causes a very fast decay of photovoltage. For $d/L_n \ll 1$, only first term of the series on the right hand side of equation (2.47) needs be retained. Equation (2.47) under such conditions reduces to

$$\Delta V(z) = -\varrho_1^2 z\tau_n + \ln\left(\frac{A_1\pi}{2d}\right) \qquad .. (2.51)$$

where

$$\varrho_1^2 = \left[1 + \left(\frac{\pi/2}{d/L_n}\right)^2\right]/\tau_n \qquad .. (2.52)$$

Equation (2.51) predicts a linear decay of $\Delta V(z)$ with z. For $d/L_n \ll 1$, unity in side the brackets in equation (2.52) can be neglected in comparison to the diffusive term viz. $(\pi/2)^2/(d/L_n)^2$, which justifies the dominance of diffusion effects in the present case.

For $d/L_n = 1$, both the diffusion as well as recombination processes contribute to the decay rate. The

increased distance between junction and the ohmic contact causes the decay in the present case to be slower than that for $d/L_n = 0.1$. The first term in the PVD series still suffices the purpose and, consequently decay is linear. For $d/L_n = 1$, it may be verified that the recombination term in equation (2.52) is no more negligible in comparison to the diffusion term which emphasises the importance of bulk recombination in this case.

$d/L_n = 3$ corresponds to infinite base approximation. The presence of an ideal ohmic contact at a finite distance from the junction in the present theory causes the slope of steady-state excess minority carrier profile to be larger than that in Jain's (1981) theory. The moment we switch off light, junction in both the theories loses carriers by diffusion and recombination. In the beginning of the transient in both the theories diffusion effect predominate and the effect of surface on the processes occuring at the junction is very small. Consequently, both the theories predict nearly the same decay rate. However as time increases, diffusion in Jain's (1981) theory loses its effect much faster than in the present theory because of the different slopes of steady-state carrier profiles, which explains the deviation between the two theories for larger times. Decay in Jain's (1981) theory for large times is mainly recombination controlled whereas in the

present theory both recombination and some diffusion of carriers to ohmic contact contribute to it. This explains the faster decay of $\Delta V(z)$ with z as predicted by the present theory in observation (iii).

It may be mentioned here that the deviation between the two theories decreases as c increases. In figure 2.4 we have also plotted $\Delta V(z)$ against z for $c = 0.1$ and 100 for $d/L_n = 3$ and ∞. The two observations of this figures are given below:

(i) For $c = 0.1$, the deviation for $z = 5$ is 18%

(ii) For $c = 100$, the deviation for same z is reduced to about 8% only.

The above two observations can be understood as follows. As c increases, the absorption length of light $L_a (= 1/\alpha)$ decreases and consequently the distance upto which carrier generation in the base occures also decreases.

For $c = 0.1$, $L_a = 10\, L_n$ but the thickness of the base is only $3L_n$. Moreover, carrier concentration at the back surface owing to an ideal ohmic contact has to be zero. Consequently, the slope of the steady-state excess minority carrier profile in the present theory becomes much larger than that in Jain's (1981) theory where infinitely thick base allows carrier generation upto the desired value of

L_a. This therefore following the reasoning given earlier in this section explains observation (i).

For $c = 100$, $L_a = 0.01\ L_n$. Since $d/L_n = 3$, the carrier generation in the present theory occures only upto a distance $d/300$ from the junction leaving the back surface far away. For large values of c, carrier generation in Jain's (1981) theory also takes place in the same region though the base is infinitely thick. Consequently, the slopes of steady-state carrier profiles in both the theories are nearly same which accounts for the improved agreement between the two theories for large values of c. This explains observation (ii).

From above discussion it is obvious that the value of L_a (or c) relative to d/L_n also contributes to the validity of the infinite base approximation. On quantitative grounds we find that the infinite base approximation is valid provided $d/L_a < 0.3$.

The aforementioned reasoning may also be used to explain the occurrence of a kink in the beginning of the transient in all those curves for which $L_a < L_n$. The kink becomes more and more pronounced as the difference between L_a and L_n increases.

To conclude we can say that the infinite base approximation is valid provided $d/L_n > 3$ or equivalently if $d/L_a < 0.3$.

2.5 Effect of Built-in-Electric Field on PVD

In section 2.3 we have seen that the presence of built-in-electric field in the base of a solar cell in steady-state alters the distribution of excess minority carriers; an accelerating field decreases the number of carriers at the junction as compared to field-free value whereas a retarding field exhibits the opposite effect. How such a change in the nature of steady-state carrier profile affects PVD in the transient case will be discussed in the present section.

PVD as calculated by using equation (2.47) for $fL_n = -5$, 0 and +5 have been shown in figures 2.5, 2.6 and 2.7 for $d/L_n = 0.1$, 1 and 3 respectively.

To analyze the effect of field on PVD, in table 2.1 we give the magnitude of the slope of the straight line portion (S) of these curves. This table shows that as compared to field-free case; a retarding field slows down the decay by about 19, 64 and 20% whereas an accelerating field enhances it by about 22, 275 and 572% for $d/L_n = 0.1$, 1 and 3 respectively. The number of terms of the PVD series (equation 2.47) taken in these calculations are 3, 10 and 40 for $d/L_n = 0.1$, 1 and 3 respectively.

Before we proceed to analyze above observations, let us examine the convergence of the series in equation (2.47). For this purpose we calculate the slopes of the aforementioned PVD curves by taking only the first term of the PVD series. The expression for S under these conditions can be written as follows:

$$S = (fL_n/2)^2 + 1 - \left(\frac{\mu_1}{d/L_n}\right)^2 \qquad .. (2.53)$$

Values of S as calculated by using equation (2.53) are given in table 2.2.

Now we compare table 2.1 with table 2.2. Let us first consider the case $d/L_n = 0.1$. In this case we see that whole of the decay is due to the first term only and therefore we need to retain only the first term of PVD series. It should be mentioned here that though equation (2.31) also exhibits a real root for $fL_n = +5$ in this case but it is so small (0.36×10^{-18}) that its contribution can be safely neglected.

For $d/L_n = 1$, the first term describes the decay with a tolerable error. For $fL_n = +5$, however, it is the real root at $\mu_1 = 2.46$ which accounts for the decay rate.

For $d/L_n = 3$ and $fL_n = +5$, it is again the real root at $\mu_1 = 7.5$ which accounts for the entire decay rate. For $fL_n = -5$, first term yields a decay rate with 5% inaccuracy.

It is important to mention here that above analysis examines convergence at the junction ($x = 0$). For higher values of x, the need of number of terms rises as the ratio d/L_n increases. For $d/L_n = 3$ and $fL_n = -5$, we have found that the convergence is slow for $x > 0$ and to calculate excess minority carrier profile in this case we have to retain as many as 40 terms of the series.

Referring back to the effect of field on PVD, aforementioned effect of field on PVD can be physically explained as follows. An accelerating field as mentioned earlier in this section drags the carriers away from the junction and hence adds to the decay rate. For small values of d/L_n ($= 0.1$) since the decay is diffusion controlled, field is not able to show its full effect on PVD. However, as d/L_n increases, diffusion effects become weaker and weaker and consequently, the contribution of drift of carriers to the decay rate increases.

A retarding field pushes the carriers towards the junction and hence slows down the decay. The effect of field increases with d/L_n upto $d/L_n = 1$. For $d/L_n = 3$, however, the effect of field has decreased to 20% from 64% corresponding to $d/L_n = 1$. To explain this observation let us recall that for $d/L_n = 3$ decay is described by the real root alone which is located at $\mu_1 = 7.5$. We

also know that the maximum value which tanh μ_1 can take is 1. For $\mu_1 = 7.5$, tanh $\mu_1 = 1$. Furthermore, we see that for $\mu_1 = 7.5$ and $d/L_n = 3$ the drift and diffusion terms in equation (2.53) cancel each other exactly because $(fL_n/2)^2$ and $(\frac{\mu_1}{d/L_n})^2$ are equal. Consequently, the decay in this case is governed only by the bulk recombination of carriers which yields unit slope of the PVD curve.

In view of the exponential nature of the decay modes (equation 2.47), after a long enough time only the leading mode corresponding to the lowest value of ϱ_r^2 survives. In this region, $\Delta V(z)$ is linear with z. For a retarding field a simple estimate of the real root may be easily obtained in the limit $fd \to \infty$. Since tanh μ_r saturates to unity, we obtain from equation (2.31) that $\mu_r \approx fd/2$. From here we obtain an interesting result that for $fd \to \infty$, S is independent of f and d and is equal to unity. This shows that for large fd, the decay is controlled by recombination only. Physically this can be explained by recalling that a field does not generate or absorb carriers; it only redistributes them. When a field is strong enough to counteract the diffusive loss of carriers for any value of d, then the loss of carriers at the junction will occur by recombination only and will not be affected by a further increase in the value of the field.

A change in the value of the surface recombination velocity (s) does not alter the aforementioned behaviour of PVD in the presence of a retarding field for large value of d/L_n. This statement can be easily verified with the help of table 2.3. In this table we have tabulated S for $s = 10^3$ cms^{-1} as obtained from figures 2.8, 2.9 and 2.10. All other parameters are same as for table 2.1.

It should be mentioned that although PVD in the presence of a retarding field for $d/L_n = 1$ too is described by the real root alone but the root in this case is located at $\mu_1 = 2.46$ and $\tanh \mu_1 = 0.985$. This is well below the saturation limit of $\tanh \mu_1$. Consequently, $(fL_n/2)^2 > (\frac{\mu_1}{d/L_n})^2$ which explains the increased contribution of field for $d/L_n = 1$ as compared to that for $d/L_n = 0.1$.

Lastly to conclude, we can say that the effect of accelerating field on PVD increases with d/L_n. The effect of retarding field on PVD though increases with d/L_n but only upto that value of d/L_n for which $\tanh \mu_1$ where μ_1 denotes the dominating root is less than 1.

2.6 Spectral Dependence of PVD

Spectral dependence of PVD for $d/L_n = 0.1$, 1 and 3 as calculated by using equation (2.47) has been shown in

figures 2.11 to 2.19. Figures 2.11 - 2.13, 2.14 - 2.16 and 2.17 - 2.19 are for $fL_n = -5$, 0 and +5 respectively.

A common feature exhibited by all these figures is that the effect of variation of c on PVD is substantial only when $d/L_n \geq 1$. The effect of field on PVD has already been discussed in the last section and may be observed here also.

To analyse the effect of c on PVD let us recall that as we increase c, the slope of the steady-state excess minority carrier profile increases which enhances the decay rate of photovoltage in the transient case. In fact the importance of contribution of c to the decay rate depends upon its magnitude relative to d/L_n. If L_n is comparable to d, the perfect sink at the ohmic contact makes the decay quite sensitive to d. On the other hand if L_n is very much smaller than d, the decay will not be sensitive to the value of d.

Mathematically the effect of c on PVD comes through the coefficients A_r (equation 2.36). For $d/L_n = 0.1$, since it is the first term of the PVD series that describes the decay, we can rewrite the equation (2.47) as follows:

$$\Delta V(z) = -\xi_1^2 s\tau_n + \ln\left(\frac{\mu_1}{d}\right) + \ln(A_1) \quad .. (2.54)$$

It can be shown analytically that the dependence of A_1 on c for $d/L_n \ll 1$ is very weak. In our calculations

for $fL_n = 0$, A_1 for $c = 0.1$, 1 and 5 is 0.66×10^{-3}, 0.66×10^{-3} and 0.65×10^{-3} cm respectively. Physically this would mean that all the values of c correspond nearly to the same profile of excess minority carriers which when decays, yields our observation for $d/L_n \ll 1$.

For $d/L_n = 1$, $c = 0.1$ and 1 correspond nearly to the same profile of excess minority carriers whereas $c = 5$ yields a different one. This follows from the fact that although the absorption lengths L_a for $c = 0.1$ and 1 are different but the presence of an ideal ohmic contact ($s = \infty$) at $d = L_n$ forces the profile with $c = 0.1$ to merge into the profile with $c = 1$. This explains the occurrence of degenerate curves a and b in figures 2.11, 2.14 and 2.17. For $c = 5$, $L_a = 0.2\ L_n$ only and consequently, the slope of the carrier profile is higher than in the first two cases which explains the faster decay of photovoltage in these figures for $c = 5$.

Above reasoning may be applied to show that for $d/L_n = 3$, all the three carrier profiles corresponding to $c = 0.1$, 1 and 5 have different slopes. Consequently, as soon as light is switched off, the three profiles decay with individual decay rates.

Another characteristic of PVD which has also been observed by Jain (1981) is that for $c \ll 1$ and $c \gg 1$,

$\Delta V(z)$ is independent of c. We find that all $\Delta V(z)$ vs z curves corresponding to $c \ll 1$ and $c \gg 1$ pile up together into two curves (one each for $c \ll 1$ and $c \gg 1$). This behaviour of PVD is observed regardless of the value of d/L_n and field (magnitude as well as direction).

2.7 Effect of Back Surface Recombination on PVD

Effect of surface recombination velocity (s) on PVD is shown in figures 2.20, 2.21 and 2.22 for $d/L_n = 0.1$, 1 and 3 respectively. The main observation of these figures is that the effect of surface recombination velocity on PVD decreases as the ratio d/L_n increases.

We know that the presence of an ohmic contact in the vicinity of the junction accelerates the leakage of excess minority carriers from the base and, therefore, accelerates the transient process in open circuit. As ratio d/L_n increases, back surface is shifted further and further away from the junction and consequently, theeffect of surface on the process occuring at the junction viz. PVD decreases.

2.8 Interpretation of Experimental Results on PVD

In this section, as an example, we shall apply our theory to interpret the experimental results of Madan and Tewary (1981) on PVD in a silicon pn junction solar cell. The experimental results were obtained on a Plessy 304 solar cell at 19°C by using the same circuit as given by

Mahan et. al. (1979) and using a General Radio (USA) Type-1531-AB Electronic Stroboscope as the source of light. Monochromatic light was obtained by using appropriate interference filters. We have chosen the experimental results of Madan and Tewary (1981) because they refer to monochromatic light and therefore are amenable to the present theoretical analysis. The only other available experimental data on PVD is due to Mahan et. al. (1979). However, they have used a composite light source whose spectral composition has not been given. It is not possible therefore to analyse their data quantitatively.

The experimental results on PVD corresponding to monochromatic light of wave lengths 5000 A°, 5600 A°, 5900 A° and 6900 A° are given in figures 2.23 and 2.24. The values of the absorption coefficient α for these wavelengths as obtained by using the formula of Shumka (1970) are 9441 cm^{-1}, 6126 cm^{-1}, 4937 cm^{-1} and 2362 cm^{-1} respectively. Using these values of α, we estimate the values of r_n, L_n, d/L_n and fL_n by fitting the theoretical values obtained from equation (2.47) to the experimental results. Two sets of values of these parameters are obtained, one in which the field is forced to be zero ($f = 0$) and the other in which f is allowed to be finite. In both these cases s is taken to be infinite because the cell is known to have no back surface field (BSF). These cases are described below.

(1) Zero Built-in-Electric Field

In this case which corresponds to an uniform doping in the base, f is forced to be zero and τ_n, L_n and d/L_n are allowed to vary. The best fit between the theoretical and experimental results as obtained by using a least square fitting computer programme is shown in figure 2.23. The 'best' values of these parameters corresponding to this fit are $\tau_n = 47\ \mu s$, $L_n = 458\ \mu m$ (which gives $D_n = 44.6\ cm^2 s^{-1}$) and $d/L_n = 1.57$.

It may be noted that if the life time is obtained following the usual method in terms of the slope of the linear region of the PVD curve at large times, as done by for example Mahan et. al. (1979), τ_n comes out to be 23 μs. The discrepancy between this value of τ_n (indicated by $\tau_{n\infty}$) and our value $\tau_n = 47\ \mu s$ is explained by observing that $\tau_{n\infty}$ is an effective life time which does not take into account the finite thickness of the base layer. An approximate relation between $\tau_{n\infty}$ and τ_n can be obtained by keeping only the first term of the series in equation (2.47) and relating the excess carrier life time to the slope of the PVD curve (Nosov 1969, Choo and Masur 1970 and Bassett et. al. 1973). Using equation (2.53), this gives

$$\frac{1}{\tau_{n\infty}} = \frac{1}{\tau_n}\left[1 + (fL_n/2)^2 - \left(\frac{\mu_1}{d/L_n}\right)^2\right] \qquad .. (2.55)$$

For $f = 0$, μ_1 as obtained from equation (2.31) is $\pi i/2$. Using $d/L_n = 1.57$ and $\tau_n = 47\ \mu s$ as obtained by the least square fitting, we find $\tau_{n\infty} = 23\ \mu s$ as would be expected from the conventional analysis. This clearly shows that if finite thickness of the base is not accounted for, a totally misleading value of life time may be obtained.

(ii) Finite Built-in-Electric Field

As a further refinement, we also allowed f to vary in the least square fitting programme. The resulting fit between the theoretical and experimental results is shown in figure 2.24. We see that there is no real improvement in the fitting by introducing another parameter f but the values of the parameters come out to be quite different and are as follows: $\tau_n = 19.6\ \mu s$, $L_n = 128.2\ \mu m$ (this gives $D_n = 8.38\ cm^2 s^{-1}$), $d/L_n = 1.55$ and $fL_n = 7.69$. This value of f corresponds to the field $E = 15.5\ V\ cm^{-1}$.

The discrepancy between the value of τ_n and the effective life time $\tau_{n\infty} = 23\ \mu s$ can also be explained by using equation (2.55) and by taking the fitted values of fL_n and d/L_n. In order to use equation (2.55), it may be noted that in this case the value of real root μ_1 as obtained by solving equation (2.31) is 5.98.

We find that in this case the experimental data and the analysis is not adequate to yield an unique set of

material parameters except for d/L_n which is roughly same in the both the cases. However, it can be safely concluded that both the thickness of the base and the field make significant contributions to PVD. The excess carrier life time obtained by neglecting these contributions and only considering the slope of the linear region of the PVD curve will be only an effective life time and may be quite different than the actual excess carrier life time in the base.

2.9 Conclusions

The normal mode analysis of the solar cell base based upon the Sturm Liouville R-transform technique has been presented. The theory considers a base with (i) an arbitrary thickness, (ii) an arbitrary surface recombination velocity at the back contact which can account for an ohmic contact as well as back surface field (BSF) and (iii) a constant built-in-electric (drift) field which may be present due to the gradient of the doping concentration. Following results have been reported.

I. The infinite base approximation for solar cells is valid provided $d/L_n > 3$.

II. In the absence of built-in-electric field we find that (i) for $d/L_n << 1$, the decay of open circuit photovoltage with time is very fast and linear and (iii) for

$d/L_n >> 1$, the decay curve exhibits a kink in the beginning of the transient which is more pronounced for larger values of the absorption coefficient of light. For larger values of time, however, the decay is still linear.

III. The presence of a built-in-electric field affects PVD in the following manner:

(i) An accelerating field enhances the decay whereas a retarding field has the opposite effect.

(ii) The effect of an accelerating field on PVD increases with d/L_n. The effect of a retarding field on the decay rate though increases with d/L_n but only upto that value for which $\tanh \mu_r < 1$. Beyond this limit the effect of retarding field on decay rate is balanced by the diffusion and is independent of the values of d/L_n and s.

IV. The theory has been used to interpret some experimental data on PVD. The values of τ_n, L_n, d and E have been obtained by fitting the theory with this experimental data. It is shown that the conventional analysis of the excess minority carrier life time based upon the slope of the linear region of PVD curve for large time yields only an effective life time which may be quite different than the actual value.

References

1. Bassett R.J., Fulop W. and Hogarth C.A. (1973) Int. J. Electronics 35 177-92.

2. Carslaw H.S. and Jaeger J.C. (1959) Conduction of Heat in Solids (Oxford University Press).

3. Choo S.C. and Mazur R.G. (1970) Solid State Electronics 13 553-64.

4. Dhariwal S.R., Kothari L.S. and Jain S.C. (1976) J. Phys. D: Appl. Phys. 9 631-41.

5. Dhariwal S.R., Kothari L.S. and Jain S.C. (1977) Solid State Electronics 20 297-304.

6. Dhariwal S.R. and Vasu N.K. (1981) IEEE Electron Device Letters EDL-2 53-55.

7. Jain S.C. (1981) Solid State Electronics 24 179-83.

8. Kennedy D.P. (1962) IRE Trans. Electron Devices ED-9 174-82.

9. Lindholm F.A. and Sah C.T. (1976) J. Appl. Phys. 47 4203-05.

10. Linholm F.A., Neugroschel A., Sah C.T., Godlewski M.P. and Brandhorst Jr. H.W. (1977) IEEE Transactions on Electron Devices ED-24 402-10.

11. Madan M.K. and Tewary V.K. (1981) Submitted to J. Phys. D: Appl. Phys.

12. Mahan J.E., Ekstedt T.W., Frank R.I. and Kaplow R.(1979) IEEE Trans. Electron Devices ED-26 733-39.

13. McKelvey J.P. (1966) Solid State and Semiconductor Physics (N.Y.: Harper and Row).

14. Moll J.L., Krakauer S. and Shen R. (1962) Proc. IRE 50 43-53.

15. Neugroschel A., Lindholm F.A. and Sah C.T. (1977) IEEE Trans. on Electron Devices ED-24 662-71.

16. Neugroschel A., Chen P.J., Pao S.C. and Lindholm F.A. (1978) IEEE Trans. on Electron Devices ED-25 485.

17. Nosov Y.R. (1969) Switching in Semiconductor Diodes (N.Y: Plenum Press).

18. Shumka (1970) The Conference Record of Eighth IEEE Photovoltaic Specialists Conference 96.

19. Sneddon I.N. (1972) The Use of Integral Transforms (N.Y. McGraw-Hill).

20. Tada H.Y. (1966) J. Appl. Phys. 37 4595-96.

21. Wolf M. (1963) Proc. IEEE 51 674-93.

Table 2.1

Slope S as obtained from figures 2.5, 2.6 and 2.7 as a function of d/L_n and fL_n for c = 1 and s = ∞.

fL_n \ d/L_n	0.1	1	3
+ 5	200	1.25	1
0	247	3.47	1.25
- 5	300	13	8.4

Table 2.2

Slope S as calculated by taking only the first term of the PVD series as a function of d/L_n and fL_n for c = 1 and s = ∞.

fL_n \ d/L_n	0.1	1	3
+ 5	201	1.2	1
0	248	3.46	1.27
- 5	301	12.9	8

Table 2.3

Slope S for $s = 10^3$ $ohms^{-1}$ and $\sigma = 1$ as obtained from figures 2.8, 2.9 and 2.10.

f/L_n \ d/L_n	0.1	1	3
+ 5	8.46	1.03	1.0
0	10.66	1.74	1.16
- 5	13.33	5.13	7.64

Captions for Figures

Figure 2.1: Relative excess minority carrier concentration $\frac{n(x,z)}{n(0)}$, as a function of x/d. fL_n, s, c and d/L_n for these curves are -5, 10^3 cms^{-1}, 5 and 1 respectively. Curves a, b and c in this figure are for z = 0, 0.1 and 0.2 respectively.

Figure 2.2: Relative excess minority carrier concentration $\frac{n(x,z)}{n(0)}$, as a function of x/d. fL_n, s, c and d/L_n for these curves are 0, 10^3 cms^{-1}, 5 and 1 respectively. Curves a, b and c are for z = 0, 0.1 and 0.2 respectively.

Figure 2.3: Relative excess minority carrier concentration, $\frac{n(x,z)}{n(0)}$, as a function of x/d. fL_n, s, c and d/L_n for these calculations are +5, 10^3 cms^{-1}, 5 and 1 respectively. Curves a, b and c are for z = 0, 0.1 and 0.2 respectively.

Figure 2.4: $\Delta V(z)$ as a function of z for s = ∞ and fL_n = 0. For curves 1, 2 and 3; d/L_n = 1, 3 and ∞ respectively. For curves a, b and c; c = 0.1, 5 and 100 respectively.

Figure 2.5: $\Delta V(z)$ as a function of z for d/L_n = 0.1, c = 1 and s = ∞ cms^{-1}. Curves 1, 2 and 3 in this figure are for fL_n = -5, 0 and +5 respectively.

Figure 2.6: $\Delta V(z)$ as a function of z for $d/L_n = 1$, $c = 1$ and $s = \infty$ cms^{-1}. Curves 1, 2 and 3 in this figure are for $fL_n = -5$, 0 and +5 respectively.

Figure 2.7: $\Delta V(z)$ as a function of z for $d/L_n = 3$, $c = 1$ and $s = \infty$ cms^{-1}. Curves 1, 2 and 3 in this figure are for $fL_n = -5$, 0 and +5 respectively.

Figure 2.8: $\Delta V(z)$ as a function of z for $d/L_n = 0.1$, $s = 10^3$ cms^{-1} and $c = 1$. Curves 1, 2 and 3 are for $fL_n = -5$, 0 and +5 respectively.

Figure 2.9: $\Delta V(z)$ as a function of z for $d/L_n = 1$, $s = 10^3$ cms^{-1} and $c = 1$. Curves 1, 2 and 3 are for $fL_n = -5$, 0 and +5 respectively.

Figure 2.10: $\Delta V(z)$ as a function of z for $d/L_n = 3$, $s = 10^3$ cms^{-1} and $c = 1$. Curves 1, 2 and 3 are for $fL_n = -5$, 0 and +5 respectively.

Figure 2.11: $\Delta V(z)$ as a function of z for $fL_n = -5$, $d/L_n = 0.1$ and $s = \infty$ cms^{-1}. All the three curves corresponding to $c = 0.1$, 1 and 5 overlap.

Figure 2.12: $\Delta V(z)$ as a function of z for $fL_n = -5$, $d/L_n = 1$ and $s = \infty$ cms^{-1}. Curves corresponding to $c = 0.1$ and 1 overlap and are represented by curve a in this figure. Curve b is for $c = 5$.

Figure 2.13: $\Delta V(z)$ as a function of z for $fL_n = -5$, $d/L_n = 3$ and $s = \infty$ cms^{-1}. Curves a, b and c in this figure are for $c = 0.1$, 1 and 5 respectively.

Figure 2.14: $\Delta V(z)$ as a function of z for $fL_n = 0$, $d/L_n = 0.1$ and $s = \infty$ cms^{-1}. All the three curves corresponding to $c = 0.1$, 1 and 5 respectively.

Figure 2.15: $\Delta V(z)$ as a function of z for $fL_n = 0$, $d/L_n = 1$ and $s = \infty$ cms^{-1}. Curves corresponding to $c = 0.1$ and 1 overlap and are represented by curve a in this figure. Curve b is for $c = 5$.

Figure 2.16: $\Delta V(z)$ as a function of z for $fL_n = 0$, $d/L_n = 3$ and $s = \infty$ cms^{-1}. Curves a, b and c in this figure are for $c = 0.1$, 1 and 5 respectively.

Figure 2.17: $\Delta V(z)$ as a function of z for $fL_n = +5$, $d/L_n = 0.1$ and $s = \infty$ cms^{-1}. All the three curves corresponding to $c = 0.1$, 1 and 5 overlap.

Figure 2.18: $\Delta V(z)$ as a function of z for $fL_n = +5$, $d/L_n = 1$ and $s = \infty$ cms^{-1}. Curves corresponding to $c = 0.1$ and 1 overlap and represented by curve a in this figure. Curve b is for $c = 5$.

Figure 2.19: $\Delta V(z)$ as a function of z for $fL_n = +5$, $d/L_n = 3$ and $s = \infty$ cms^{-1}. Curves a, b and c in this figure are for $c = 0.1$, 1 and 5 respectively.

Figure 2.20: $\Delta V(z)$ as a function of z for $fL_n = 0$, $d/L_n = 0.1$ and $c = 10$. Curves a and b in this figure are for $s = 10^3$ and ∞ cms^{-1} respectively.

Figure 2.21: $\Delta V(z)$ as a function of z for $fL_n = 0$, $d/L_n = 1$ and $c = 10$. Curves a and b in this figure are for $s = 10^3$ and ∞ cms^{-1} respectively.

Figure 2.22: $\Delta V(z)$ as a function of z for $fL_n = 0$, $d/L_n = 3$ and $c = 10$. Curves a and b in this figure are for $s = 10^3$ and $= \infty$ cms^{-1} respectively.

Figure 2.23: V(t) as a function of t curves 1, 2, 3 and 4 are for wavelengths (in nm) 690, 590, 560 and 500 respectively. Corresponding experimental points are shown by X, O, △ and □ respectively.

Figure 2.24: V(t) as a function of t curves 1, 2, 3 and 4 are for wavelengths (in nm) 690, 590, 560 and 500 respectively. Corresponding experimental points are shown by X, O, △ and □ respectively.

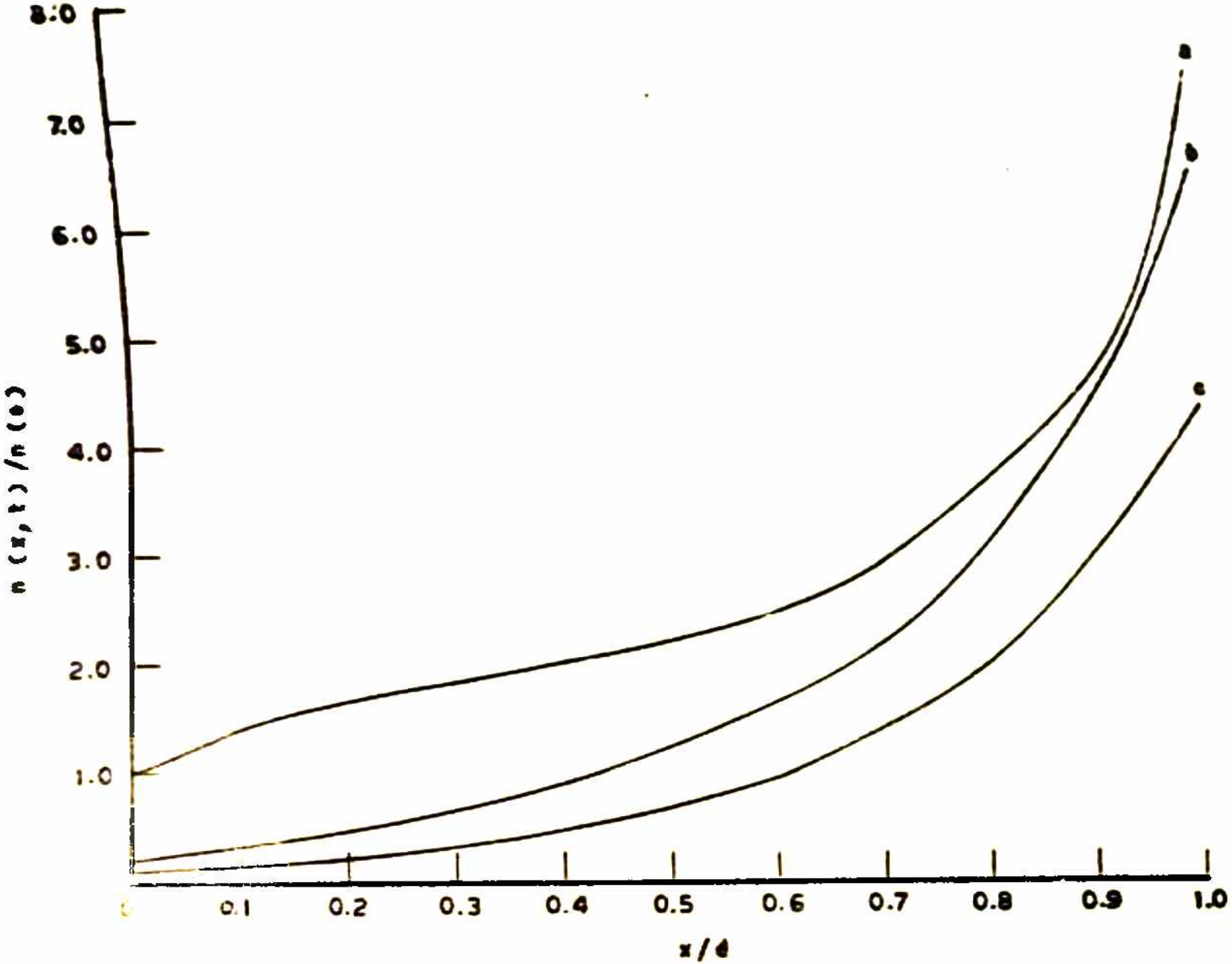

FIG. 2.1

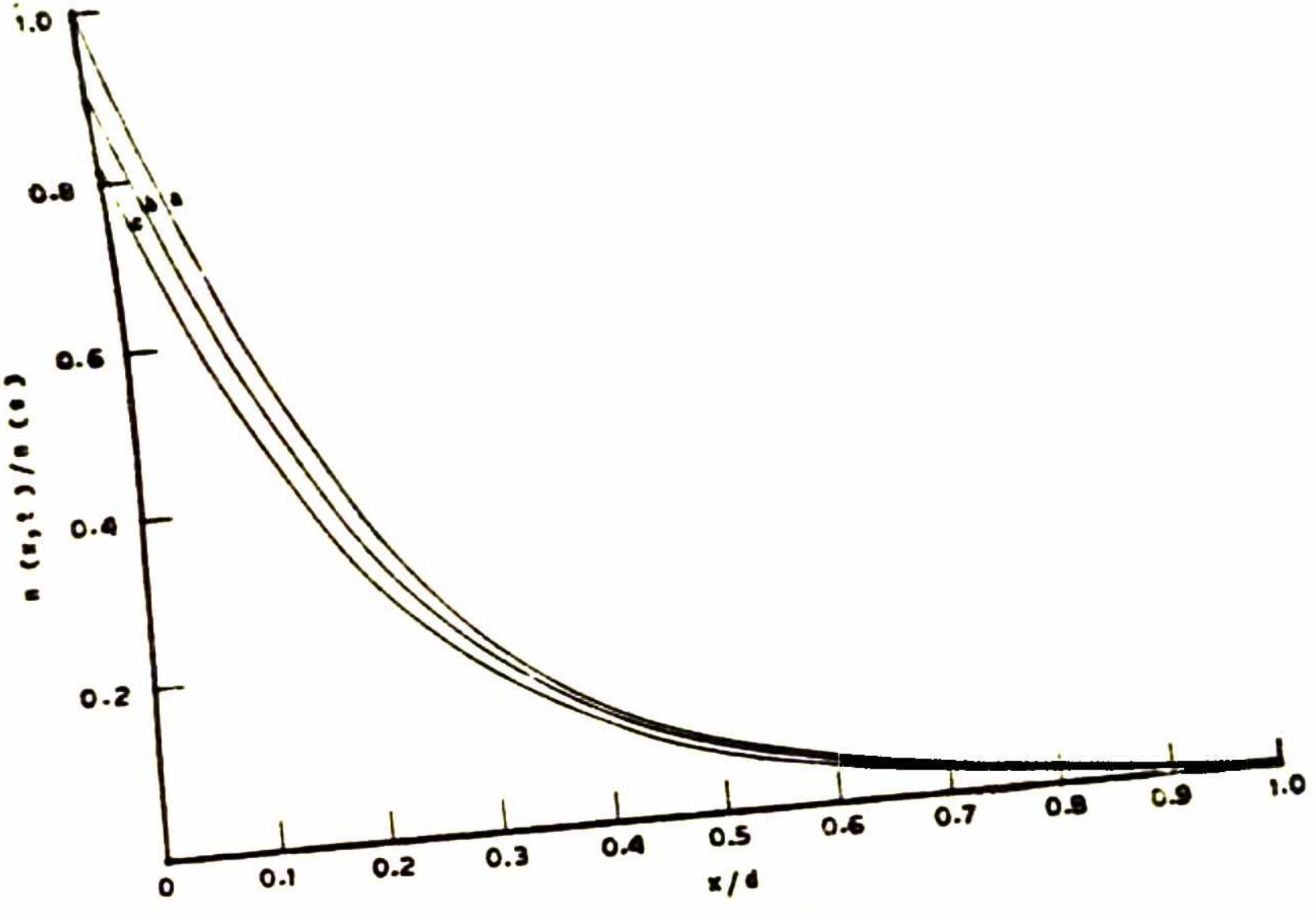

FIG. 2.3

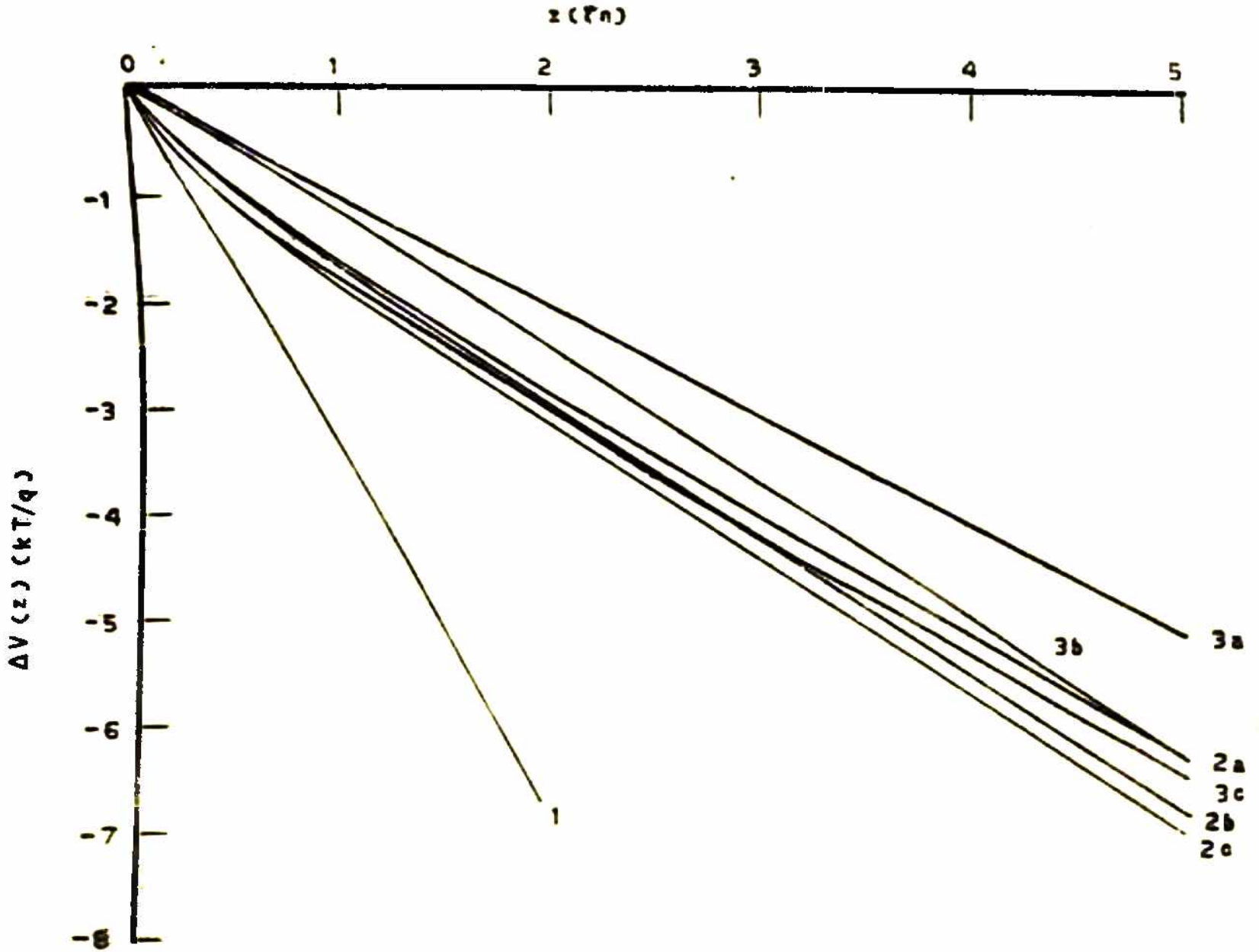

FIG. 2.4

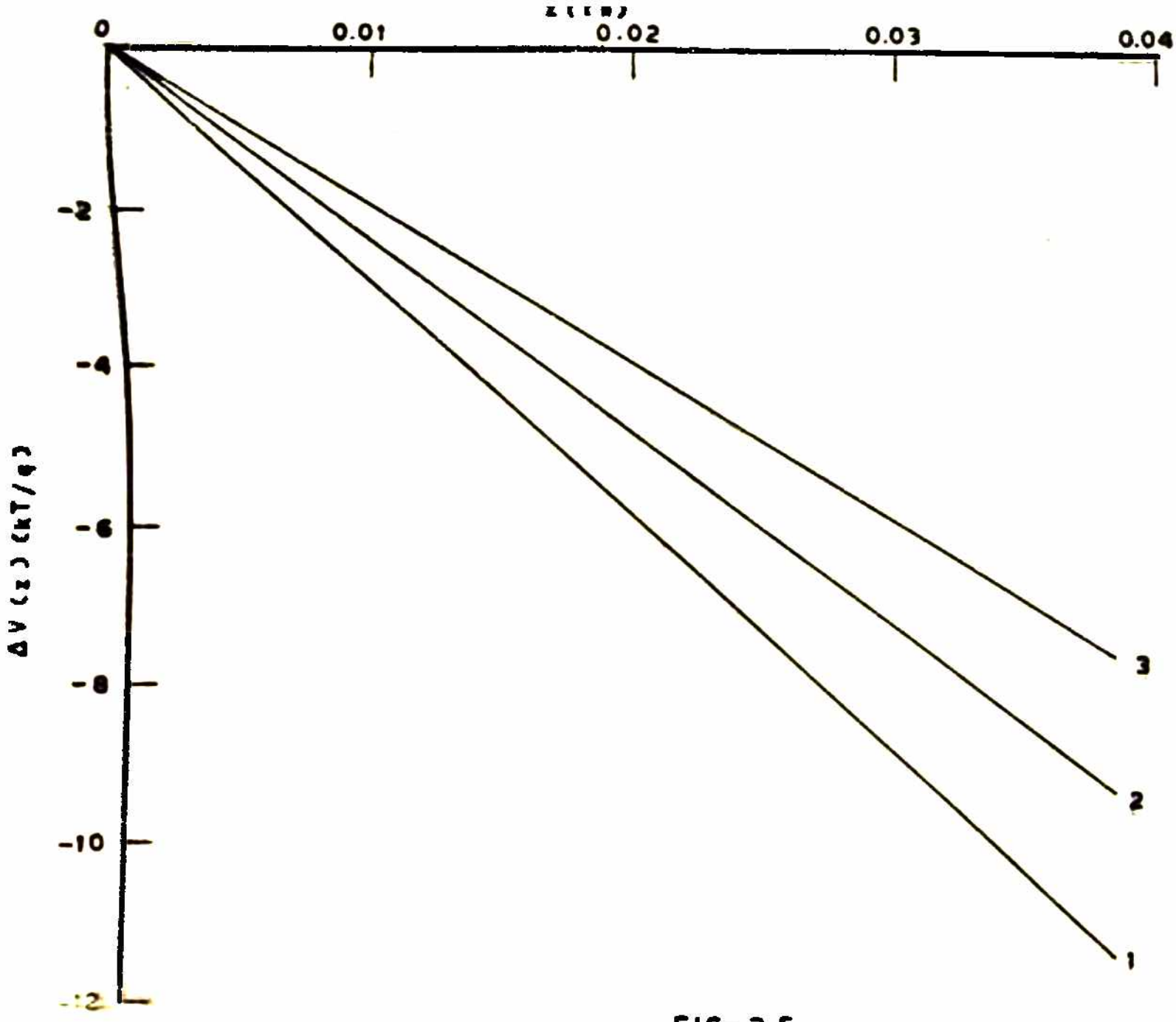

FIG. 2.5

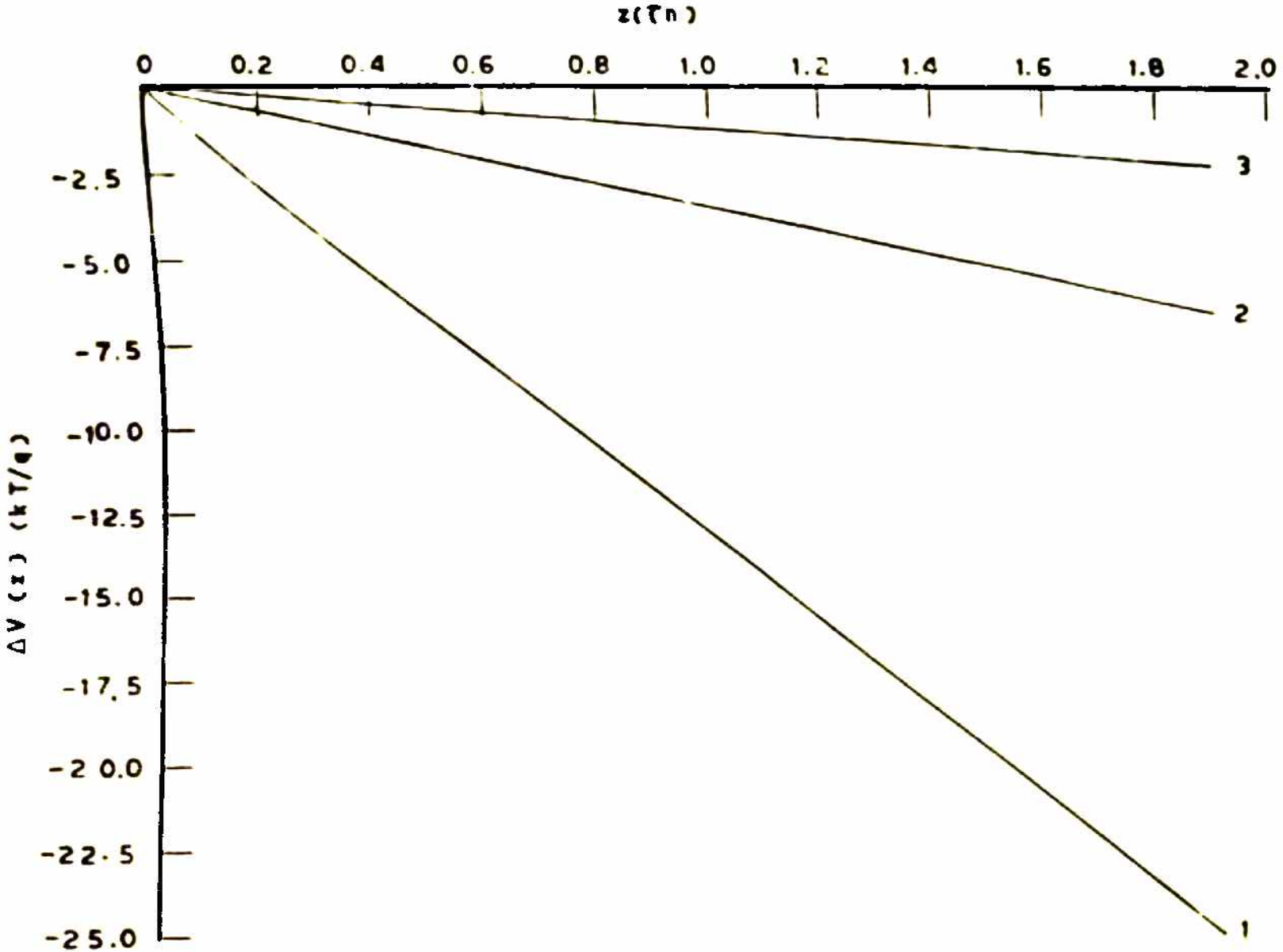
z(Tn)
0
0.2
0.4
0.6
0.8
1.0
1.2
1.4
1.6
1.8
2.0
-2.5
-5.0
-7.5
-10.0
-12.5
-15.0
-17.5
-20.0
-22.5
-25.0
ΔV (x) (kT/q)
1
2
3

FIG. 2.6

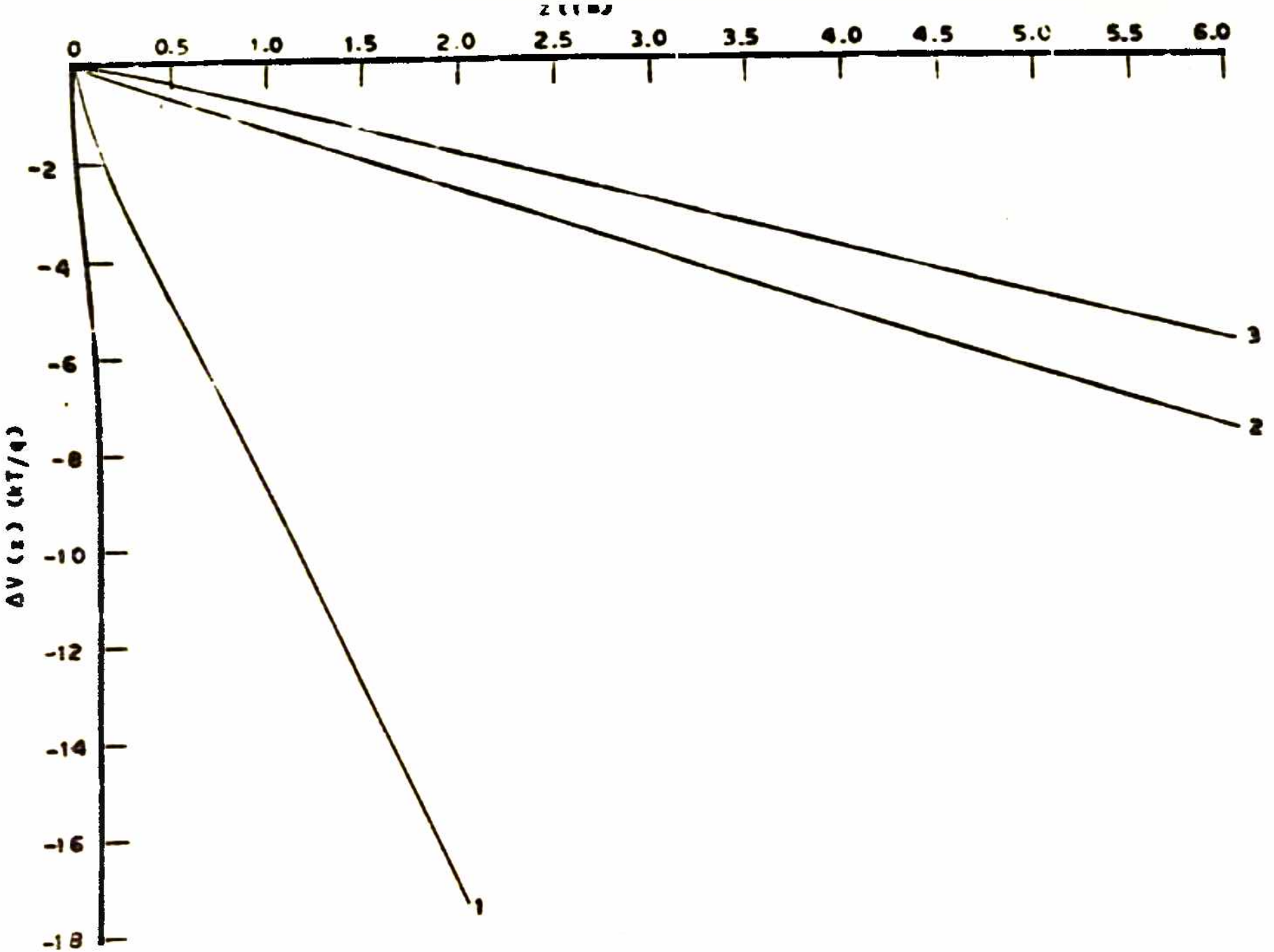

FIG. 2.3

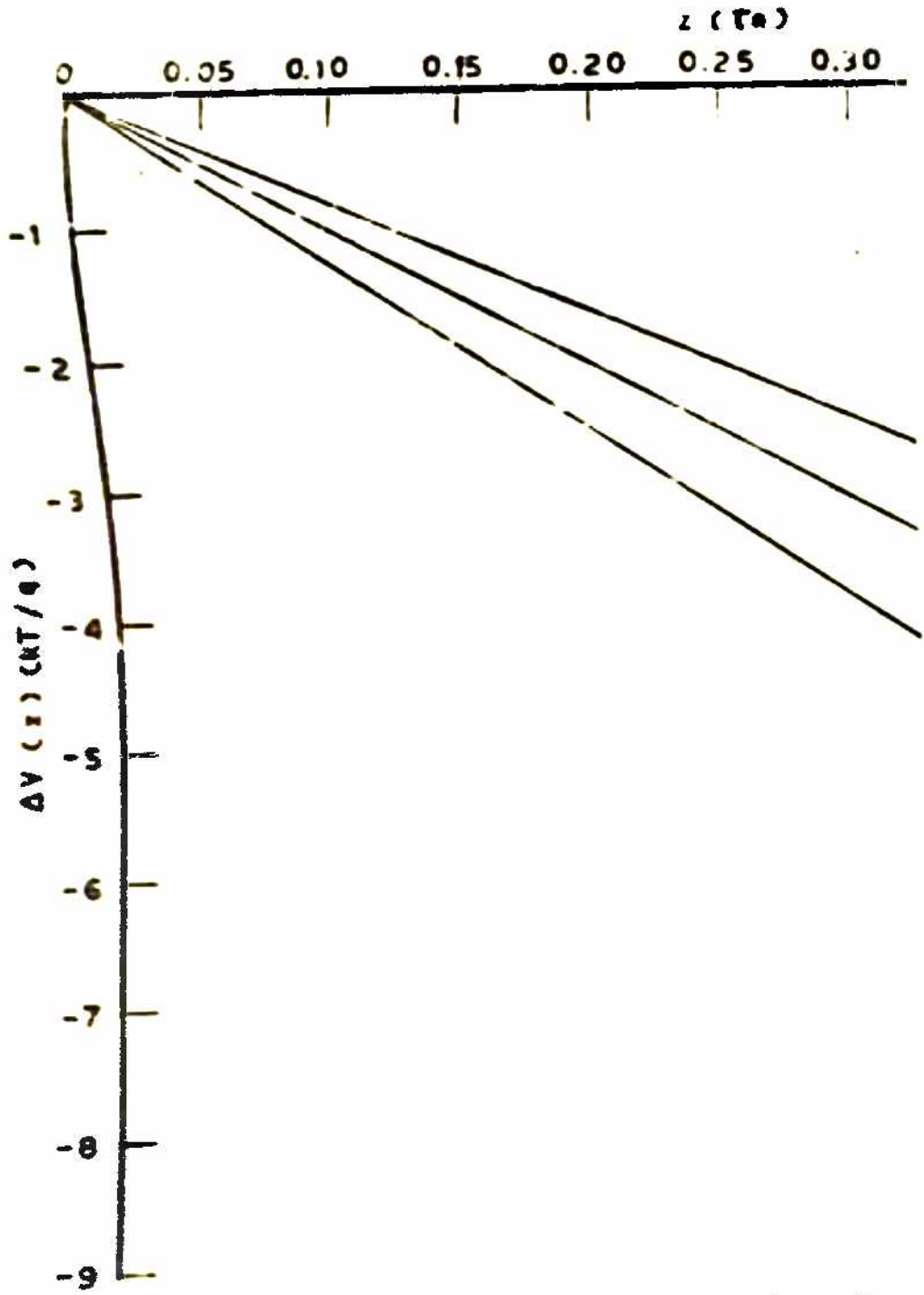

FIG. 2.8

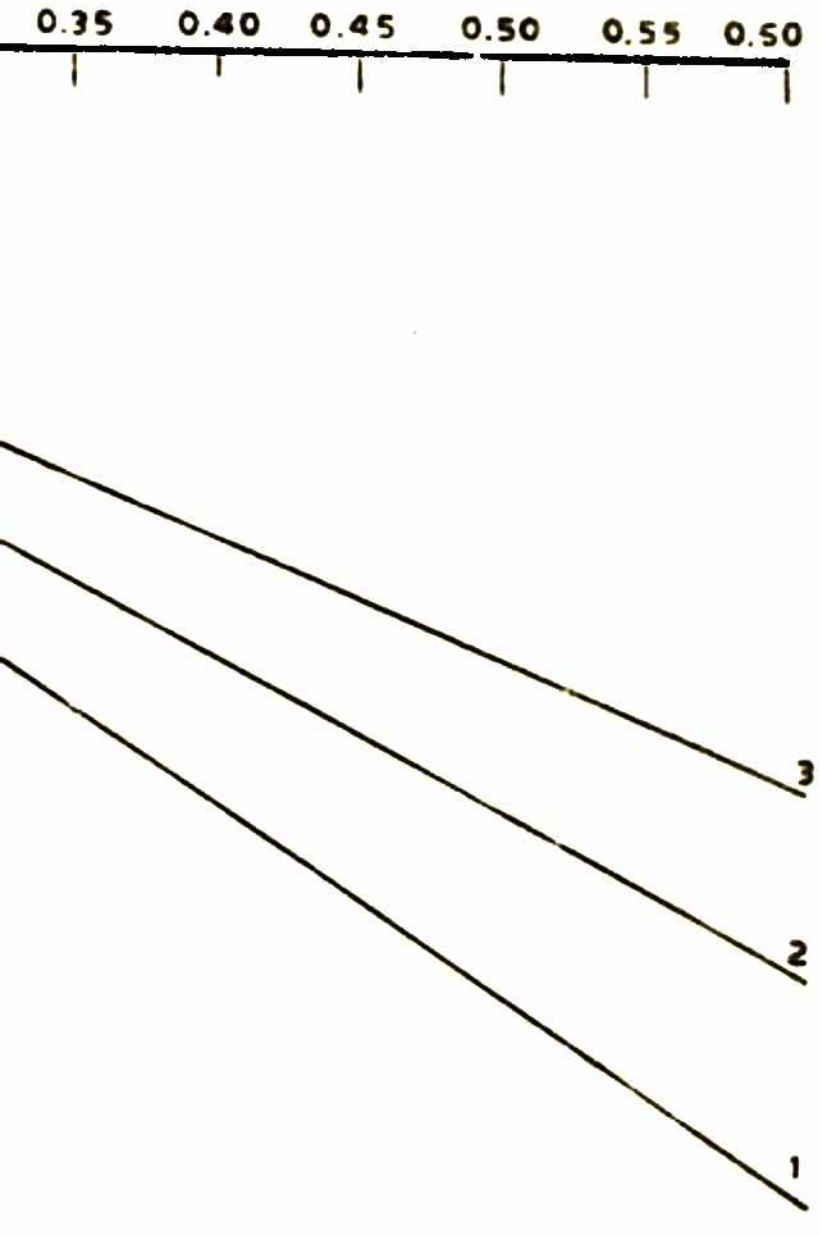
0.35
0.40
0.45
0.50
0.55
0.50
3
2
1

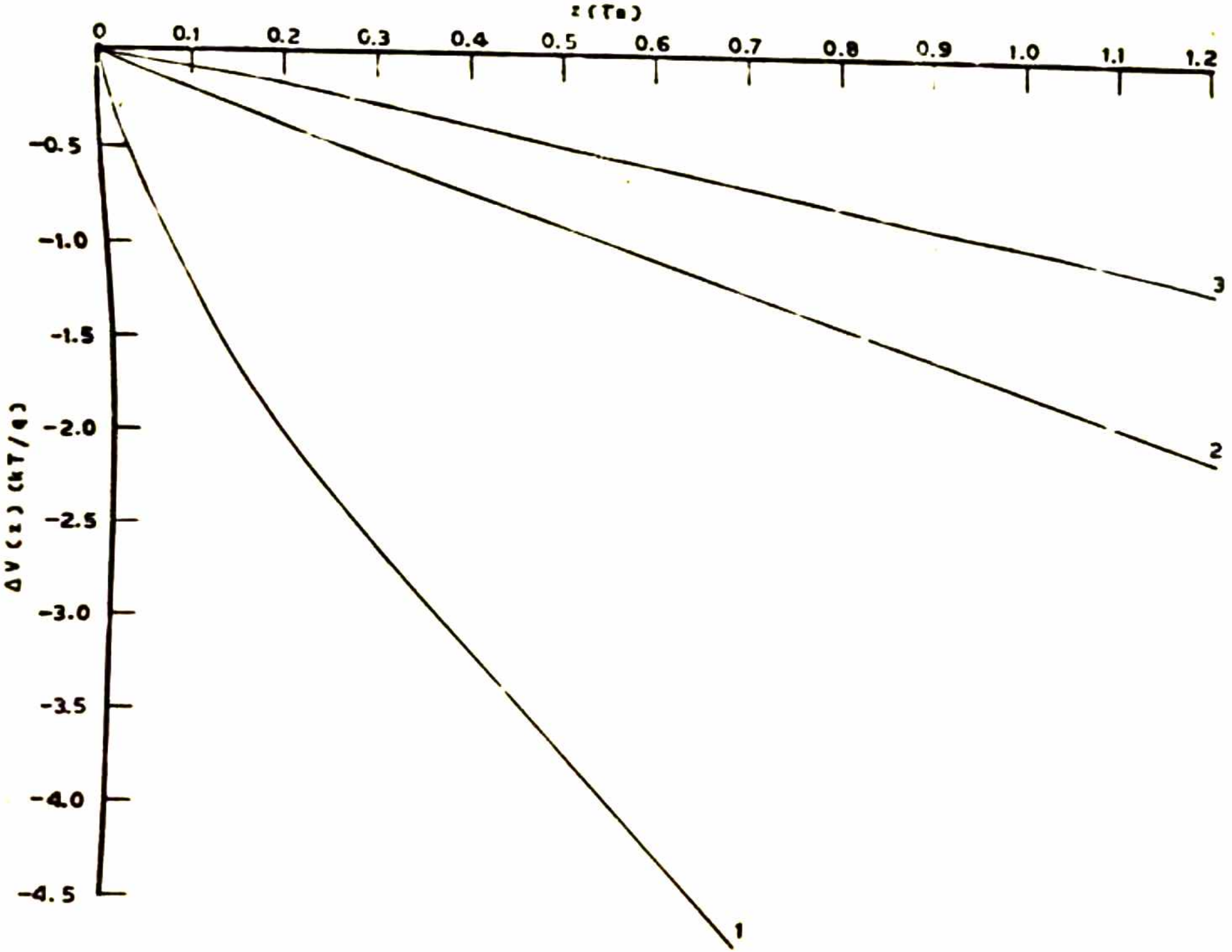
z (Ta)
0
0.1
0.2
0.3
0.4
0.5
0.6
0.7
0.8
0.9
1.0
1.1
1.2
-0.5
-1.0
-1.5
-2.0
-2.5
-3.0
-3.5
-4.0
-4.5
ΔV (z) (kT/e)
1
2
3

FIG. 2.9

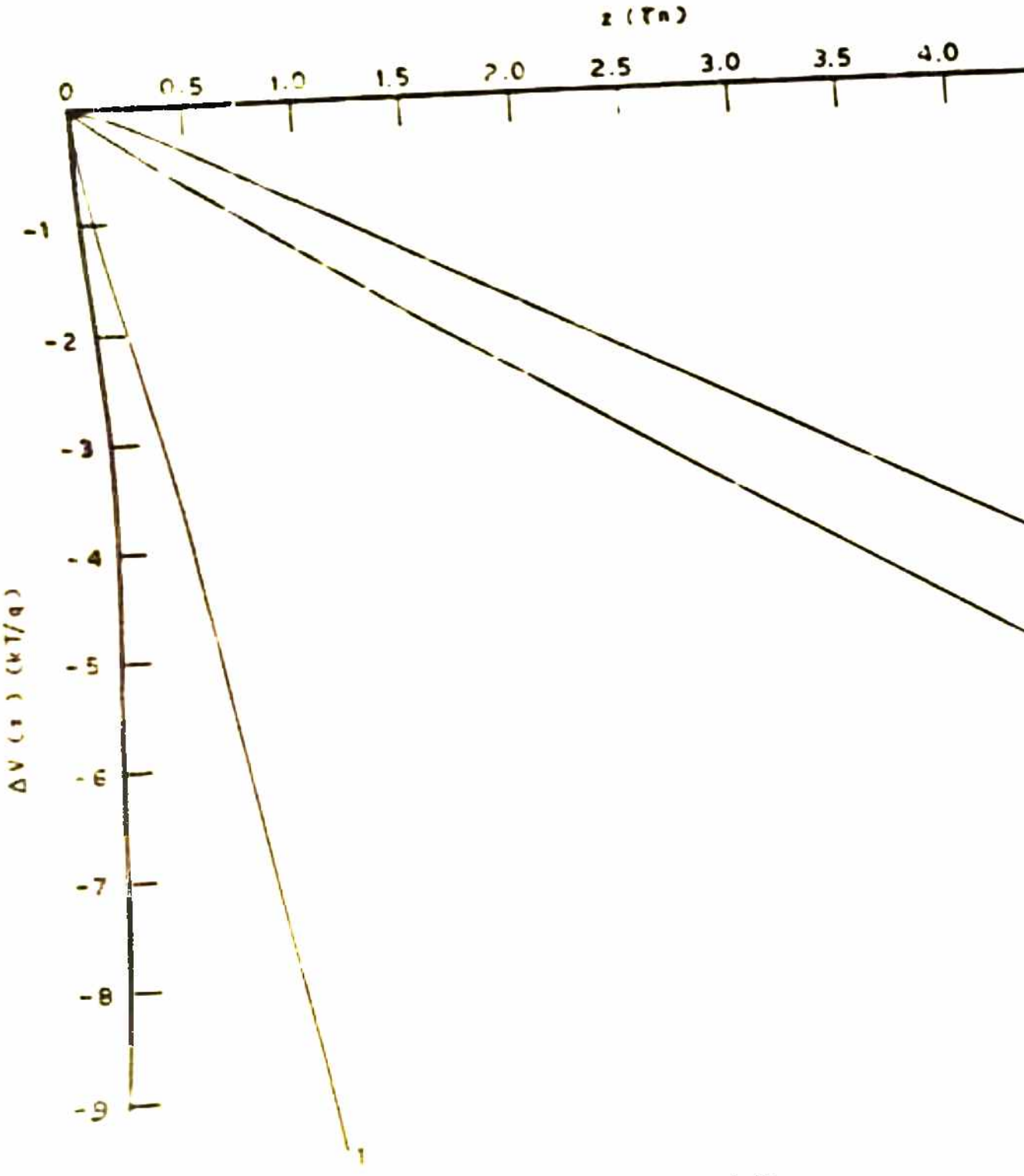

FIG. 2.10

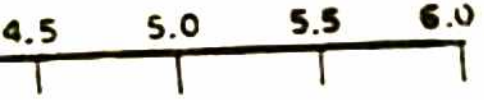
4.5
5.0
5.5
6.0

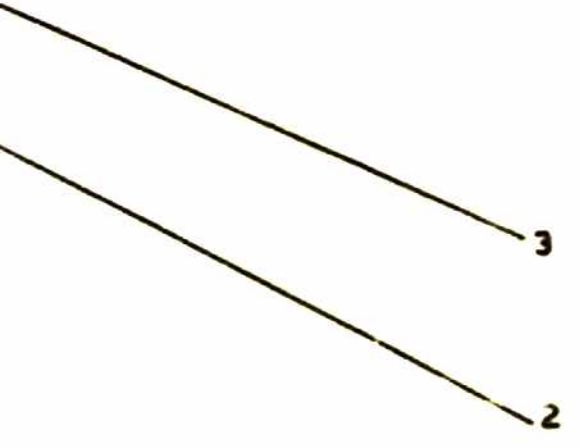
3
2

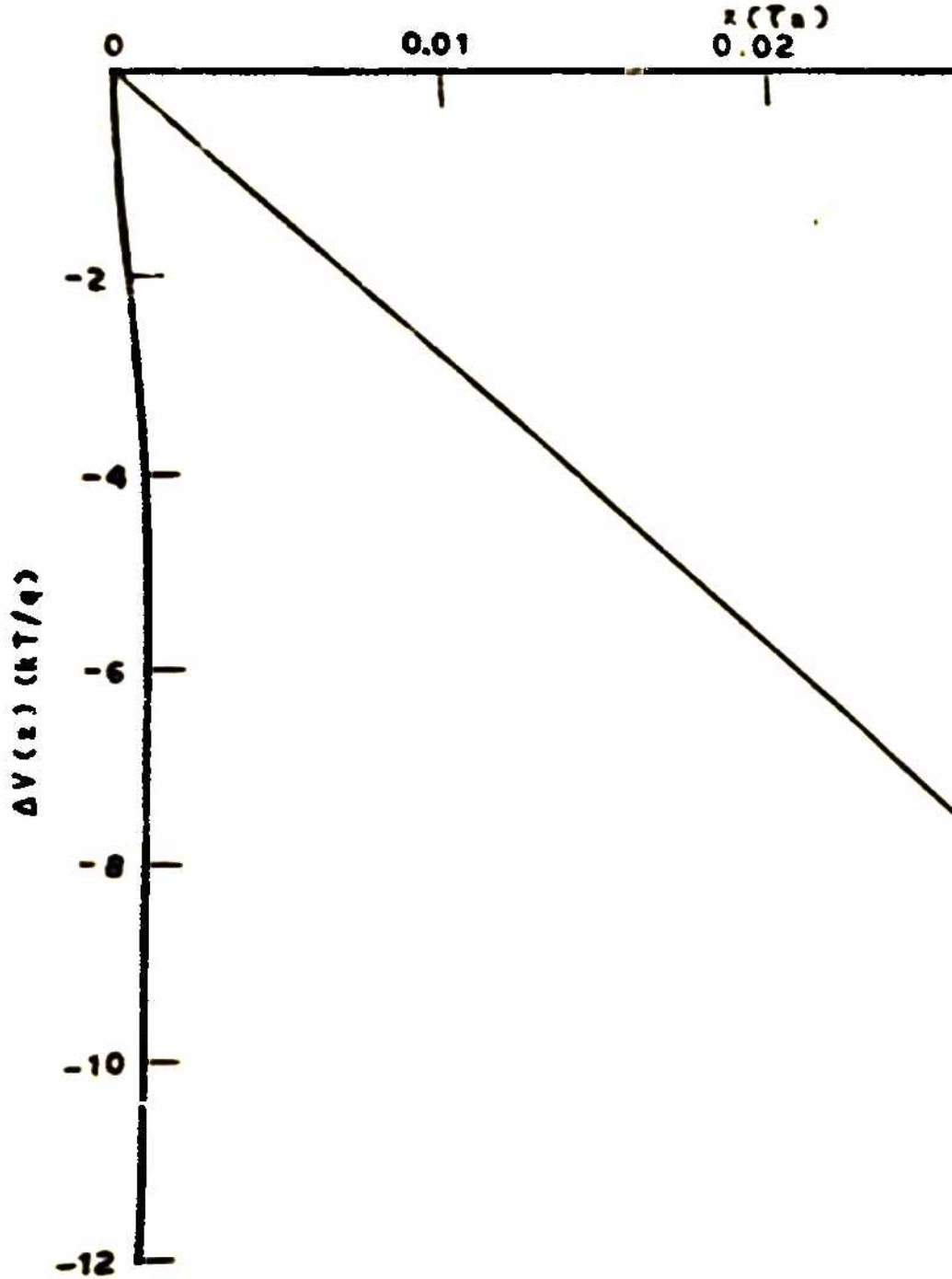

FIG. 2.11

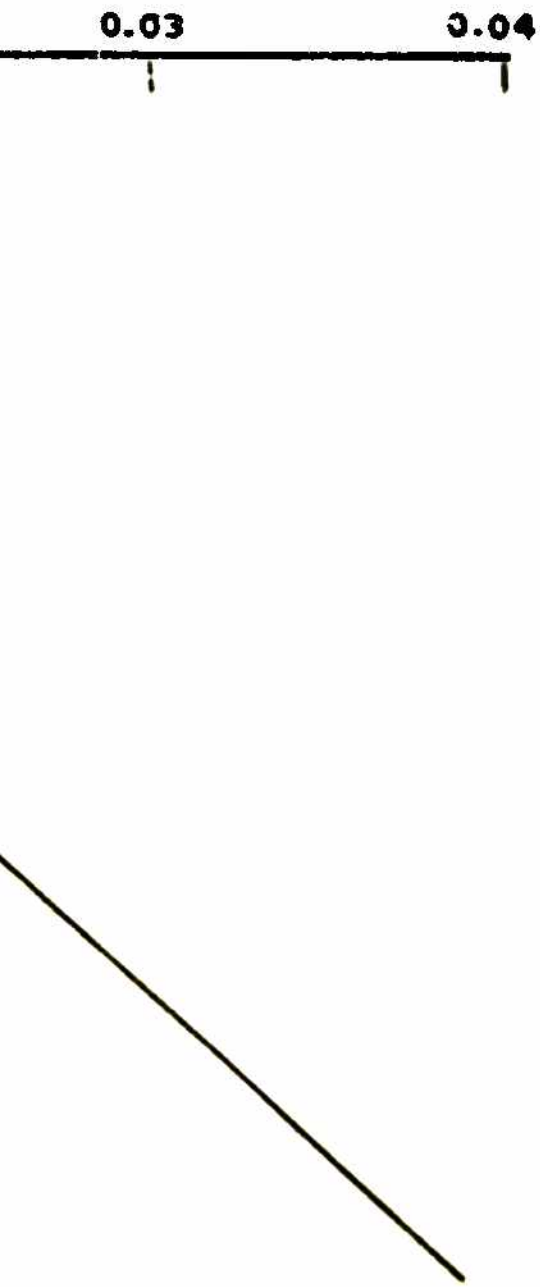
0.03
0.04

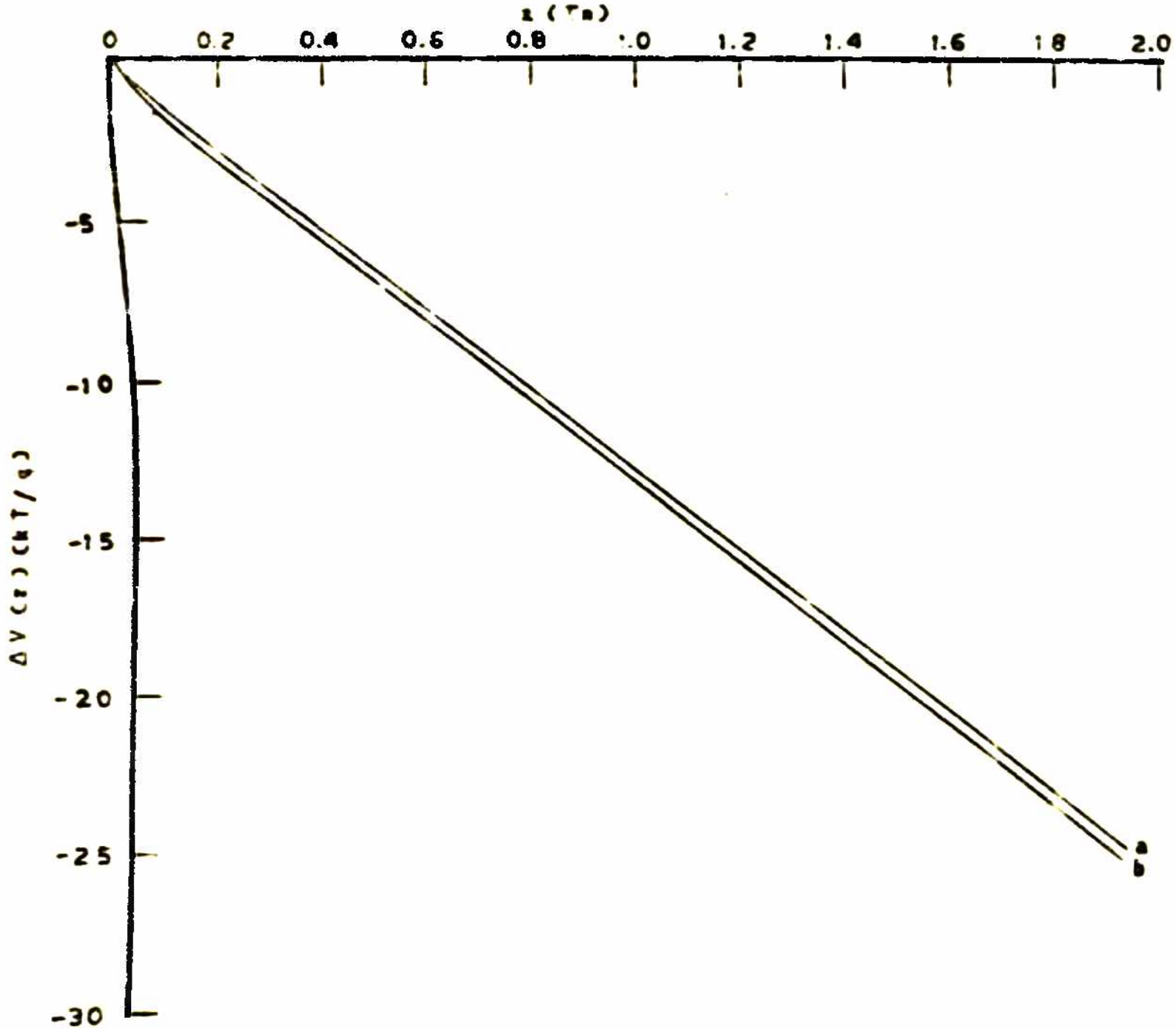

FIG. 2.12

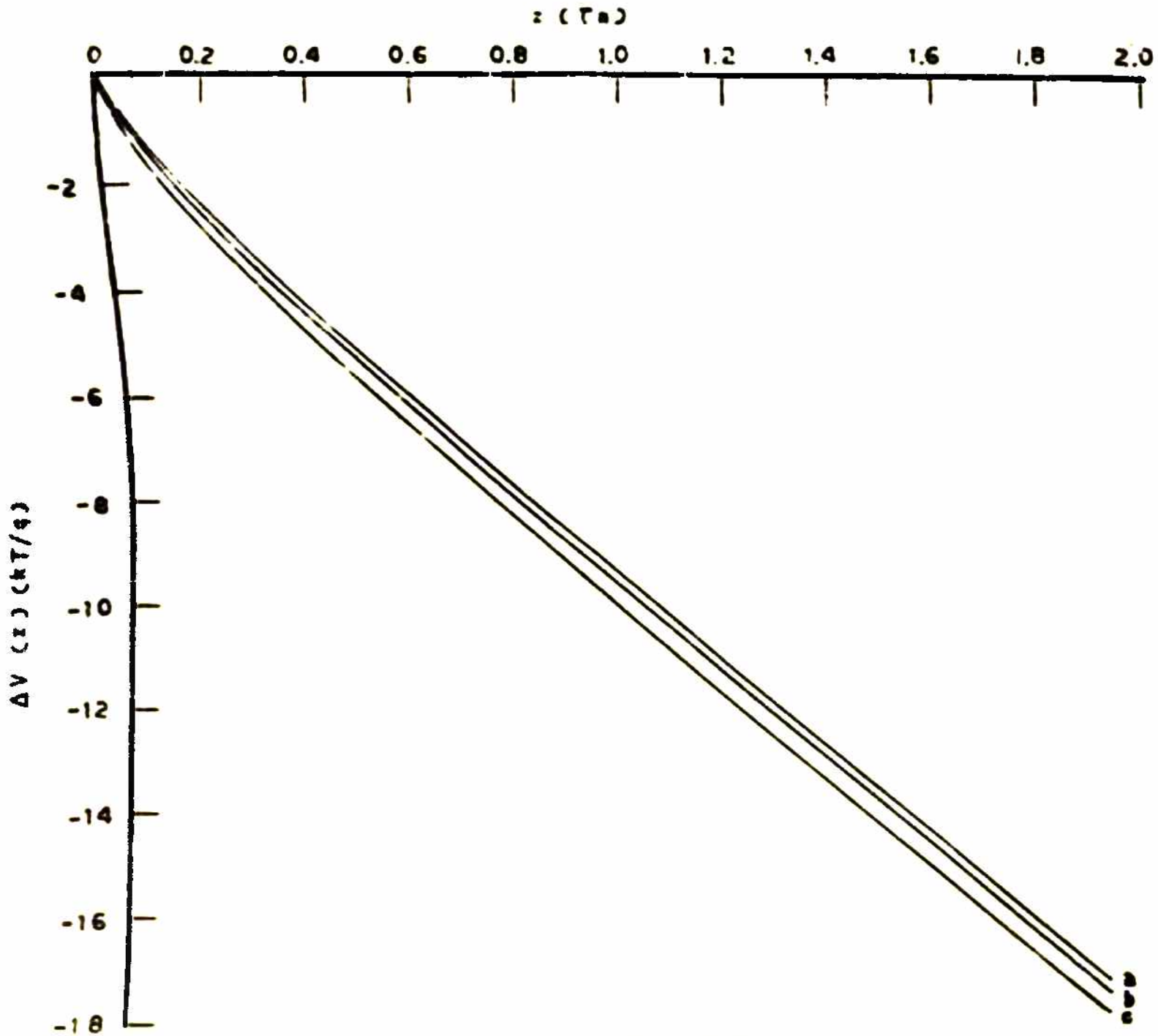

FIG. 2.13

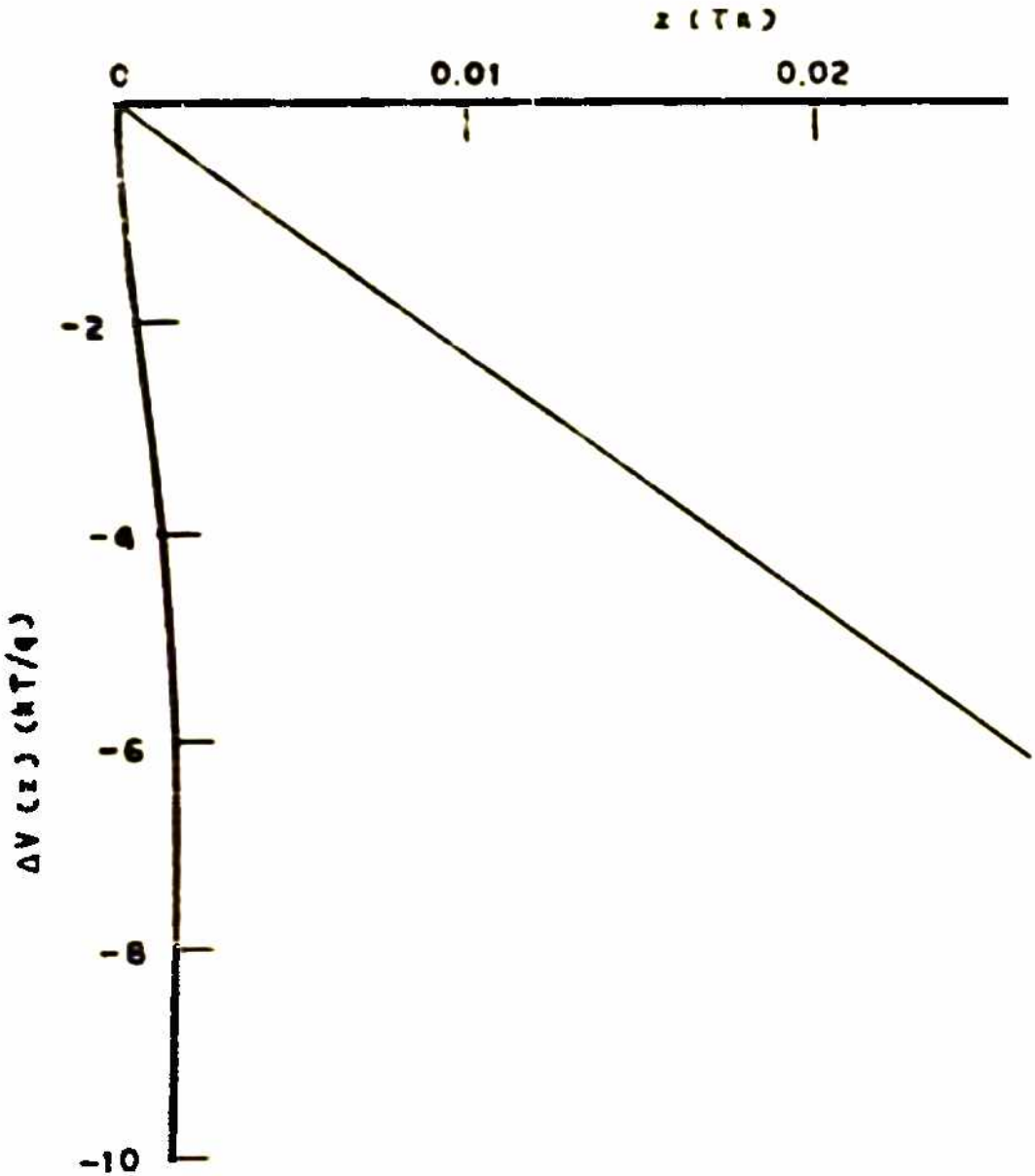

FIG. 2.14


0.03
0.04

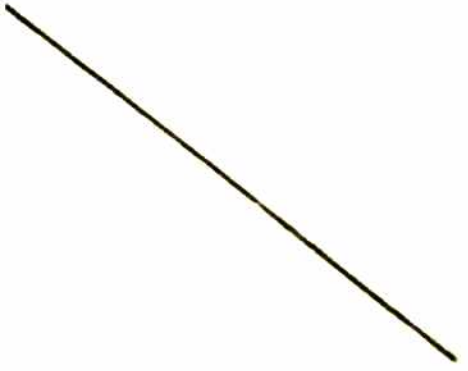

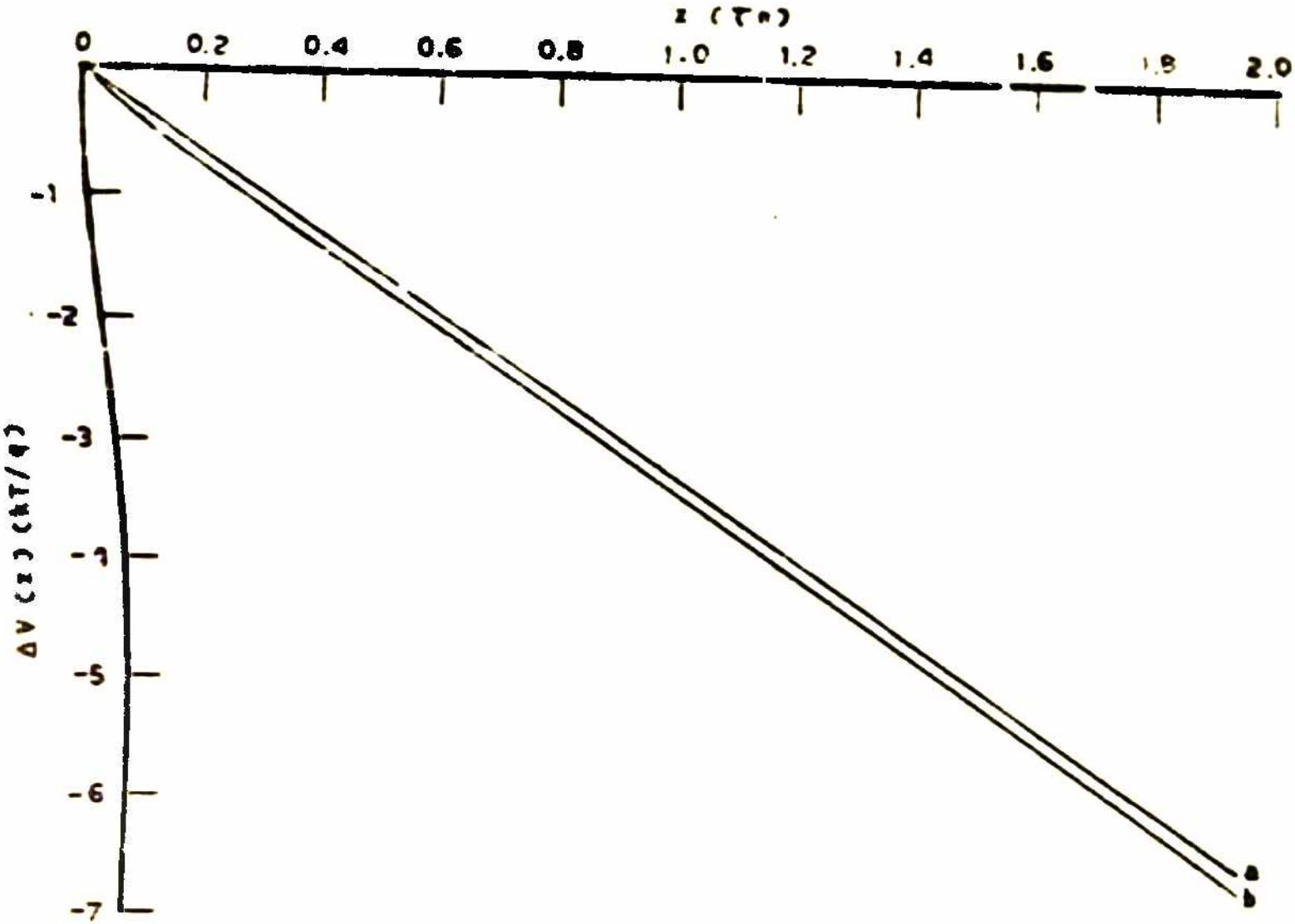

FIG. 2.15

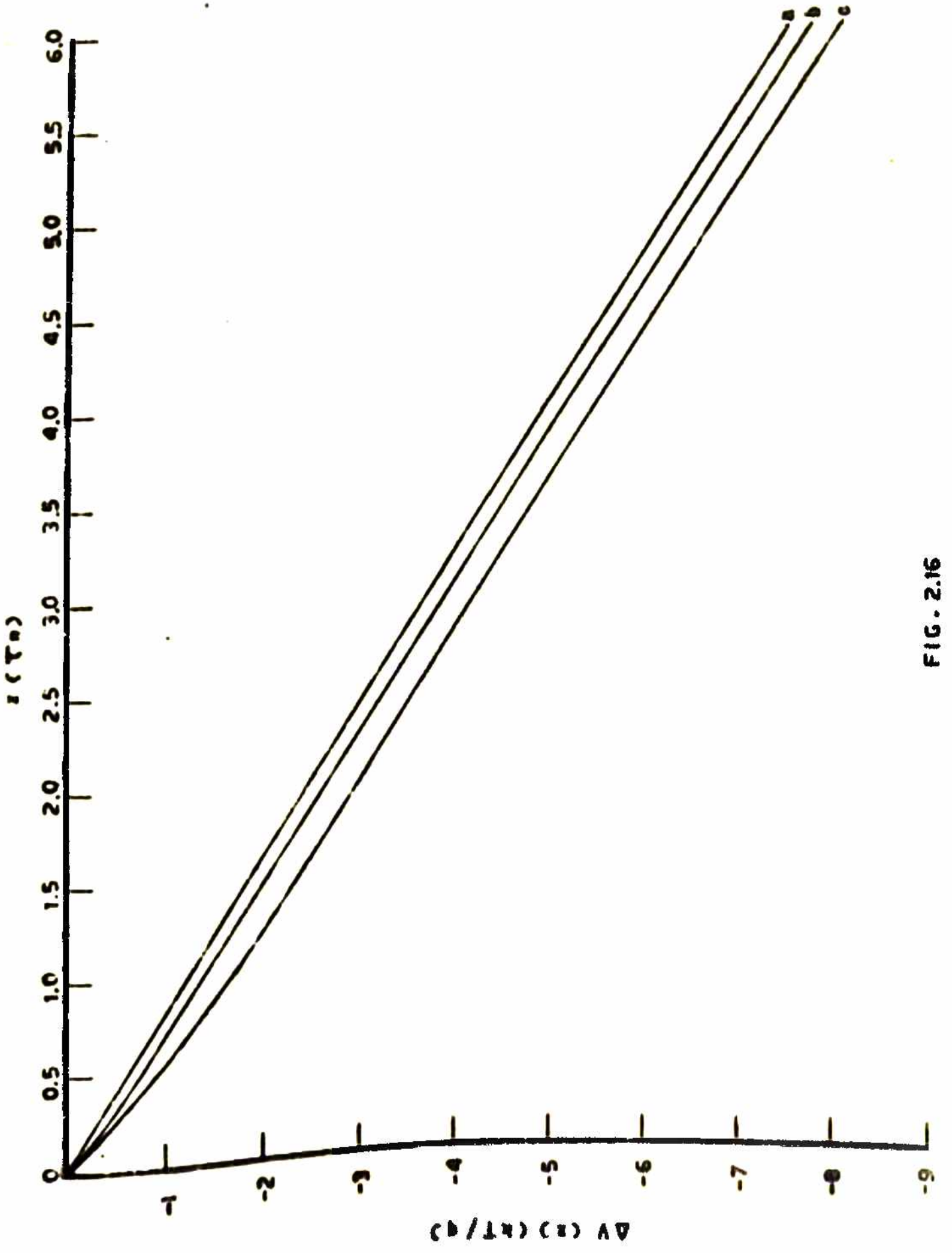

FIG. 2.16

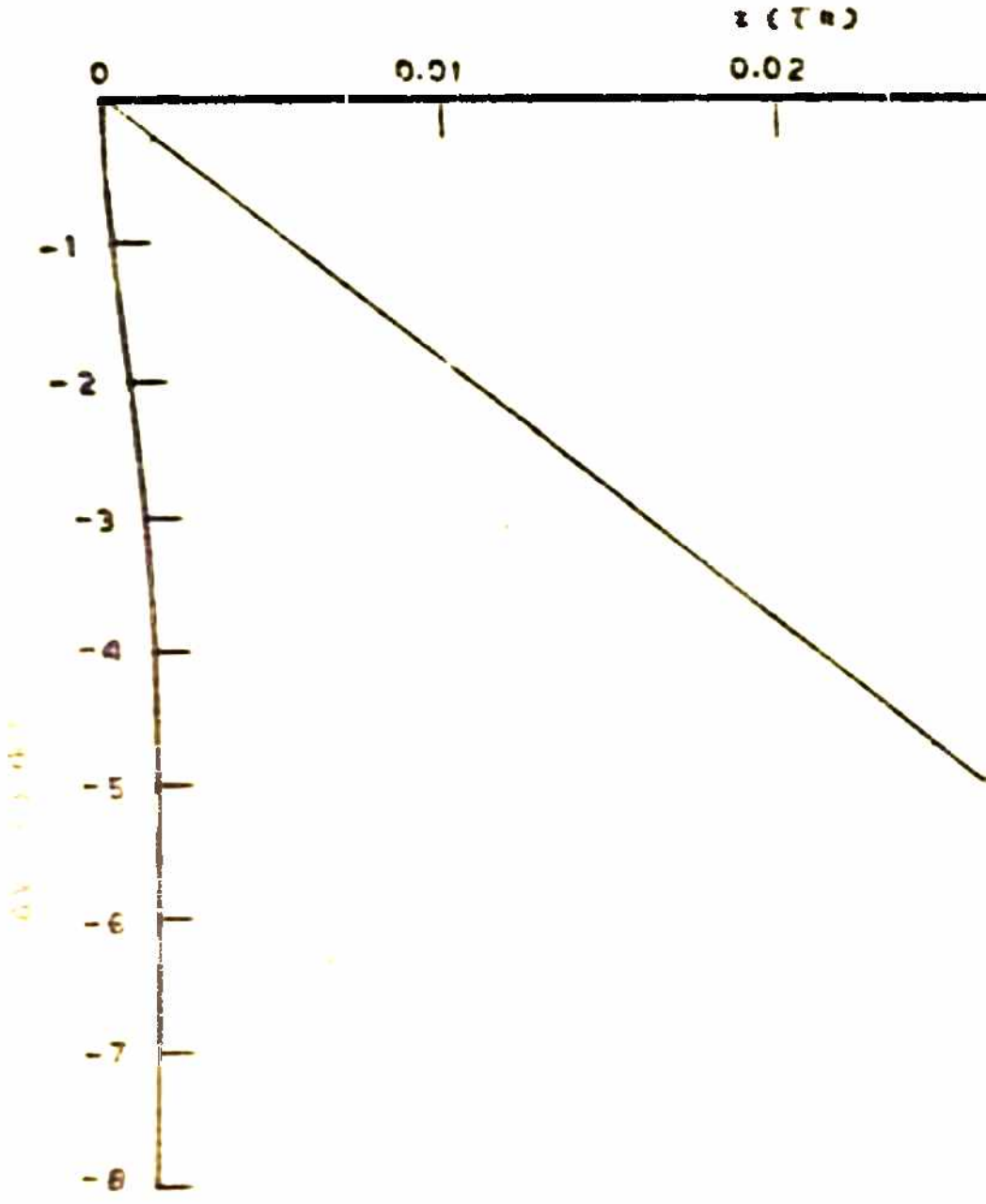

FIG. 7.17

0.03
0.04

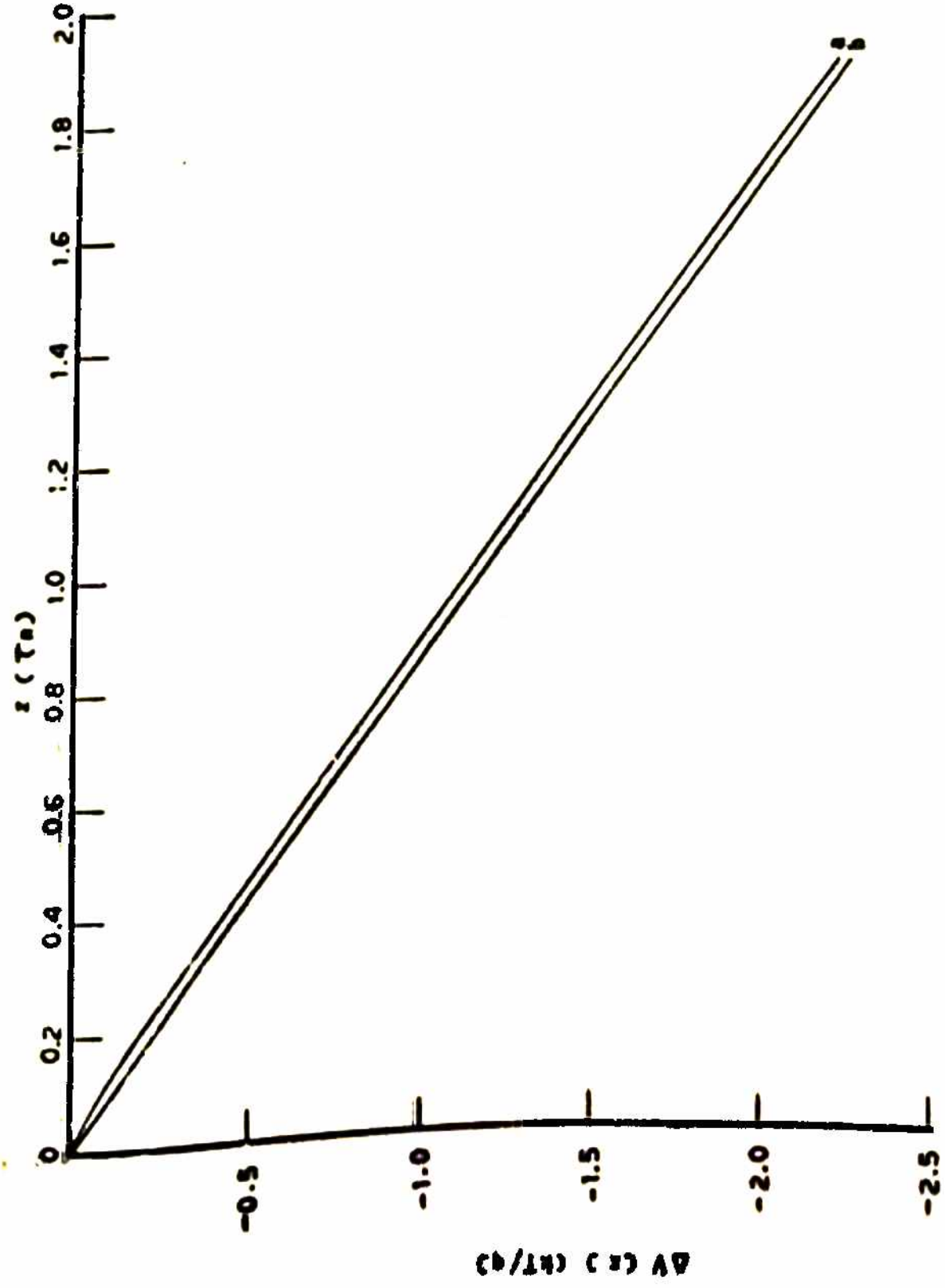

FIG. 2.18

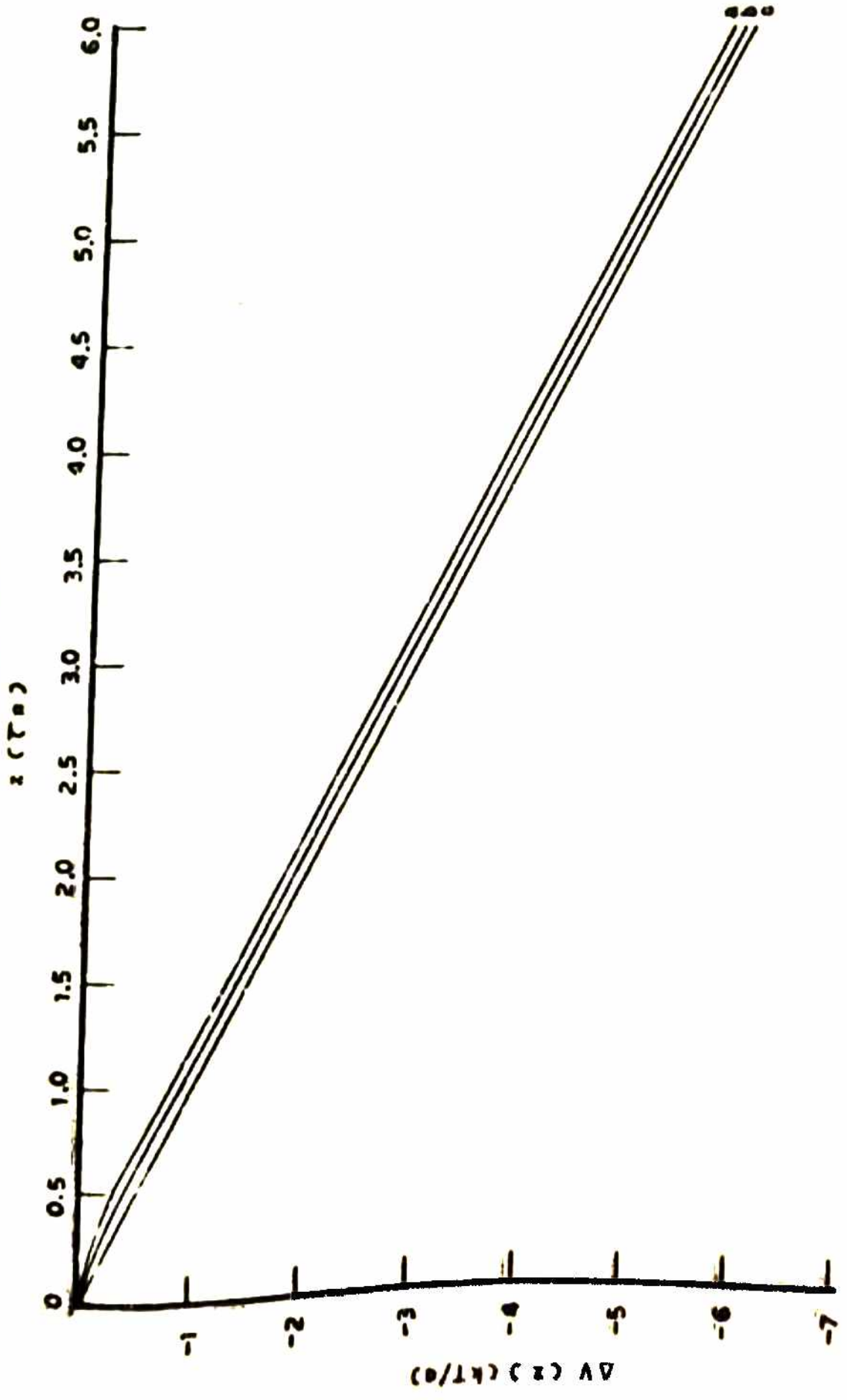

FIG. 2.19

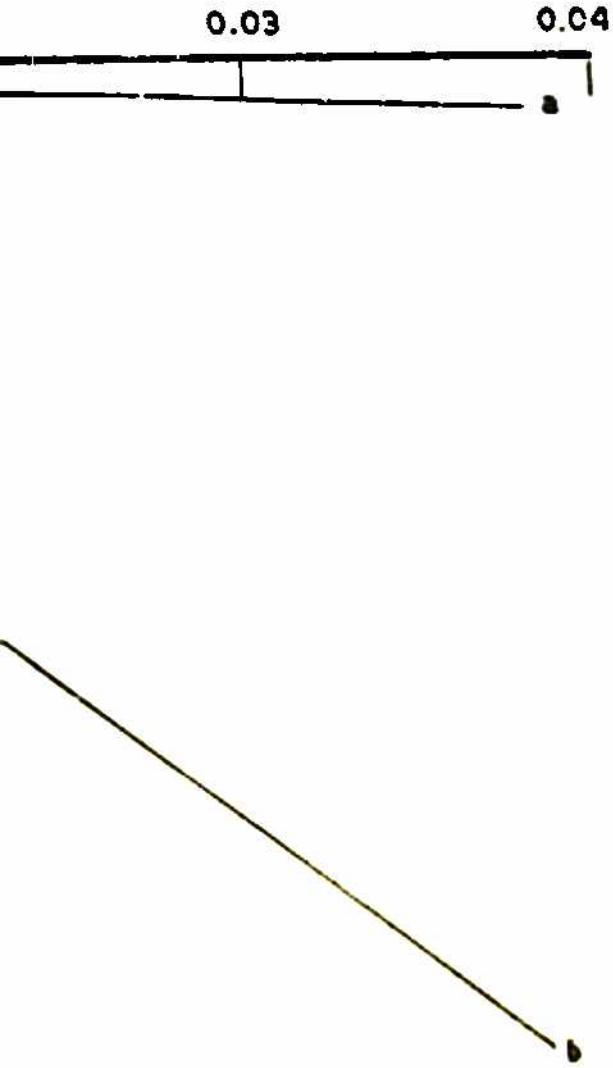

2.20

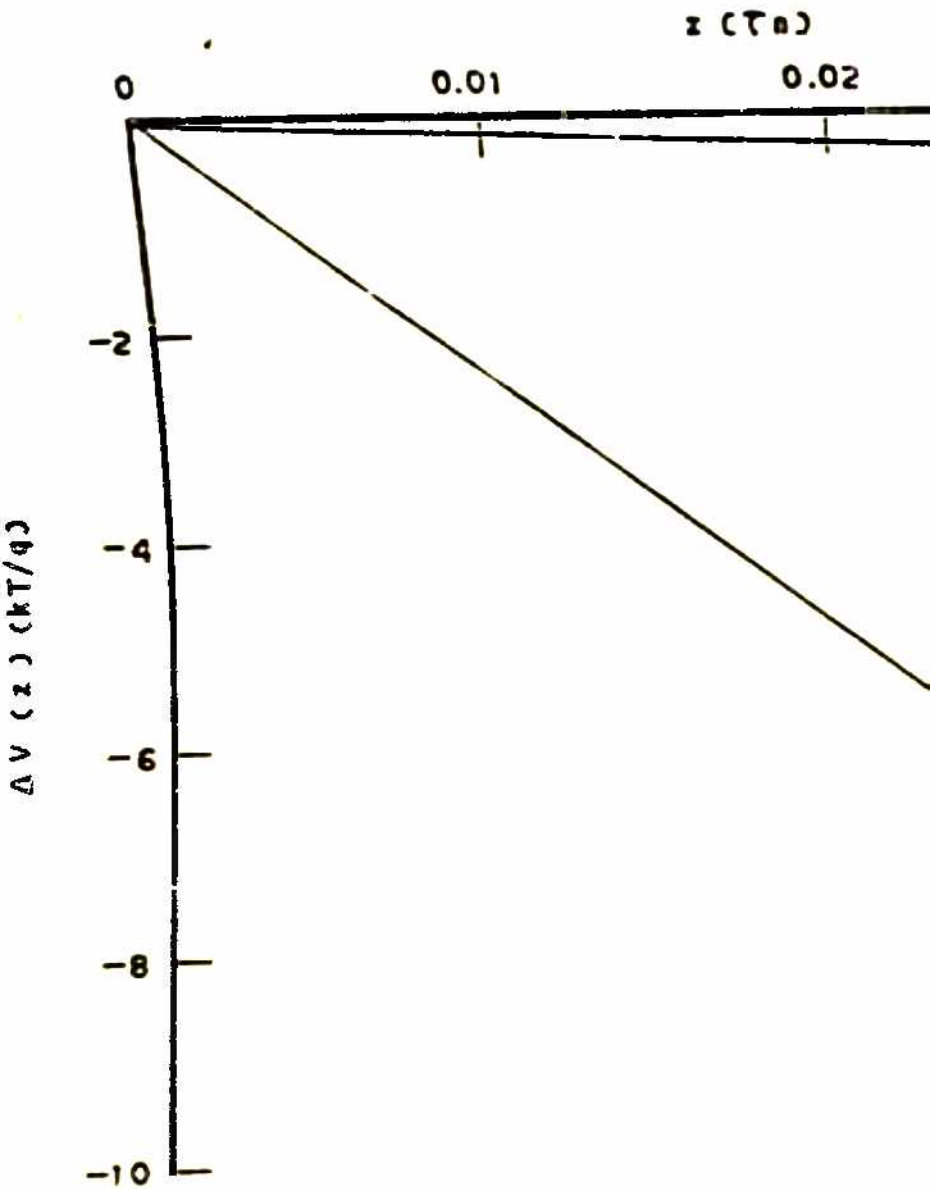

FIG.

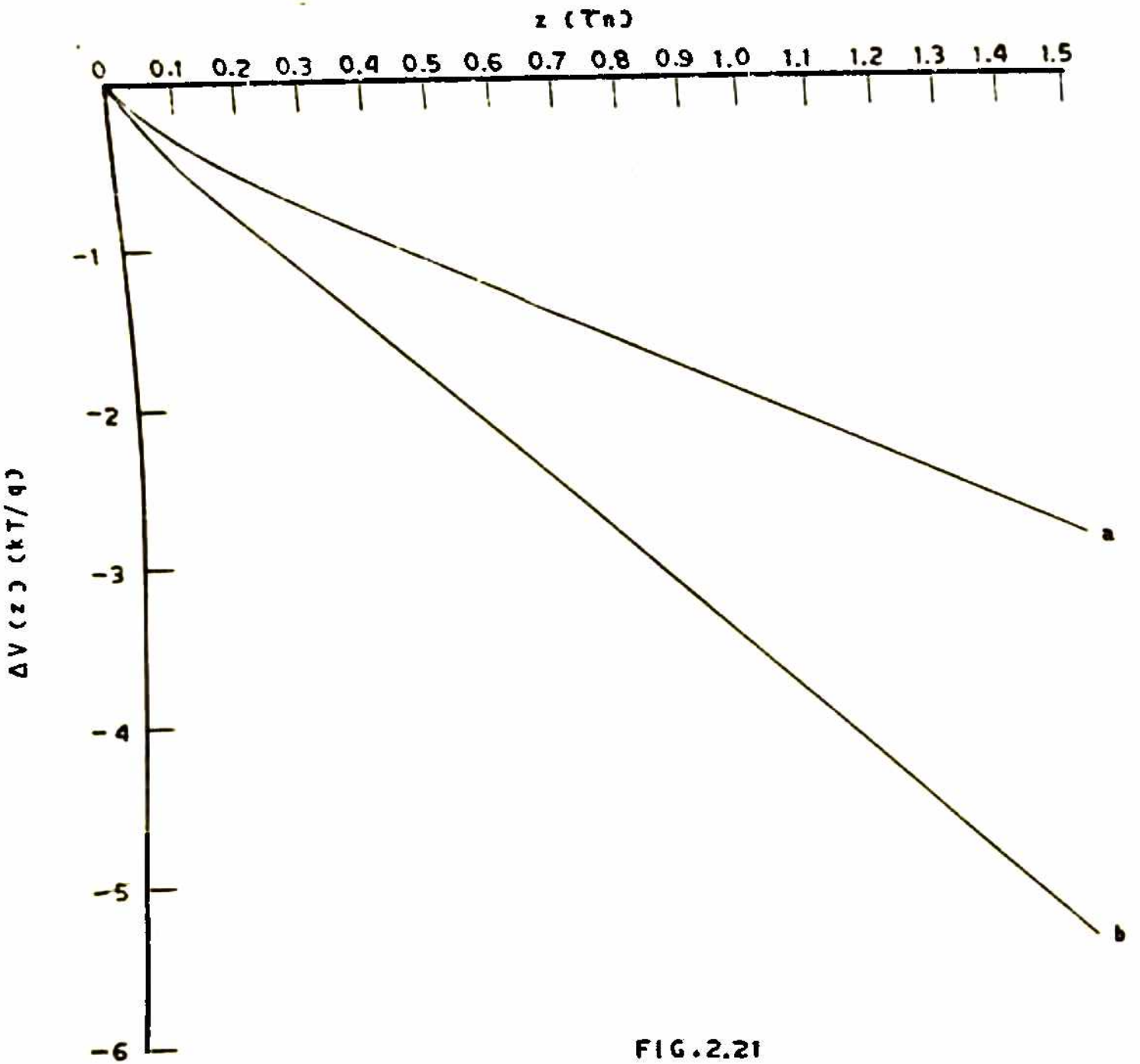

FIG.2.21

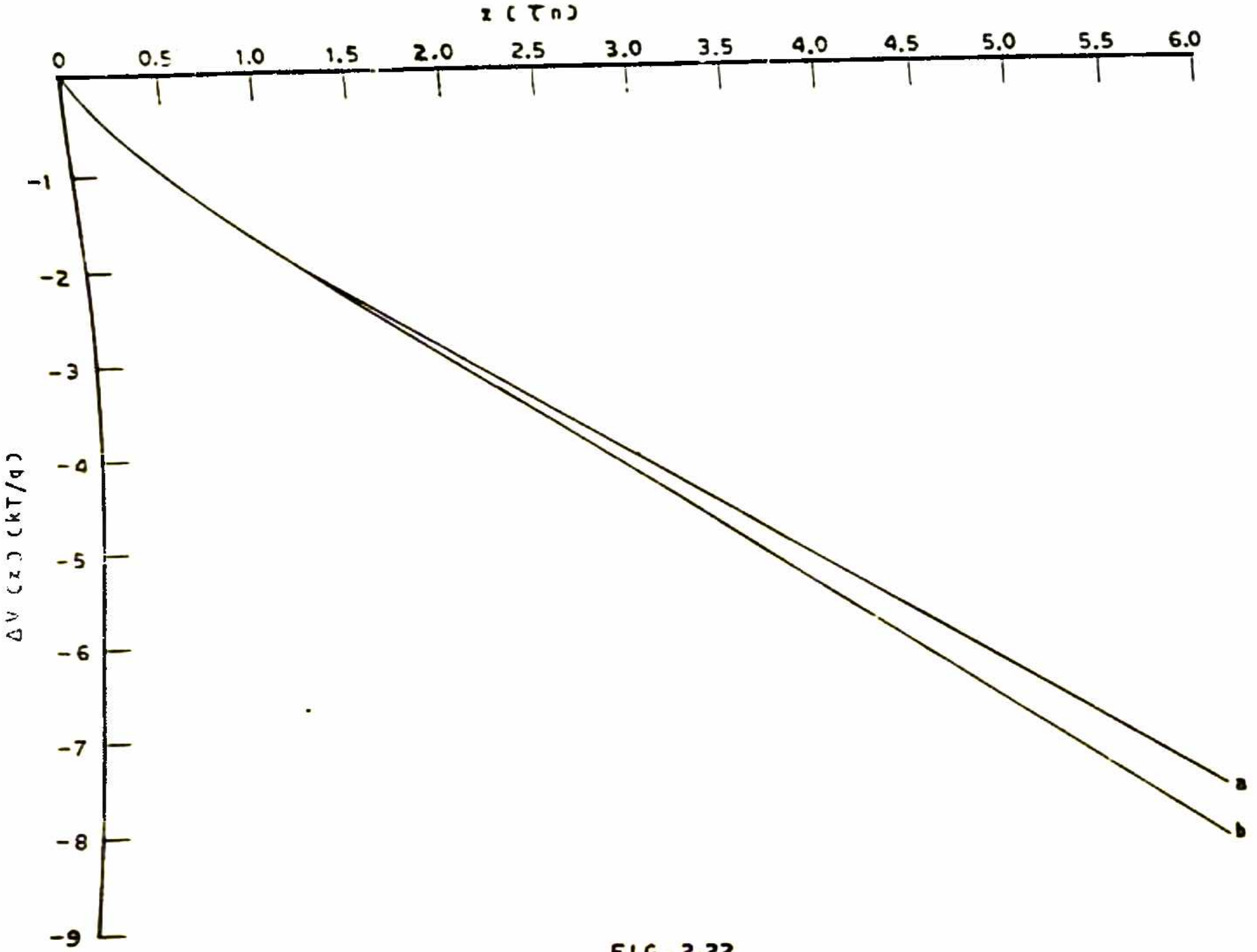

FIG. 2.22

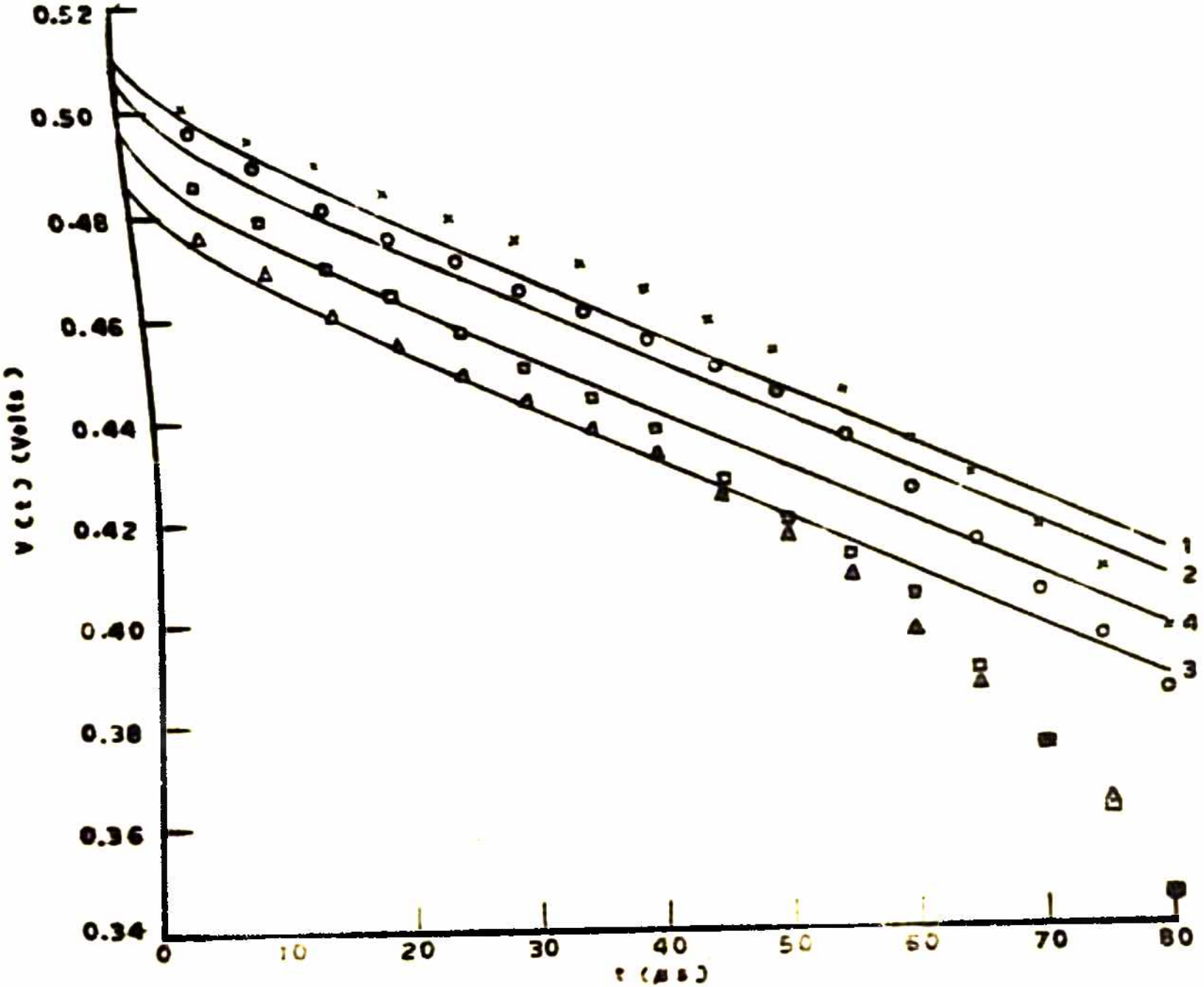
0.52
0.50
0.48
0.46
0.44
0.42
0.40
0.38
0.36
0.34
V (t) (Volts)
0
10
20
30
40
50
60
70
80
t (μs)
1
2
4
3

FIG. 2.23

50
60
70
80
3
4
2
1

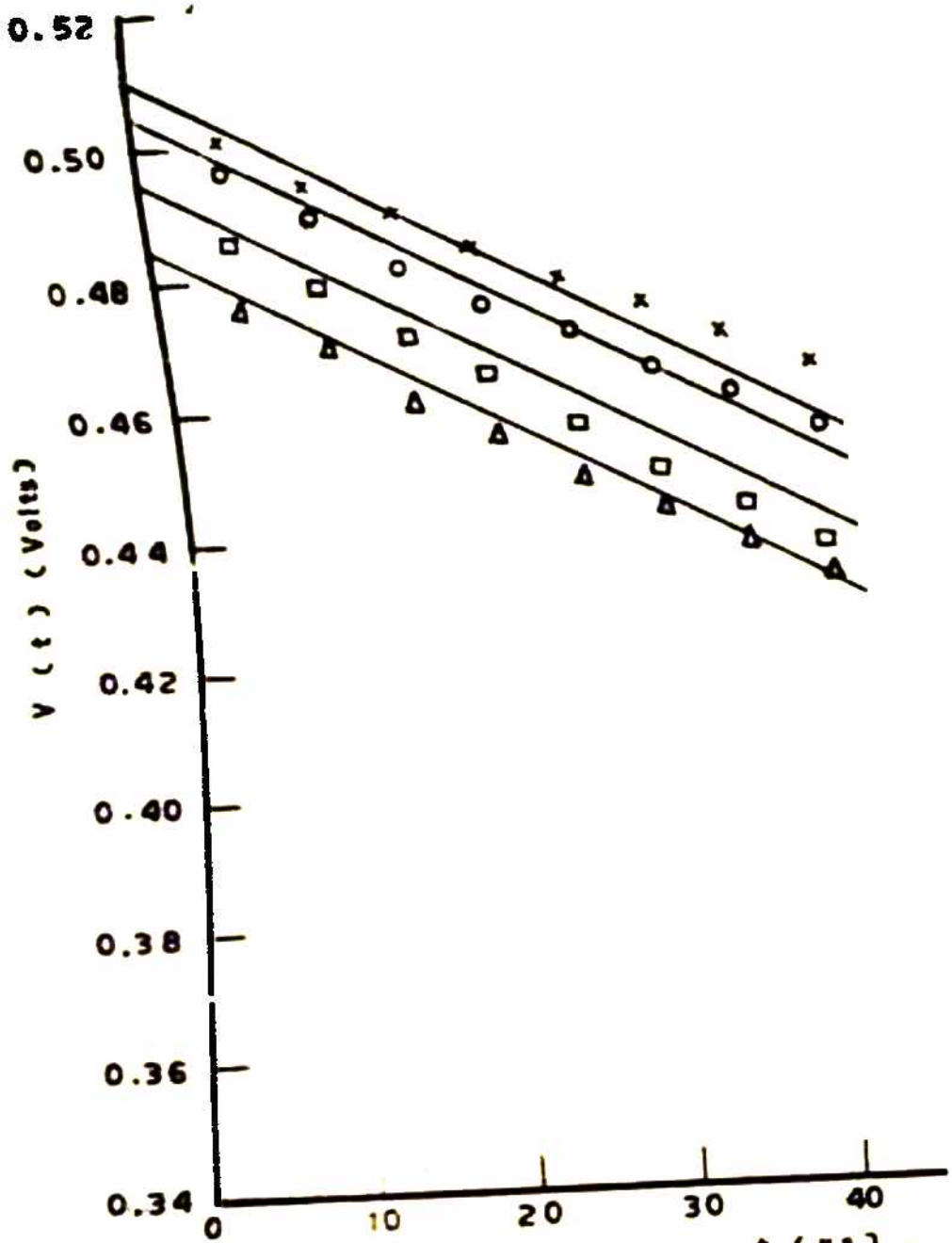

FIG. 2.24

CHAPTER 3

EFFECT OF pn COUPLING ON STEADY-STATE RESPONSE OF A SOLAR CELL

3.1. Introduction

The theory presented in the last chapter is based on the assumption that the contribution of the diffused layer and its coupling with base to the solar cell response is negligible, and thus considered only the base. This is justified in many cases because the thermal equilibrium concentration of minority carriers in the diffused layer is much smaller than that in the base. However as described in section 1.5, in modern n^+p (or p^+n) solar cells, the heavy doping in the diffused layer causes band gap narrowing which increases the thermal minority carrier concentration in the diffused layer so much that it becomes comparable to or even exceed that in the base. In such cases the diffused layer makes an important contribution to the steady-state as well as transient response of the solar cell.

Recent experimental results of Fossum et. al. (1979) on the sensitivity of the steady-state open circuit photovoltage of a solar cell to its surface treatment clearly show

the importance of the contribution of the diffused layer. Fossum et. al. (1979) have analysed their results on the basis of a simple model in which they have neglected the contribution of the base to the dark saturation current and the contribution of the diffused layer to the generation current. In this chapter we present a more rigorous theory which accounts for the pn coupling and includes the contributions of both the diffused layer as well as the base.

In this thesis our main interest is to investigate the transient response of the cell i.e. when the light has been switched off. However, the transient calculations require a prior knowledge of the steady-state calculations. In view of this in this chapter we have studied the effect of pn coupling on the steady-state response of the solar cell in as much as it is applicable to the transient response presented in the next chapter.

In the theory given in this chapter we have modelled the front (illuminated) surface of the solar cell by using the Tewary and Jain (1980) boundary condition which accounts for the recombination as well as generation of carriers at the surface. The dependence of short-circuit current and open circuit photovoltage of an n^+p solar cell on the absorption coefficient of light, surface recombination velocity

and surface generation coefficient have been calculated. The effect of surface generation of carriers has not been included in any calculations so far but we find that it makes a significant contribution to the solar cell characteristics. We have also calculated the excess minority carrier profile in the base in the open circuit configuration and find that pn coupling shifts the position of the maxima of the profile away from the junction. The same in the absence of pn coupling however as dictated by the open circuit requirement always occures right at the junction.

In section 3.2 the theory of the steady-state response of an n^+p solar cell is given. The dependence of short-circuit current and open circuit photovoltage on the absorption coefficient of light, surface generation coefficient and surface recombination velocity have been calculated in subsections 3.2.1 and 3.2.2 respectively. In subsection 3.2.3 the excess minority carrier profile in the base in the open circuit configuration has been calculated and in subsection 3.2.4 the expression for the maxima in the carrier profile in the diffused layer is given.

3.2 Theory

To study the effect of pn coupling on the solar cell response in steady-state, one has to solve a set of

two diffusion equations subject to appropriate boundary conditions. Here we consider an n^+p solar cell with abrupt junction at $x = 0$, front surface at $x = -d$ and back surface at $x = \infty$. The approximation that the base is infinitely thick has been made for the sake of mathematical simplicity and is valid if base thickness is much larger than the corresponding excess minority carrier diffusion length. The effect of finite size of base has already been discussed in chapter 2 which changes the slope of PVD curve by certain amount.

The diffusion equations for excess minority carrier concentrations p and n respectively in the diffused layer and the base are given below (see, for example, McKelvey 1966).

$$D_p\left(\frac{d^2p}{dx^2}\right) - \frac{p}{\tau_p} = -g \exp(-\alpha x) \qquad -d \leq x < 0 \qquad (3.1)$$

$$D_n\left(\frac{d^2n}{dx^2}\right) - \frac{n}{\tau_n} = -g \exp(-\alpha x) \qquad x > 0 \qquad (3.2)$$

where $g = \alpha N_o \exp(-\alpha d)$. $D_{p,n}$ and $\tau_{p,n}$ denote respectively the diffusion coefficient and life time of the p or n type carriers, N_o is the number of incident photons (assumed to be monochromatic) per unit area per unit time at the front surface and α is the absorption coefficient of light. The boundary conditions for p and n in the open circuit case are given below:

(a) at $x = -d$: We use the boundary condition derived by Tewary and Jain (1980) which takes into account recombination as well as the generation of excess carriers at the surface viz.

$$D_p\left(\frac{dp}{dx}\right)_{-d} = sp(-d) - \eta N_o \qquad .. (3.3)$$

where s denotes the surface recombination velocity and η is the surface generation coefficient.

(b) at $x = 0$: The usual Shockley boundary condition gives

$$\frac{p(0)}{p_{no}} = \frac{n(0)}{n_{po}} = \exp\left(\frac{qV}{kT}\right) - 1 \qquad .. (3.4)$$

where p_{no} and n_{po} denote respectively the thermal equilibrium values of p and n and V is voltage across the junction.

The open circuit condition at $x = 0$ requires total current J_t (not necessarily the individual diffused layer or base current) to be zero i.e.

$$J_t = qD_p\left(\frac{dp}{dx}\right)_o - qD_n\left(\frac{dn}{dx}\right)_o = 0 \qquad .. (3.5)$$

(c) at $x = \infty$: Assuming an ohmic contact at the base, we take

$$n(\infty) = 0 \qquad .. (3.6)$$

The solutions of equations (3.1) and (3.2) subject to above boundary conditions can be easily obtained (see, for example, McKelvey 1966). We give below the expressions for V_o - the steady-state open circuit photovoltage, J_g - the light generated or the short-circuit current, J_o - the dark saturation current, and $n(x)$ and $p(x)$ - the excess minority carrier concentrations in the base and the diffused layer respectively, in the open circuit configuration

$$V_o = \left(\frac{kT}{q}\right) \ln\left(1 + \frac{J_g}{J_o}\right) \qquad .. (3.7)$$

$$J_g = J_p + J_n \qquad .. (3.8)$$

$$J_p = J_{ps} + J_{pb} \qquad .. (3.9)$$

$$J_{ps} = \frac{qN_o D_p \eta}{D_p \cosh d/L_p + sL_p \sinh d/L_p} \qquad .. (3.10)$$

$$J_{pb} = \left[\frac{(sL_p \cosh d/L_p + D_p \sinh d/L_p) \exp(-\alpha d) - sL_p - \alpha D_p L_p}{D_p \cosh d/L_p + sL_p \sinh d/L_p} + \alpha L_p \exp(-\alpha d)\right] \frac{qN_o \alpha L_p}{(1-\alpha^2 L_p^2)} \qquad .. (3.11)$$

$$J_n = \frac{qN_o \alpha L_n \exp(-\alpha d)}{1 + \alpha L_n} \qquad .. (3.12)$$

$$J_o = J_{no} + J_{po} \frac{sL_p \cosh d/L_p + D_p \sinh d/L_p}{D_p \cosh d/L_p + sL_p \sinh d/L_p} \qquad .. (3.13)$$

$$J_{no} = qn_{po} L_n/\tau_n$$

$$J_{po} = qp_{no} L_p/\tau_p \qquad \text{.. (3.14)}$$

$$n(x) = K \exp(-x/L_n) + \frac{\alpha N_o \tau_p}{(1-\alpha^2 L_n^2)} \exp[-\alpha(x+d)] \qquad \text{.. (3.15)}$$

$$\text{.. (3.16)}$$

$$K = n_{po}[\exp(qV_o/kT) - 1] - \frac{\alpha N_o \tau_n \exp(-\alpha d)}{1-\alpha^2 L_n^2} \qquad \text{.. (3.17)}$$

$$p(x) = A_1 \cosh x/L_p + B_1 \sinh x/L_p + \frac{\alpha N_o \tau_p \exp[-\alpha(x+d)]}{1-\alpha^2 L_p^2}$$

$$A_1 = p_{no}[\exp(qV_o/kT) - 1] - \frac{\alpha N_o \tau_p}{1-\alpha^2 L_p^2} \exp(-\alpha d) \qquad \text{.. (3.18)}$$

$$\text{.. (3.19)}$$

$$B_1 = A_1 \frac{sL_p \cosh d/L_p + D_p \sinh d/L_p}{D_p \cosh d/L_p + sL_p \sinh d/L_p} + \frac{\alpha L_p N_o \tau_p (\alpha D_p + s)}{(1-\alpha^2 L_p^2)(D_p \cosh d/L_p + sL_p \sinh d/L_p)} - \frac{qN_o L_p}{D_p \cosh d/L_p + s \sinh d/L_p} \qquad \text{.. (3.20)}$$

where q is the electronic charge and L denotes the diffusion length of the minority carriers. The suffices p and n refer to minority carriers in the diffused layer and the base respectively. J_p and J_n denote the contributions to the short-circuit current, J_g, from the diffused layer and the base respectively. J_{ps} and J_{pb} denote the contributions to J_p from surface and the bulk

of the diffused layer respectively. J_o is the dark saturation current of the cell. The two terms on the right hand side of equation (3.13) denote the contribution to J_o from the base and the diffused layer respectively.

pn coupling in the present theory arises from equations (3.4) and (3.5) which couple the values of p and n and their derivatives across the junction. If the band gap narrowing effects in the diffused layer are neglected, $p_{no} \ll n_{po}$ and since $\tau_p \ll \tau_n$, then the contribution of the diffused layer becomes small. The usual calculations in this case neglect pn coupling by taking $(dn/dx)_o = 0$ instead of equation (3.5) and use only the second equality in equation (3.4). However, as remarked earlier, and as shown by Lindholm and Sah (1976), Neugroschel et. al. (1977) and Fossum et. al (1979), the band gap narrowing caused by heavy doping in the diffused layer in a modern n^+p solar cell makes p_{no} comparable to or even larger than n_{po} and therefore pn coupling can not be neglected.

To investigate the effect of pn coupling on the solar cell response, we have considered an n^+p silicon solar cell as used by Fossum et. al. (1979). For this cell material parameters as quoted by Fossum et. al (1979) are $d = 0.1\ \mu m$ and $J_{no} = 6.2 \times 10^{-14}$ A cm^{-2}. For the other

material parameters we have chosen the following values on the basis of various estimates and other data given by Fossum et. al. (1979):

$D_n = 15.5\ cm^2\ s^{-1}$, $\tau_n = 4.1\ \mu s$, $L_n = 80\ \mu m$, $n_{po} = 200\ cm^{-3}$, $D_p = 1\ cm^2\ s^{-1}$, $\tau_p = 1\ ns$, $L_p = 0.3\ \mu m$, $p_{no} = 368\ cm^{-3}$, and $J_{po} = 18.6 \times 10^{-13}\ A\ cm^{-2}$.

The effect of band gap narrowing in the diffused layer is included in the chosen values of p_{no} and J_{po} which are larger than the corresponding values in the base viz. $p_{no}/n_{po} = 1.8$ and $J \equiv J_{po}/J_{no} = 30$.

3.2.1 Steady-State Short-Circuit Current

The dependence of J_g on s, η and α as calculated from equation (3.8) is shown in figure (3.1). The main observations of figure 3.1 are summarised below:

(i) For $\eta = 0$, J_g is sensitive to s for large $\alpha (\geq 10^5\ cm^{-1})$ only.

(ii) For nonzero η, J_g is sensitive to s in almost the whole range of α.

(iii) J_g is very sensitive to η for low $\alpha (\leq 1\ cm^{-1})$.

(iv) For large $s (\approx 10^7\ cm\ s^{-1})$, J_g is not sensitive to η for moderate and large values of $\alpha (\geq 10^2\ cm^{-1})$.

(v) For low s ($\leq 10^4$ cm s^{-1}), J_g is sensitive to η in almost the whole range of α.

(vi) In general, as remarked by Tewary and Jain (1980), J_g increases with η.

The above behaviour of J_g can be understood from equation (3.8). J_g is the sum of J_p and J_n, the contributions from the diffused layer and the base respectively, as given by equation (3.9) and (3.12). J_p is made up of J_{ps}, the contribution arising from the surface absorption of photons given by equation (3.10), and J_{pb}, the contribution from the bulk of the diffused layer, given by equation (3.11).

For $\eta = 0$ as in observation (i), which is the well known case, unless $\alpha d \gg 1$, $J_p \ll J_n$ because $L_p \ll L_n$. In this case the contribution of the diffused layer is negligible. If $\alpha d \gg 1$, $J_n \sim 0$ and the diffused layer makes a significant contribution to J_g which therefore is sensitive to s and other parameters of the diffused layer such as L_p, d etc.

For nonzero η as long as $\exp(-\alpha d) \approx 1$, $J_{pb} \ll J_n$ and the relative contribution of J_{ps} depends upon η, s, α and L_p as follows:

$$\frac{J_{ps}}{J_n} = \frac{\eta(1 + \alpha L_n)D_p}{\alpha L_n(D_p \coth d/L_p + sL_p) \sinh d/L_p} \quad .. (3.21)$$

The ratio J_{ps}/J_n will be sensitive to s for large enough η unless $s \ll (D_p/L_p) \coth d/L_p$. In the present calculations $(D_p/L_p) \coth d/L_p \sim 10^5$ cm s^{-1}. This therefore explains observations (ii) and (v). Observation (iii) is apparent from equation (3.21) because J_{ps}/J_n will obviously be quite large for low α. In the limit $s \to \infty$, $J_{ps}/J_n \to 0$, which explains observation (iv).

Thus we find that the surface absorption of photons introduced in the boundary condition by Tewary and Jain (1980) makes an important contribution to the short-circuit current through η as well as s. No measurement of η has been reported in the literature as yet, but it should be possible to estimate η by using the behaviour of J_g as discussed above. In addition to this, in all these calculations η has been assumed to be independent of α. It is expected that η will have an implicit, perhaps weak, dependence on α because both η and α depend upon photon energy (Tewary and Jain 1980). In the absence of any theoretical or experimental information about the values of η, we have made the approximation in these calculations that η is independent of α; so as to get atleast a qualitative idea regarding the dependence of J_g on η.

We have also neglected the effect of band gap narrowing on α by assuming that α has the same value in the diffused layer and the base. This effect can be easily included in a more refined calculation. However, this effect is likely to be much smaller than the effect of band gap narrowing on p_{no} which has been included in the present calculations. This is because p_{no} has an exponential dependence on energy gap whereas the dependence of α on energy gap is relatively weaker: α is proportional to the square of the difference between the photon energy and the energy gap (Pankov 1971).

3.2.2 Steady-State Open Circuit Photovoltage

The dependence of V_o on s, η and α as calculated from equation (3.7) has been shown in figure (3.2). This figure reflects the dependence of V_o on η and α through J_g (equation 3.8) and on s through J_g and J_o (equation 3.13). As s increases, J_g decreases and J_o increases, which causes a decrease in V_o. An increase in η increases J_g which results in an increase in V_o.

If the dependence of J_g on η and s is not accounted for, as for example is the case considered by Fossum et. al. (1979), V_o depends upon s only through J_o. If $J_{po} \ll J_{no}$ then J_o and therefore V_o will not

be sensitive to s. This would be the case if diffused layer were more heavily doped than the base layer and the band gap narrowing effect was negligible. In modern n^+p diodes, as discussed by Fossum et. al. (1979), $J_{po} >> J_{no}$ and hence V_o becomes sensitive to s through J_{po}. In this limit, as expected, our results are similar to those obtained by Fossum et. al. (1979).

Our results on the dependence of V_o on s are in qualitative agreement with the experimental results of Fossum et. al. (1979). However, a quantitative comparison with their experimental results is not possible because the nature of light which was used by Fossum et al. (1979) to generate the photovoltage is not known.

3.2.3 Steady-state Carrier Profile in the Base

The steady-state carrier profile in the base in the open circuit configuration as calculated from equation (3.16) for $\alpha = 10^2$ cm^{-1} and 10^5 cm^{-1} have been shown in figure (3.3). We notice that n(x) has a maximum when $\alpha = 10^2$ cm^{-1} and decreases monotonically with x for $\alpha = 10^5$ cm^{-1}. If pn coupling is neglected the behaviour of n(x) is qualitatively different. In this case the boundary condition given by equation (3.5) simply becomes $(dn/dx)_o = 0$ which forces n(x) to have maximum at junction (x = 0) for all values of α, in contrast to the behaviour shown in figure 3.3.

The occurrence of the maximum in $n(x)$ away from the junction caused by the pn coupling for low α can be physically understood as follows. The value of $n(x)$ at the junction is defined by the junction voltage in accordance with equation (3.4). If α is small so that the concentration of carriers generated in the base close to the junction is larger than $n(0)$, as allowed by the equation (3.4), then some carriers near the junction will cross over to the other side. This will affect the carrier concentration within a diffusion length of the junction. Further away from the junction the carrier concentration will not be very much affected and apart from some diffusive contribution it will be determined mainly by the absorption of photons which decreases exponentially. Thus the carrier concentration in this case increases as we move away from the junction and then starts decreasing which explains the occurrence of the maximum in the base. It may be remarked that in the open circuit case, the current due to the movement of carriers across the junction in order to satisfy equation (3.4) is just balanced by the current due to crossing over of other type of carriers in accordance with equation (3.5).

If on the other hand α is large, so that the concentration of carriers generated by photon absorption

We see from equation (3.22) that in the limit $\alpha \to \infty$ the logarithmic term and hence x_m will be negative. Thus there will be no maximum in $n(x)$ in the base ($x > 0$) for large α. Further, if we neglect pn coupling by putting $J_{po}/J_{no} = 0$ in J_o (equation 3.13) and $L_p = 0$ in J_g (equation 3.8), we see that x_m as given by equation (3.22) becomes zero. This is the usual case in which the maximum in $n(x)$ occures at the junction. The effect of pn coupling is to shift this maximum to positive x for low α and to negative x for large α.

Aforementioned effect of α on x_m in the presence of pn coupling can also be seen from figure (3.4). Curves (a) and (b) in this figure are for $J = 30$ and 0.01 respectively. As we are interested in studying only the effect of pn coupling on x_m, we have taken s and η equal to zero. It is obvious from this figure that pn coupling shifts the maximum to positive values of x for low α and to negative values of x for large α. For $J = 30$, x_m is positive for $\alpha \leq 10^4$ cm^{-1}. However for $J = 0.01$, x_m is positive only for $\alpha \leq 10$ cm^{-1}.

3.2.4 Steady-state Carrier Profile in the Diffused Layer

The profile of theexcess minority carriers $-p(x)$ in the diffused layer can be calculated by using equation (3.18). pn coupling in $p(x)$ comes because of the dependence

of constants A_1 (equation 3.19) and B_1 (equation 3.20) on p_{no} and V_o which, as shown earlier, strongly depend upon band gap narrowing and pn coupling. In the absence of pn coupling $p(x)$ as dictated by open circuit boundary condition (equation 3.5), always has an extremum at the junction. pn coupling shifts this extremum away from the junction.

To obtain the position of extremum in $p(x)$ in the diffused layer, we differentiate equation (3.18) with respect to x and equate it to zero. The result is

$$A_1 \sinh x/L_p + B_1 \cosh x/L_p - \frac{\alpha^2 L_p N_o \tau_p}{(1-\alpha^2 L_p^2)} \exp[-\alpha(x+d)] = 0 \quad \ldots (3.23)$$

For a given set of physical constants equation (3.23) has to be solved numerically for x.

3.3 Conclusions

Effect of pn coupling on the steady-state response of the solar cell has been analysed. It is shown that pn coupling shifts the position of the maxima of the excess minority carrier profile in the base (in the open circuit configuration) away from the junction which in the absence of pn coupling as dictated by the open circuit condition always occures right at the junction.

Effect of surface generation coefficient as introduced by Tewary and Jain (1980) in the surface boundary condition for solar cells is found to be more pronounced for lower values of the absorption coefficient of light. This as predicted by Tewary and Jain (1980) increases the short-circuit current and hence also the open circuit photovoltage of the solar cell.

Surface recombination velocity increases the dark saturation current and decreases the short-circuit current and thus in accordance with equation (3.7) decreases the open circuit photovoltage of the solar cell.

References

(1) Possum J.G., Lindholm F.A. and Shibib M.A. (1979) IEEE Transactions on Electron Devices ED-26 1294-98.

(2) Lindholm F.A. and Sah C.T. (1976) J. Appl. Phys. 47 4203-05.

(3) McKelvey J.P. (1966) Solid State and Semiconductor Physics (N.Y. Harper and Row).

(4) Neugroschel A., Lindholm F.A. and Sah C.T. (1977) IEEE Transactions on Electron Devices ED-24 662-71.

(5) Pankov J.I. (1971) Optical Processes in Semiconductors (New Jersey: Prentice-Hall, Inc.).

(6) Tewary V.K. and Jain S.C. (1980) J. Phys. D. Appl. Phys. 13 835-7.

Figure Captions

Figure 1: Variation of steady-state short-circuit current with absorption coefficient of light (α) for different values of surface recombination velocity(s) and surface generation coefficient (η) in a n^+p solar cell. A full curve is composed of three labelled segments. For curves amu, bmu, and cmu, $s = 10^7$ cms^{-1} and $\eta = 0$, 0.01 and 0.1 respectively. For curves amv, dmv and enw, $s = 10^4$ cms^{-1} and $\eta = 0$, 0.01 and 0.1 respectively.

Figure 2: Variation of steady-state open circuit photovoltage (V_o) with absorption coefficient of light (α). For curves a, b and c, $s = 10^7 cms^{-1}$ and $\eta = 0$, 0.01 and 0.1 respectively and for curves d, e and f, $s = 10^4$ cms^{-1} and $\eta = 0$, 0.01 and 0.1 respectively.

Figure 3: Excess minority carrier concentration (n(x)) in the base in the open circuit configuration as a function of the distance (x) from the junction in a n^+p solar cell. The values of the absorption coefficient of light (α) for curves a and b are 10^5 cm^{-1} and 10^2 cm^{-1} respectively.

Figure 4: Variation of position of maxima (x_m) in the carrier profile in the base in the open circuit configuration as a function of the absorption coefficient of light (α). For curves a and b J = 30 and 0.01 respectively. s and η in these calculations have been taken as zero.

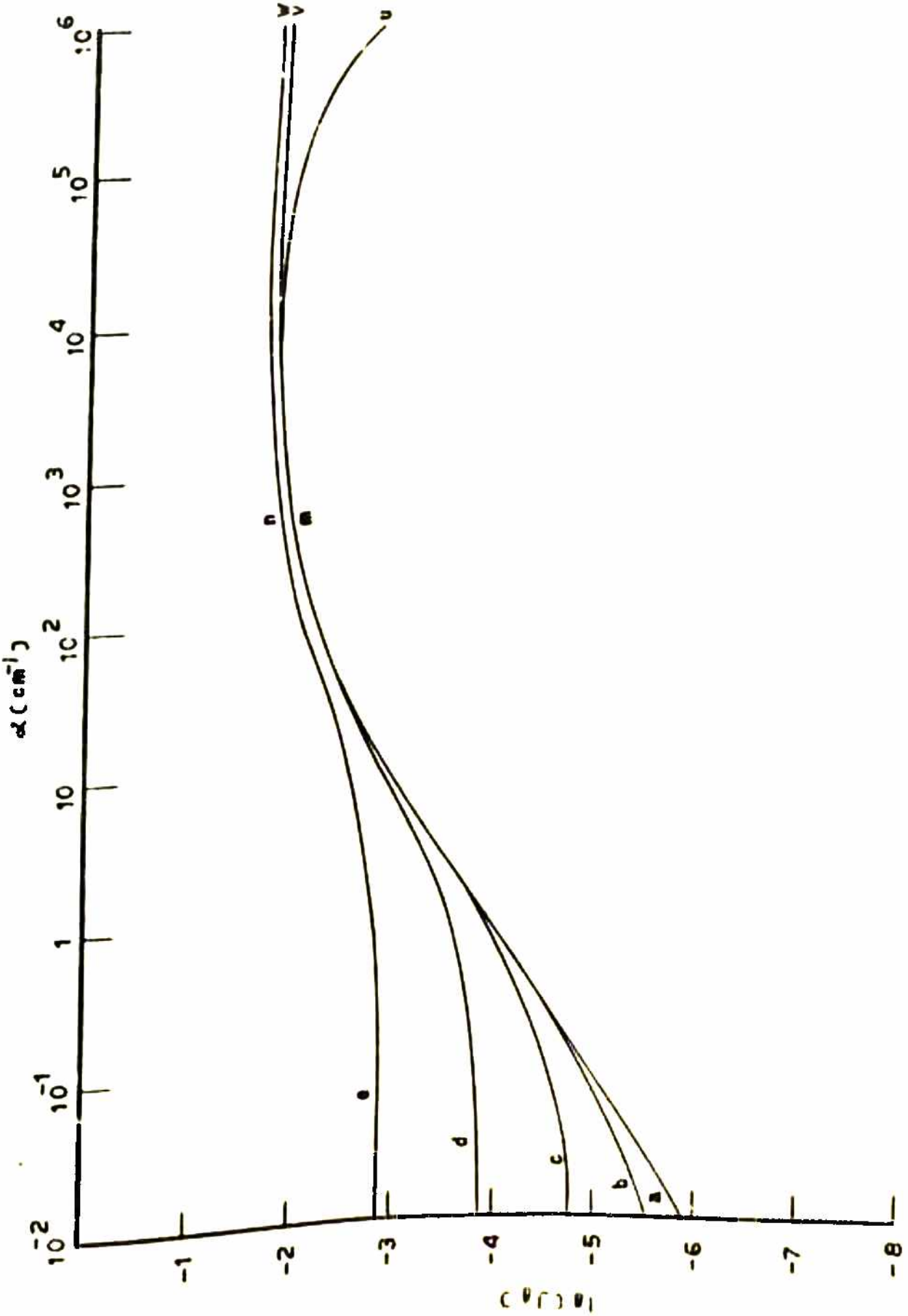

FIG. 3.1

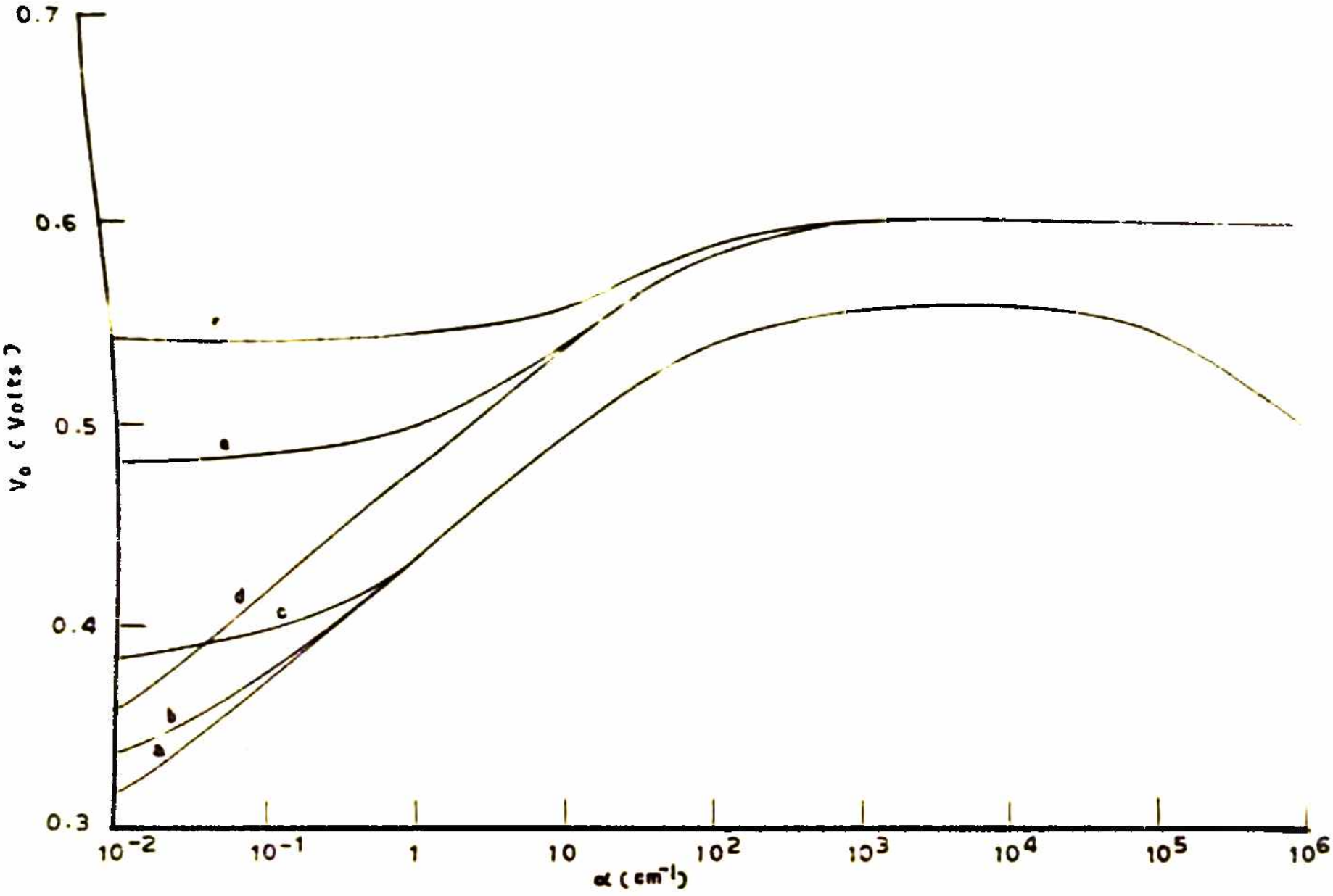
0.7
0.6
0.5
0.4
0.3
V_o (Volts)
e
a
d
c
b
a
10^{-2}
10^{-1}
1
10
10^2
10^3
10^4
10^5
10^6
α (cm^{-1})

FIG. 3.2

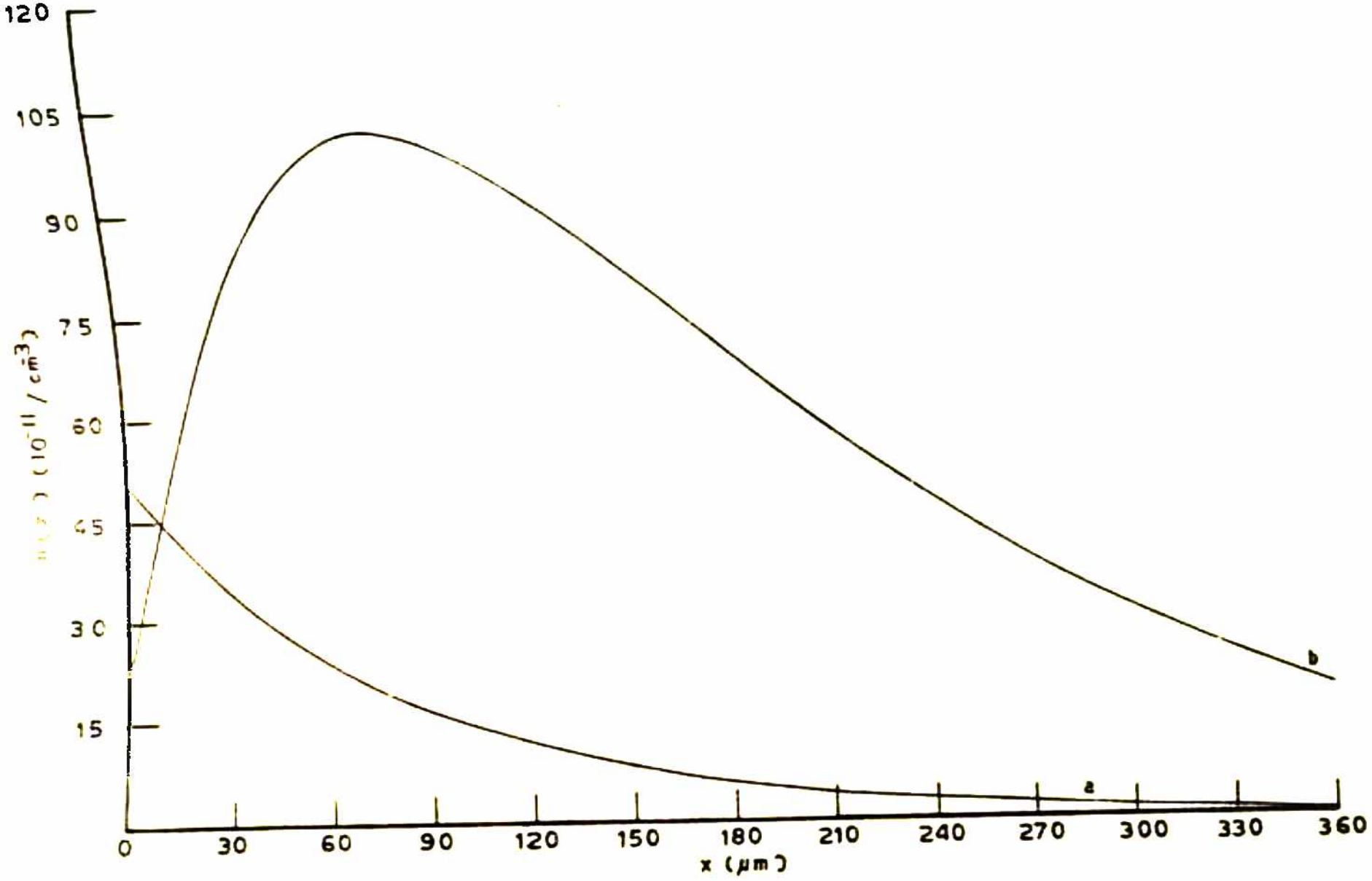
120
105
90
75
60
45
30
15
0
30
60
90
120
150
180
210
240
270
300
330
360
x (μm)
a
b

FIG. 3.3

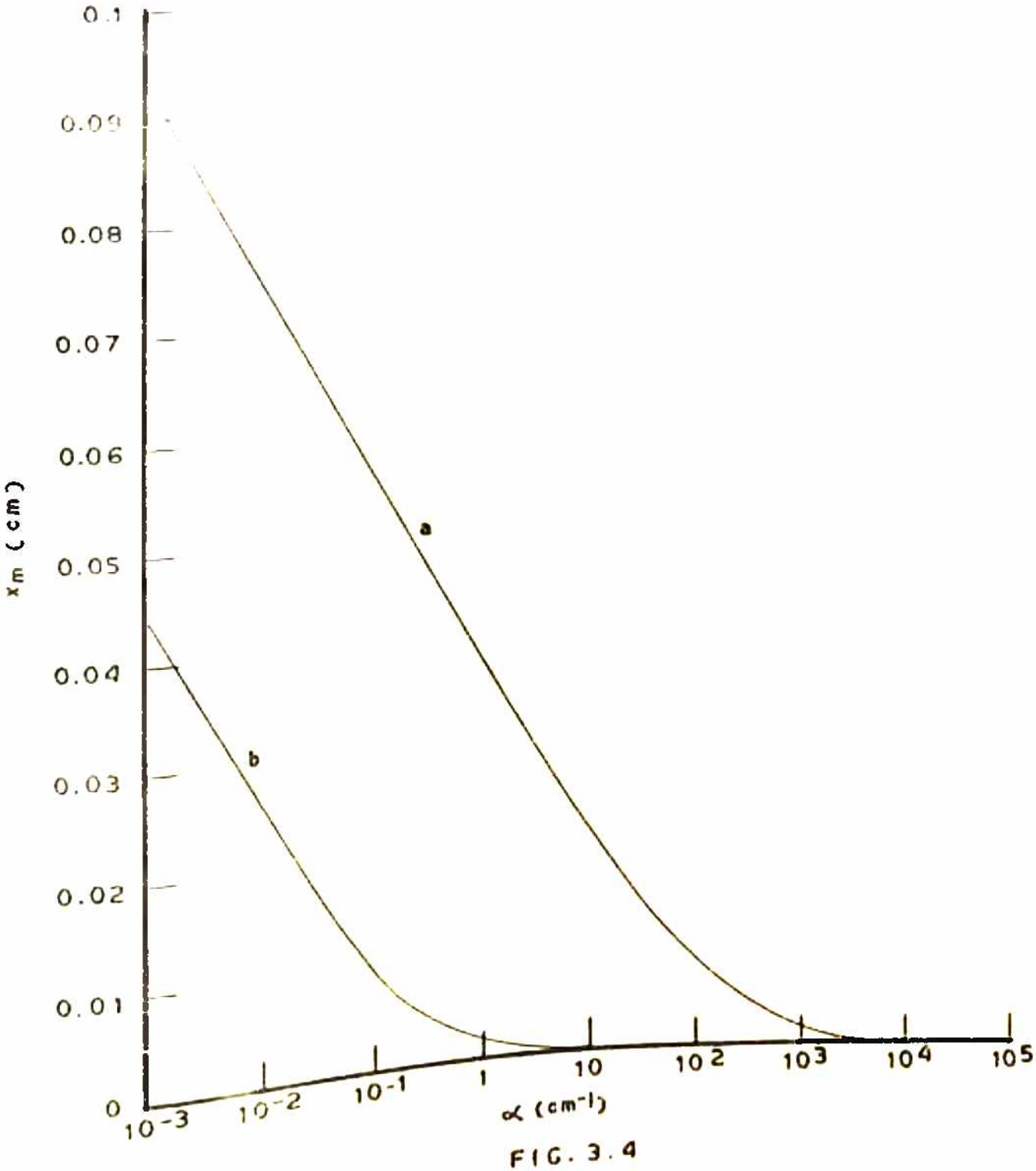
0.1
0.09
0.08
0.07
0.06
0.05
0.04
0.03
0.02
0.01
0
x_m (cm)
a
b
10^{-3}
10^{-2}
10^{-1}
1
10
10^2
10^3
10^4
10^5
α (cm^{-1})

FIG. 3.4

CHAPTER 4

EFFECT OF pn COUPLING ON THE TRANSIENT RESPONSE OF A SOLAR CELL

4.1 Introduction

In the last chapter we analysed the effect of pn coupling on the steady-state response of a solar cell and found that it is quite sensitive to the pn coupling. The importance of pn coupling in the transient case has been emphasized by Lindholm and Sah (1976) and Tewary and Jain (1981). These authors have considered only the dark transient response of a solar cell or diode viz. FCVD after rapid termination of forward current. However, as shown by Mahan et. al. (1979) the decay of open circuit photovoltage (PVD) after switching off the illumination is a convenient method for measurement of life time of excess minority carriers and possibly the other parameters of a solar cell.

In this chapter we have studied the transient response of a solar cell including the effect of pn coupling. In particular we have studied the open circuit photovoltage decay in a solar cell which as mentioned in chapter 2 is a measure of the transient response of the solar cell.

The effect of pn coupling on PVD in a solar cell has not been theoretically analysed before. In the present chapter we have calculated PVD in an n^+p solar cell and find that under certain conditions it is quite sensitive to the pn coupling. Effect of various diffused layer parameters on PVD has been analysed and it is suggested that the measurement of PVD in its initial stages would yield useful information about the diffused layer excess minority carrier life time and also front surface parameters.

In section 4.2 the theory of PVD has been developed by applying Laplace transform technique (Sneddon 1972). In section 4.3 it is assumed that the absorption of incident radiation is uniform and the low time behaviour of PVD is discussed. It is shown that the leading term in the low time behaviour of PVD is proportional to t. The low time behaviour of PVD following exponential absorption of radiation is given in section 4.4 and results similar to those in section 4.3 have been obtained. In section 4.5 the importance and applications of Tricomi method (Sneddon 1972 and Ward 1954) in inverting Laplace transform have been discussed. In section 4.6 and its subsections the effect of various diffused layer parameters on PVD is analysed. The convergence of the PVD series obtained by applying Tricomi method is discussed in section 4.7.

4.2 Theory

n^+p solar cell as discussed by us in chapter 3 has been considered here also. The time dependent diffusion equations which describe the distribution of excess minority carriers in the diffused layer and the base respectively are given below

$$D_p(\partial^2 p/\partial x^2) - p/\tau_p + g\ \exp(-\alpha x) = \partial p/\partial t \qquad -d \leq x < 0 \qquad .. (4.1)$$

$$D_n(\partial^2 n/\partial x^2) - n/\tau_n + g\ \exp(-\alpha x) = \partial n/\partial t \qquad x > 0 \qquad .. (4.2)$$

where $g = \alpha N_o \exp(-\alpha d)$ and other symbols have their usual meaning (defined in section 3.2). In steady-state the time derivatives $\partial p/\partial t$ and $\partial n/\partial t$ are zero.

The solar cell under consideration has been exposed to light such that steady-state is reached for $t < 0$ and light is switched off at $t = 0$ which marks the beginning of the transient state. The equations which describe the transient behaviour of the solar cell are obtained by deleting the generation term in equations (4.1) and (4.2). These are given below

$$D_p(\partial^2 p/\partial x^2) - p/\tau_p = \partial p/\partial t \qquad -d \leq x < 0 \qquad .. (4.3)$$

and $$D_n(\partial^2 n/\partial x^2) - n/\tau_n = \partial n/\partial t \qquad x > 0 \qquad .. (4.4)$$

The boundary conditions for equations (4.3) and (4.4) in the transient state are given below

(i) at $x = -d$: The surface boundary condition as obtained by putting $\eta = 0$ in equation (3.3) is given below

$$D_p(\partial p/\partial x)_{-d} = sp(-d) \qquad .. (4.5)$$

(ii) at $x = 0$: The usual Shockley boundary condition gives

$$p(0)/p_{no} = n(0)/n_{po} = \exp(qV/kT) - 1 \qquad .. (4.6)$$

where p_{no} and n_{po} denote the thermal equilibrium values of p and n respectively. q is the electronic charge and kT represents the thermal energy at temperature T. V denotes the voltage across the junction.

(iii) at $x = \infty$: We take an ohmic contact at the back so that

$$n(\infty) = 0 \qquad .. (4.7)$$

In addition to these, in transient case we also impose the initial condition that the time dependent functions $p(x,t)$ and $n(x,t)$ reduce to their steady-state values $n_s(x)$ and $p_s(x)$ for $t = 0$, i.e.

(iv) $$p(x,t)|_{t=0} = p_s(x) \qquad .. (4.8)$$

and

$$n(x,t)\big|_{t=0} = n_s(x) \qquad .. (4.9)$$

where $p_s(x)$ and $n_s(x)$ are given by equations (3.18) and (3.16) respectively.

The open circuit condition at x = 0 requires that

$$qD_p(\partial p/\partial x)_o - qD_n(\partial n/\partial x)_o = 0 \qquad .. (4.10)$$

To solve equations (4.3) and (4.4), we apply the Laplace transform technique (Sneddon 1972). Upon taking the Laplace transform of equation (4.3), we get

$$\frac{\partial^2 p(x,s)}{\partial x^2} - \frac{(1+S\tau_p)\,p(x,S)}{L_p^2} = -\frac{\tau_p}{L_p^2}\,p_s(x) \qquad .. (4.11)$$

Upon substituting the value of $p_s(x)$ in equation (4.11) from equation (3.18), we get

$$\frac{\partial^2 p(x,S)}{\partial x^2} - \frac{(1+S\tau_p)\,p(x,S)}{L_p^2}$$

$$= -\frac{\tau_p}{L_p^2}\left[A_1 \cosh\frac{x}{L_p} + B_1 \sinh\frac{x}{L_p} + \frac{g\tau_p \exp(-\alpha x)}{(1-\alpha^2 L_p^2)}\right] \qquad .. (4.12)$$

Similarly for the excess minority carriers on the base side we can write

$$\frac{\partial^2 n(x,S)}{\partial x^2} - \frac{(1+S\tau_n)\,n(x,S)}{L_n^2}$$

$$= -\frac{\tau_n}{L_n^2}\left[K \exp\left(-\frac{x}{L_n}\right) + \frac{g\tau_n \exp(-\alpha x)}{1-\alpha^2 L_n^2}\right] \qquad .. (4.13)$$

Solutions of equations such as these can be written as the sum of the corresponding homogeneous equation solution and any particular solution to the homogeneous equation. The same are as follows:

$$p(x,S) = C\cosh(1+S\tau_p)^{1/2}x/L_p + D\sinh(1+S\tau_p)^{1/2}x/L_p + \frac{A_1}{S}\cosh x/L_p + \frac{B_1}{S}\sinh x/L_p + \frac{g\tau_p^2\exp(-\alpha x)}{(1-\alpha^2L_p^2)[S\tau_p+(1-\alpha^2L_p^2)]} \quad .. (4.14)$$

and

$$n(x,S) = E\exp[-(1+S\tau_n)^{1/2}x/L_n] + \frac{K}{S}\exp(-x/L_n) + \frac{g\tau_n^2\exp(-\alpha x)}{(1-\alpha^2L_n^2)[S\tau_n+(1-\alpha^2L_n^2)]} \quad .. (4.15)$$

where the constants of integration C and E can be evaluated by applying boundary condition (11) (equation 4.6) and D by applying equation (4.5). These are given below

$$C = p_{no}f_p(S) - \frac{A_1}{S} - \frac{g\tau_p^2}{(1-\alpha^2L_p^2)[S\tau_p+(1-\alpha^2L_p^2)]} \quad .. (4.16)$$

$$D = C(s\cosh X_1 + D_p X_2 \sinh X_1)/A(S)$$
$$+ \frac{A_1}{S}[s\cosh d/L_p + (D_p/L_p)\sinh d/L_p]/A(S)$$
$$- \frac{B_1}{S}[s\sinh d/L_p + (D_p/L_p)\cosh d/L_p]/A(S)$$
$$+ T'/A(S) \qquad .. (4.17)$$

where

$$X_1 = (1 + S\tau_p)^{1/2}\, d/L_p \qquad .. (4.18)$$

$$X_2 = X_1/d \qquad .. (4.19)$$

$$A(S) = D_p X_2 \cosh X_1 + s\sinh X_1 \qquad .. (4.20)$$

$$T' = \frac{g\exp(\alpha d)\,\tau_p^2(\alpha D_p + s)}{(1-\alpha^2 L_p^2)[S\tau_p + (1-\alpha^2 L_p^2)]} \qquad .. (4.21)$$

$$E = n_{po} f_n(S) - \frac{K}{S} - \frac{g\tau_n^2}{(1-\alpha^2 L_n^2)[S\tau_n + (1-\alpha^2 L_n^2)]} \qquad ..(4.22)$$

and $$f_n(S) = f_p(S) = \mathcal{L}[\exp(qV/kT) - 1] \equiv f(S) \qquad .. (4.23)$$

Now on applying open circuit condition (equation 4.10), we get

$$\frac{f(S)}{f(0)} = -\frac{I_o(S)}{I(S)} - \frac{I_g(S)}{I(S)}\,\frac{J_o}{J_g} \qquad .. (4.24)$$

where

$$f(0) = \exp(qV_o/kT) - 1 \qquad .. (4.25)$$

V_o denotes the steady-state open circuit photovoltage as given by equation (3.7). J_g and J_g are given by equation (3.13) and (3.8) respectively.

$$I(S) = J_{po}\, S_1 (1+S\tau_p)^{1/2} + J_{no}(1+S\tau_n)^{1/2} \qquad \text{.. (4.26)}$$

$$S_1 = \frac{s\cosh(1+S\tau_p)^{1/2} d/L_p + (D_p/L_p)(1+S\tau_p)^{1/2}\sinh(1+S\tau_p)^{1/2} d/L_p}{(D_p/L_p)(1+S\tau_p)^{1/2}\cosh(1+S\tau_p)^{1/2} d/L_p + s\sinh(1+S\tau_p)^{1/2} d/L_p} \qquad \text{.. (4.27)}$$

where J_{po} and J_{no} are given by equations (3.15) and (3.14) respectively.

$$I_o(S) = \frac{J_{po} M_1}{S} - \frac{J_{po}(1+S\tau_p)^{1/2} S_1}{S} + \frac{J_{no}}{S} - \frac{J_{no}(1+S\tau_n)^{1/2}}{S} \qquad \text{.. (4.28)}$$

$$M_1 = \frac{s\cosh d/L_p + (D_p/L_p)\sinh d/L_p}{(D_p/L_p)\cosh d/L_p + s\sinh d/L_p} \qquad \text{.. (4.29)}$$

$$U_2 = \frac{D_p}{L_p}(1 + S\tau_p)^{1/2} \cosh(1 + S\tau_p)^{1/2} d/L_p + s \sinh(1 + S\tau_p)^{1/2} d/L_p \quad .. (4.33)$$

$$U_3 = s \sinh d/L_p + (D_p/L_p) \cosh d/L_p \quad .. (4.34)$$

Now the inverse Laplace transform of equation (4.24) will yield the desired expression for PVD. However, it was not found possible to obtain an analytical closed expression for the inverse Laplace transform of this equation. We therefore used a semianalytical method viz. Tricomi method (Sneddon 1972 and Ward 1954) to obtain the inverse Laplace transform of equation (4.24). Before that in order to qualitatively study the behaviour of PVD we assume the approximation that absorption of light is uniform as given in section 4.3; and also obtain the law time behaviour of PVD for exponential absorption in section 4.4.

4.3 PVD by Assuming Uniform Absorption of Incident Radiation

For a qualitative analysis of PVD in this section we make the following three approximations:

(i) the absorption of radiation is uniform which amounts to putting $\alpha = 0$ in equations (4.1) and (4.2) while keeping g finite.

(ii) thickness of the diffused layer as well as base is infinite i.e. much larger than the corresponding diffusion length.

(iii) the surface recombination velocity (s) and the surface generation coefficient (η) are zero.

This case although does not simulate the actual operation of solar cell exposed to the sun light but is good for qualitative analysis and also for understanding the physical processes (Dhariwal et. al. 1976). Some of the cases to which it is applicable are given below;

(i) solar cells irradiated by X-rays

(ii) solar cells when the photon energy is just short(!) of the band gap energy i.e. when photon energy is very close to the absorption edge on its lower energy side

(iii) this is often used for analysis of photoconductivity (see, for example, McKelvey 1966).

The equations which describe the distribution of excess minority carriers in this case can be obtained by putting $\alpha = 0$ while keeping g constant in equations (4.1) and (4.2). The boundary conditions (ii) - (iv) (equations 4.6 - 4.9) along with the open circuit condition (equation 4.10) apply to this case also. The surface boundary condition (equation 4.5) however due to infinite thickness of the diffused layer in the present case assumes the following form

$$(\partial p/\partial x)_{\infty} = 0 \qquad .. (4.35)$$

Solutions of equations thus obtained subject to these boundary conditions in steady-state can be easily obtained (see, for example, McKelvey 1966). Below we give expressions for $p(x)$ and $n(x)$ - the excess minority carrier profiles in the diffused layer and the base respectively, J_g - the short-circuit current, J_o - the dark saturation current and V_o - the steady-state open circuit photovoltage.

$$p(x) = F_1 \exp(x/L_p) + g\tau_p \quad .. (4.36)$$

$$n(x) = F_2 \exp(-x/L_n) + g\tau_n \quad .. (4.37)$$

where

$$F_1 = p_{no}[\exp(qV_o/kT) - 1] - g\tau_p \quad .. (4.38)$$

$$F_2 = n_{po}[\exp(qV_o/kT) - 1] - g\tau_n \quad .. (4.39)$$

$$V_o = (kT/q) \ln(1 + J_g/J_o) \quad .. (4.40)$$

$$J_g = qg(L_n + L_p) \quad .. (4.41)$$

$$J_o = J_{po} + J_{no} \quad .. (4.42)$$

$$J_{po} = p_{no}\, q\, D_p/L_p \quad .. (4.43)$$

$$J_{no} = n_{po}\, q\, D_n/L_n \quad .. (4.44)$$

where J_{po} and J_{no} denote the contributions to J_o from the diffused layer and the base respectively.

In transient case, solutions of equations (4.3) and (4.4) for this case can be obtained by putting $\alpha = 0$ and taking the limit $d \to \infty$ in equations (4.14) and (4.15) respectively. The results are given below:

$$p(x,S) = E_1 \exp[(1 + S\tau_p)^{1/2}\, x/L_p] + \frac{1}{S}[f(0) - g\tau_p] \exp(x/L_p) + \frac{g\tau_p^2}{1 + S\tau_p} \quad .. (4.45)$$

$$n(x,S) = E_2 \exp[-(1 + S\tau_n)^{1/2}\, x/L_n] + \frac{1}{S}[f(0) - g\tau_n] \exp(x/L_n) + \frac{g\tau_n^2}{(1+S\tau_n)} \quad .. (4.46)$$

where

$$E_1 = p_{no} f(s) - \frac{p_{no} f(0) - g\tau_p}{S} - \frac{g\tau_p^2}{1 + S\tau_p} \quad .. (4.47)$$

and

$$E_2 = n_{po} f(s) - \frac{n_{po} f(0) - g\tau_n}{S} - \frac{g\tau_n^2}{1 + S\tau_n} \quad .. (4.48)$$

Now applying the open circuit condition equation (4.10), we get the following expression for PVD which is in terms of the Laplace variable S:

$$\frac{f(S)}{f(0)} = \frac{1}{S} - \frac{(J_{po} + J_{no})}{S[J_{po}(1 + S\tau_p)^{1/2} + J_{no}(1 + S\tau_n)^{1/2}]}$$

$$+ \frac{qJ_o g}{J_g}\left[\frac{L_p\tau_p(1 + S\tau_p)^{-1/2} + L_n\tau_n(1 + S\tau_n)^{-1/2}}{J_{po}(1 + S\tau_p)^{1/2} + J_{no}(1 + S\tau_n)^{1/2}}\right]$$

$$+ \frac{qJ_o g(L_p + L_n)}{SJ_g[J_{po}(1 + S\tau_p)^{1/2} + J_{no}(1 + S\tau_n)^{1/2}]}$$

$$- \frac{qJ_o g}{SJ_g}\left[\frac{L_p(1 + S\tau_p)^{1/2} + L_n(1 + S\tau_n)^{1/2}}{J_{po}(1 + S\tau_p)^{1/2} + J_{no}(1 + S\tau_n)^{1/2}}\right] \quad .. (4.49)$$

where J_{po} and J_{no} are given by equations (4.43) and (4.44) respectively. J_o and J_g are given by equations (4.42) and (4.41) respectively.

Inverse Laplace transform of equation (4.49) yields the following expression for PVD.

$$\frac{\exp(qV/kT)-1}{\exp(qV_o/kT)-1} = 1 - \frac{JD_o \exp(-C'z)}{J-1}(\text{Erf } Y_p - \text{Erf } Y_n)$$

$$- \exp(-C'z) F_o\{(L-J) I_o(\beta' t) \exp(-\alpha' t)$$

$$+ F'_o \int_o^t \exp(-\alpha' u) I_o(\beta' u) du\}$$

$$- \frac{\exp(-C'z)}{J-1}\{J(1-C'T)^{1/2} \text{Erf}[(\frac{1-C'T}{T})z]^{1/2}$$

$$- (1-C')^{1/2} \text{Erf}[(1-C')z]^{1/2}\}$$

$$- \frac{1}{(J-1)(L+1)}\{(JL-1)[1-\exp(-C'z)]$$

$$- \exp(-\alpha t) I_o(\beta t)(L-JT)/T^{1/2}$$

$$- \frac{(L-J)T^{1/2}}{\tau_p} \int_o^t \exp(-au) I_o(\beta u) du$$

$$+ G_o \exp[-(C'z+\alpha')t] I_o(\beta' t)$$

$$+ G'_o \exp(-C'z) \int_o^t \exp(-\alpha' u) I_o(\beta' u) du\} \quad .. (4.50)$$

where $J = J_{po}/J_{no}$ and

$$z = t/\tau_n \qquad \text{.. (4.51)}$$

$$T = \tau_p/\tau_n \qquad \text{.. (4.52)}$$

$$C' = \frac{(J^2 - 1)}{(J^2 T - 1)} \qquad \text{.. (4.53)}$$

$$Y_n = (JKz)^{1/2} \qquad \text{.. (4.54)}$$

$$Y_p = (Kz/TJ)^{1/2} \qquad \text{.. (4.55)}$$

$$L = L_p/L_n \qquad \text{.. (4.56)}$$

$$D_o = J\left(\frac{1-C'T}{1-J^2T}\right)^{1/2} \qquad \text{.. (4.57)}$$

$$F_o = \frac{C'T^{1/2}}{(L+1)(J-1)} \qquad \text{.. (4.58)}$$

$$F_o' = F_o\left[\frac{(1-C')L - J(1-C'T)/T}{\tau_n}\right] \qquad \text{.. (4.59)}$$

$$G_o = \frac{L(1-C'T) - JT(1-C')}{T^{1/2}} \qquad \text{.. (4.60)}$$

$$G_o' = \frac{(1-C')(1-C'T)(L-J)T^{1/2}}{\tau_p} \qquad \text{.. (4.61)}$$

$$K = \frac{J(T-1)}{(J^2T-1)} \qquad \text{.. (4.62)}$$

$$\alpha' = \frac{1}{2}\left(\frac{1}{\tau_p} + \frac{1}{\tau_n}\right) - \frac{C'}{\tau_n} \qquad \text{.. (4.63)}$$

$$\beta' = \frac{1}{2}\left(\frac{1}{\tau_p} - \frac{1}{\tau_n}\right) \qquad \text{.. (4.64)}$$

$$\alpha = \frac{1}{2}\left(\frac{1}{\tau_p} + \frac{1}{\tau_n}\right) \qquad .. (4.65)$$

$$\beta = \beta' \qquad .. (4.66)$$

I_o denotes the modified Bessel Function of zeroeth kind. $I_o(z)$ can be expressed as follows (see, for example, Erdelyi 1954 and Abromovitz and Stegun 1965).

$$I_o(z) = \sum_{m=0}^{\infty} \frac{(z/2)^{2m}}{(m!)^2} \qquad .. (4.67)$$

For $t = 0$, the entire right hand side of equation (4.50) reduces to unity so that voltage V is equal to the steady-stage open circuit photovoltage V_o.

If we neglect pn coupling in the present theory by putting J and L zero then equation (4.50) reduces to the following expression

$$\Delta V(t) = V(t) - V_o = - t/\tau_n \qquad .. (4.68)$$

Equation (4.68) predicts a linear decay of open circuit photovoltage with time. The slope of the PVD curve yields the excess minority carrier life time in the base.

Although the uniform absorption approximation has enabled us to obtain an analytical form for PVD but this equation (equation 4.50) is still not convenient for numerical use. Since our interest in this section is only

in the qualitative study of PVD and also since the effect of pn coupling is substantial only at low times (Tewary and Jain 1981), we obtained the low time behaviour of PVD by expanding the error functions and the Bessel functions in equation (4.50) in powers of t/τ_p and t/τ_n. The leading term in this case is found to be proportional to t which is given below. Similar dependence is obtained in the exponential case also (discussed in the next section).

$$\Delta V(t) \equiv V(t) - V_o = -(kT/q)At/\tau_n + \text{higher order terms} \quad .. (4.69)$$

where

$$A = \frac{(J+1)}{(L+1)(J^2T-1)}\left[JL-1) + (JT-L)/T^{1/2}\right] \quad .. (4.70)$$

It may be mentioned that the low time behaviour of PVD observed above is in contrast to the low time behaviour of FCVD in which leading term is proportional to $t^{1/2}$. The detailed discussion on the low time behaviour of PVD and its comparison with the low time behaviour FCVD will be given in the next section.

4.4 Low Time Behaviour of PVD - Exponential Absorption of Incident Radiation

As shown by Tewary and Jain (1981) pn coupling is more effective in the initial stages of the decay i.e. for

close to zero. Since our present interest is to analyse the effect of pn coupling, in this section we consider PVD for $t \approx 0$. The leading term in the low time expansion of PVD (equation 4.24) is given below

$$\Delta V(t) \equiv V(t) - V_o = -(kT/q)At + \text{higher order terms} \quad .. (4.71)$$

where .. (4.72)

$$A = J_o P / J_g T \quad .. (4.73)$$

$$P = qN_o \exp(-\alpha d)(\alpha L_p/\tau_p^{1/2} + \alpha L_n/\tau_n^{1/2}) \quad .. (4.74)$$

$$T = J_{no}(J\tau_p^{1/2} + \tau_n^{1/2}) \quad .. (4.75)$$

$$J \equiv J_{po}/J_{no}$$

It may be verified that the coefficient A in equation (4.69) for the low time behaviour of PVD following uniform absorption of radiation and that in the present case (equation 4.71) are same.

Equation (4.71) predicts a linear decay of open circuit photovoltage for t close to zero. The dependence of A which denotes the decay rate at $t = 0$, on α is shown in figure (4.1) for different values of η and s. The pn coupling contributes to the decay rate through all the four factors J_o, J_g, P and T. The behaviour of J_o and J_g has already been discussed in chapter 3. The

characteristics of J_g described in section 3.2.1 may also be observed in A in fugure 4.1.

We see from equations (4.73) and (4.74) that the effect of pn coupling is to increase P as well as T; the former increases A whereas the latter has the opposite effect.

Physically the effect of pn coupling on PVD arises from two factors:

(i) Nature of steady-state profile for $t < 0$

(ii) Crossing over of carriers across the junction after $t = 0$ without contributing to the total current in accordance with equation (3.5).

First we consider the effect of the steady-state profile $n(x)$ in the base. As discussed in section 3.2.3, the carrier concentration $n(x)$ increases with x away from the junction for low values of α. As soon as light is switched off the junction loses carriers due to recombination, but also gains some carriers by diffusion from the near by region which has a higher concentration of carriers. Thus the decay rate of voltage, which depends upon the number of carriers at the junction, is slowed down by pn coupling. For large α, the carrier concentration falls as x increases from zero. In this case

the junction loses carriers by recombination as well as by diffusion, which makes the voltage decay faster than that in the absence of pn coupling.

Regarding process (ii) which involves the movement of the carriers across the junction, the carriers on the diffused layer side of the junction are removed much faster than those on the base side because $\tau_p \ll \tau_n$. Hence some carriers from the base side have to cross over the junction to diffused side in order to satisfy the equation (4.6). This increases the rate of carrier loss on the base side of the junction and therefore increases the decay rate. The net decay of voltage is a resultant of these two processes.

The other important characteristic of A which is shown in figure (4.1) is that it has a maximum at about $\alpha = 1/d$. This maximum arises from the $\alpha \exp(-\alpha d)$ term in P in equation (4.73). To analyze physically the occurrence of the maximum, we identify the factor $N_o \exp(-\alpha d)$ as the intensity of light reaching the junction and αL_n and αL_p as the number of carriers in a diffusion length from the junction on its two sides which can cross over the junction. As α increases, these numbers increase which increases the contribution

of the diffusive motion to decay rate. However, the intensity of light at the junction itself decreases exponentially with α. The resultant of the two processes gives the maximum at $\alpha = 1/d$, which can also be verified mathematically. The maximum in figure (4.1) does not occur exactly at $\alpha = 1/d$ because of the dependence of J_g on α which is relatively weak as compared to the dependence of P on α.

An interesting thing to note is that the leading term in PVD at low times is proportional to t. In contrast, the leading term in FCVD in a pn diode is $t^{1/2}$, which can be seen by expanding the error functions in the result given by Tewary and Jain (1981). The $t^{1/2}$ behavious of FCVD at low times arises because of the discontinuity in the slopes of profiles at the junction at $t = 0$. In a FCVD experiment the steady-state current ($t < 0$) is not zero but is forced to be zero for $t > 0$. On the other hand, in a PVD experiment in solar cells, the current is zero at all negative and positive times so that there is no discontinuity at $t = 0$. This contrast in the behaviour of PVD and FCVDis apparent in the experimental results of Mahan et. al. (1979).

Another mathematical difference between PVD and FCVD is that the low time expansion of PVD contains even

as well as odd powers of $t^{1/2}$ whereas in FCVD only the odd powers of $t^{1/2}$ exist. The terms containing the even powers of $t^{1/2}$ in the PVD series arise only due to the photogenerated terms in the steady-state, which including the linear term in t, become zero in the limit $\alpha \to \infty$.

Unfortunately, it is not possible to make a detailed comparison between the present theory and the experimental results of Mahan et. al. (1979) because they have used a composite light source for PVD and its spectral response has not been reported. Other material parameters of the solar cell used by Mahan et. al. (1979) are also not known. It should be quite interesting to carry out a detailed experimental study of PVD, particularly its spectral response, which should yield useful information about the minority carrier life time in the diffused layer of solar cell and its surface properties.

4.5 Tricomi Method - Its Applications in Inverting the Laplace Transform

Coupled transient problem in a solar cell can, in principle, be solved by Laplace transform technique. Finite size of the diffused layer and light generated terms in steady-state, however, make it impossible (at present) to find the inverse Laplace transform. In the following

sections we shall apply Tricomi Method (Sneddon 1972 and Ward 1954) for inverting the Laplace transform in equation (4.24) and hence study the decay of open circuit photovoltage in a solar cell.

It will appear below that there are advantages in inverting such a transform in orthogonal functions. If the functions $\phi_1, \phi_2, \phi_3, \ldots\ldots \phi_n$ form a closed, normalized and orthogonal set over the interval 0 to $+\infty$ and if for some function $F(t)$ the coefficients a_n $(n = 0, 1, 2, \ldots)$ are given by the integral

$$a_n = \int_0^{\infty} \phi_n \, F(t)dt, \qquad .. (4.76)$$

supposed convergent, then under suitable conditions the sum

$$a_o\phi_o + a_1\phi_1 + a_2\phi_2 + \ldots\ldots + a_n\phi_n$$

converges to the sum $F(t)$. The advantage of this method is that it offers an approximate solution which is based on the first few terms of an infinite series. It may be shown (Courant and Hilbert 1951) that where inversion is in a series of orthogonal functions and a limited number of terms are only taken, the mean square error is at a minimum when such coefficients as are used are given the values of those in the infinite series.

Of the several orthogonal functions which are available the Laguerre polynomial is the most attractive because its Laplace transform is simple. Its use for the inversion of transforms was first described by F. Tricomi in 1935. He used the definition

$$L_n(t) = \sum_{r=0}^{n} \binom{n}{r} \frac{(-t)^r}{r!} \qquad .. (4.77)$$

so that the polynomials of the lowest order are

$$L_0(t) = 1 \qquad .. (4.78)$$

$$L_1(t) = (1-t)/1! \qquad .. (4.79)$$

$$L_2(t) = (t^2 - 4t + 2)/2! \qquad .. (4.80)$$

$$L_3(t) = (-t^3 + 9t^2 - 18t + 6)/3! \qquad .. (4.81)$$

and so on.

The Laplace Transform of this function is

$$\mathcal{L}\, L_n(t) = \frac{1}{S}\left(\frac{S-1}{S}\right)^n \qquad .. (4.82)$$

and therefore

$$\mathcal{L}\, e^{-ht} L_n(t) = \frac{1}{(S+h)}\left(\frac{S+h-1}{S+h}\right)^n \qquad .. (4.83)$$

where h is a real constant. If then the transform which is to be inverted be $F_1(S)$ and be rewritten in the form

$$F_1(S) = \frac{1}{(S+h)} \sum_{n=0}^{\infty} a_n \left(\frac{S+h-1}{S+h}\right)^n, \qquad .. (4.84)$$

the appropriate inversion is

$$F(t) = e^{-ht} \sum_{n=0}^{\infty} a_n \sigma^n = F_2(\sigma) \qquad .. (4.85)$$

where

$$\sigma = \frac{S + h - 1}{S + h} \qquad .. (4.86)$$

This equation transforms any circle $|\sigma| = r$ in the σ plane into a circle in the S plane which may be made to enclose all the singularities of $(S+h)\,F_1(S)$ by taking suitable values of r and h. The function $(S+h)\,F_1(S)$ may be expanded in powers of σ with a radius of convergence greater than one.

The procedure of inverting a transform by Tricomi Method is as follows (Sneddon 1972):

(a) Given the function $F(S)$, we make the substitution

$$S = b\left(\frac{1+\sigma}{1-\sigma}\right) \qquad .. (4.87)$$

(b) We manipulate the resulting function of σ to give the expression

$$F(S) = \frac{1-\sigma}{2b} \sum_{n=0}^{\infty} a_n \sigma^n \qquad .. (4.88)$$

(c) We interpret the original function $F(t) = \mathcal{L}[F(S), t]$ as the series

$$F(t) = \sum_{n=0}^{\infty} a_n B_n(bt) \qquad .. (4.89)$$

where the functions $B_n(x)$ are defined by the equation

$$B_n(x) = \exp(-x)\, L_n(2x) \qquad .. (4.90)$$

Here b is a real constant which has a powerful effect on the convergence of the series (Ward 1954). The functions $L_n(x)$ have been tabulated by Abramovitz and Stegun (1965) and can also be calculated numerically. Numerical calculations carried out by Ward (1954) by Tricomi method show that this method yields a high degree of accuracy.

4.6 Results and Discussions

In this section we present our results on the decay of open circuit photovoltage decay in the presence of pn coupling as obtained by applying Tricomi Method (Sneddon 1972 and Ward 1954) for inverting the Laplace transform of equation (4.24) for PVD. The expression which governs PVD is given below

$$\Delta V(t) \equiv V(t) - V_o = (-bt + \ln P)kT/q \qquad .. (4.91)$$

where

$$P = -[a_o L_o(2bt) + a_1 L_1(2bt)] \qquad .. (4.92)$$

$$a_o = \theta_o + F\phi_o \qquad .. (4.93)$$

$$a_1 = \theta_1 + F\phi_1 \qquad .. (4.94)$$

$$F = J_o/J_g \qquad .. (4.95)$$

where V_o denotes the open circuit photovoltage as given

by equation (3.7). The constants ϕ_o, ϕ_1, θ_o and θ_1 are given below:

$$\phi_o = \phi_{oa} + \phi_{ob} + \phi_{oc} + \phi_{od} + \phi_{oe} + \phi_{of} + \phi_{og} + \phi_{oh} + \phi_{oi}$$

$$\phi_{oa} = 2L_o(K_3 - K_1P_1 - K_9) \quad \text{.. (4.96)}$$

$$\phi_{ob} = 2D_p K_1 \delta L_o/L_p \quad \text{.. (4.97)}$$

$$\phi_{oc} = -\frac{2K_2 y' L_o b}{(C_j + b\tau_p)} \quad \text{.. (4.98)}$$

$$\phi_{od} = -2K_4 D_p(1 + b\tau_p)^{1/2} L_o L'/L_p T' \quad \text{.. (4.99)}$$

$$\phi_{oe} = \frac{2b K_5(1+ b\tau_p)^{1/2} mL_o}{(C_j + b\tau_p)T'} \quad \text{.. (4.100)}$$

$$\phi_{of} = \frac{2K_6 bL_o}{(C_p + b\tau_n)} \quad \text{.. (4.101)}$$

$$\phi_{og} = \frac{-2b L_o K_7}{(C_j + b\tau_p)} \quad \text{.. (4.102)}$$

$$\phi_{oh} = \frac{-2b L_o K_8(1 + b\tau_p)^{1/2}}{(C_p + b\tau_n)} \quad \text{.. (4.103)}$$

$$\phi_{oi} = \frac{2b mL_o K_5(1+ b\tau_p)^{1/2}}{T'(C_j + b\tau_p)} \quad \text{.. (4.104)}$$

$$\phi_1 = \phi_{1a} + \phi_{1b} + \phi_{1c} + \phi_{1d} + \phi_{1e} + \phi_{1f} + \phi_{1g} + \phi_{1h} + \phi_{1i} \quad \text{.. (4.105)}$$

$$\text{.. (4.106)}$$

$$\phi_{1a} = 2\beta_1(K_3 - K_1P_1 - K_9) \quad .. (4.107)$$

$$\phi_{1b} = 2D_pK_1\beta_{13}/L_p \quad .. (4.108)$$

$$\phi_{1c} = -\frac{2bK_2\beta_{14}}{(C_j+br_p)} \quad .. (4.109)$$

$$\phi_{1d} = -2D_p\beta_{12}K_4(1 + br_p)^{1/2}/L_pT' \quad .. (4.110)$$

$$\phi_{1e} = \frac{2\beta_{15}bK_5(1 + br_p)^{1/2}}{T'(C_j + br_p)} \quad .. (4.111)$$

$$\phi_{1f} = \frac{2\beta_{16}bK_6}{(C_p + br_n)} \quad .. (4.112)$$

$$\phi_{1g} = -\frac{2\beta_{17}bK_7}{(C_j+br_p)} \quad .. (4.113)$$

$$\phi_{1h} = -\frac{2\beta_{18}bK_8(1 + br_n)^{1/2}}{(C_p + br_n)} \quad .. (4.114)$$

$$\phi_{1i} = 2\beta_{19}K_9(1 + br_n)^{1/2} \quad .. (4.115)$$

$$\beta_{19} = A_1^k + k_1L_o \quad .. (4.116)$$

$$\beta_{18} = A_1^k + r_1L_o \quad .. (4.117)$$

$$\beta_{17} = A_1^k + nL_o \quad .. (4.118)$$

$$\beta_{16} = A_1^k + n_pL_o \quad .. (4.119)$$

$$\beta_{15} = mA_1^k + m_1L_o \quad .. (4.120)$$

$$\beta_{14} = y' A_1^k + n_1 L_o \quad .. (4.121)$$

$$\beta_{13} = \delta A_1^k + \delta_1 L_o \quad .. (4.122)$$

$$\beta_{12} = L' A_1^k + L_o e_1 \quad .. (4.123)$$

$$\beta_{11} = \beta_{12} \quad .. (4.124)$$

$$\beta_1 = A_1^k - L_o \quad .. (4.125)$$

$$r_1 = n_p + G_1'/2 \quad .. (4.126)$$

$$r_2 = n_p^2 + G_1' n_p/2 \quad .. (4.127)$$

$$n_p = \frac{(C_p - br_n)}{(C_p + br_n)} \quad .. (4.128)$$

$$C_p = 1 - \alpha^2 L_n^2 \quad .. (4.129)$$

$$m = L' \quad .. (4.130)$$

$$m_1 = L'n + E_1 \quad .. (4.131)$$

$$n_1 = n'y' + y_1' \quad .. (4.132)$$

$$n' = \frac{(C_j - br_p)}{(C_j + br_p)} \quad .. (4.133)$$

$$C_j = 1 - \alpha^2 L_p^2 \quad .. (4.134)$$

$$\delta = y' \quad .. (4.135)$$

$$\delta_1 = y_1' - y' \quad .. (4.136)$$

$$y' = y/J_{no} \qquad .. (4.138)$$

$$y_1' = y_1/J_{no} \qquad .. (4.139)$$

$$P_1 = \frac{D_p}{L_p} M_o \qquad .. (4.140)$$

$$P_2 = M_o D_p U_{33}/L_p \qquad .. (4.141)$$

$$P_3 = D_p U_{11}/L_p \qquad .. (4.142)$$

$$K_1 = q\alpha N_o \tau_p \exp(-\alpha d)/C_j \qquad .. (4.143)$$

$$K_2 = qL_p\alpha N_o \tau_p \exp(-\alpha d)/C_j \qquad .. (4.144)$$

$$K_3 = q\alpha L_p N_o(s+\alpha D_p)[1 - \frac{\eta C_j}{(s+\alpha D_p)\alpha\tau_p}] \qquad .. (4.145)$$

$$K_4 = K_3 U_{33} L_p/D_p \qquad .. (4.146)$$

$$K_5 = q\alpha L_p N_o \tau_p(s+\alpha D_p)/C_j \qquad .. (4.147)$$

$$K_6 = q\alpha^2 L_n^2 N_o \tau_n \exp(-\alpha d)/C_p \qquad .. (4.148)$$

$$K_7 = q\alpha^2 L_p^2 N_o \tau_p \exp(-\alpha d)/C_j \qquad .. (4.149)$$

$$K_8 = q\alpha L_n N_o \tau_n \exp(-\alpha d)/C_p \qquad .. (4.150)$$

$$K_9 = q\alpha L_n N_o \exp(-\alpha d)/C_p \qquad .. (4.151)$$

$$U_{11} = s\cosh d/L_p + \frac{D_p}{L_p} \sinh d/L_p \qquad .. (4.152)$$

$$U_{33} = s\sinh d/L_p + \frac{D_p}{L_p} \cosh d/L_p$$

$$M_o = U_{11}/U_{33} \quad .. (4.153)$$

$$\theta_o = a'\alpha^{I} + b'\alpha^{II} + c'\alpha^{III} \quad .. (4.154)$$

$$\theta_1 = a'\alpha_1^{I} + b'\alpha_1^{II} + c'\alpha_1^{III} \quad .. (4.155)$$

$$a' = -2J_{po}(1 + br_p)^{1/2} \quad .. (4.156)$$

$$b' = (M_o J_{po} + J_{no}) \quad .. (4.157)$$

$$c' = -J_{no}(1 + br_n)^{1/2} \quad .. (4.158)$$

$$\alpha^{III} = L_o \quad .. (4.159)$$

$$\alpha_1^{III} = A_1^k + k_1 L_o \quad .. (4.160)$$

$$\alpha^{II} = \alpha^{III} \quad .. (4.161)$$

$$\alpha_1^{II} = a_1^k - L_o \quad .. (4.162)$$

$$\alpha^{I} = WL_o \quad .. (4.163)$$

$$\alpha_1^{I} = WA_1^k + h_1 L_o \quad .. (4.164)$$

$$A_1^k = -C_1/C \quad .. (4.165)$$

$$k_1 = (G_1'/2) - 1 \quad .. (4.166)$$

$$h_1 = f_1 - W \quad .. (4.167)$$

$$f_1 = W_1 + (G_1 W/2) \quad .. (4.168)$$

$$e_1 = E_1 - L' \quad .. (4.169)$$

$$B_1 = A_1' + G_1 L'/2 \quad .. (4.170)$$

$$A_1' = -T_1/T' \quad .. (4.171)$$

$$T' = XR \quad .. (4.172)$$

$$T_1 = XR_1 + X_1 R \quad .. (4.173)$$

$$X = (S' + S'')/2 \quad .. (4.174)$$

$$X_1 = -XU_1/2 \quad .. (4.175)$$

$$S' = \exp\left(-\frac{d\sqrt{\tau_p}}{L_p K}\right) \quad .. (4.176)$$

$$S'' = 2d\sqrt{\tau_p}/L_p \quad .. (4.177)$$

$$K = S'' \quad .. (4.178)$$

$$K' = \left(\frac{1 + b\tau_p}{\tau_p}\right)^{1/2} \quad .. (4.179)$$

$$C_o = J_{no}(1 + b\tau_n)^{1/2} \quad .. (4.180)$$

$$C = C_o + y \quad .. (4.181)$$

$$C_1 = y_1 + G_1' C_o/2 \quad .. (4.182)$$

$$y = WC_o \quad .. (4.183)$$

$$y_1 = (W_1 + G_1 W/2)C_o \quad .. (4.184)$$

$$G_1' = 1 - u' \quad .. (4.185)$$

$$u' = \frac{1 - br_n}{1 + br_n} \quad .. (4.186)$$

$$u = \frac{1 - br_p}{1 + br_p} \quad .. (4.187)$$

$$W = J_o/R \quad .. (4.188)$$

$$W_1 = (J_o A_{11} + J_1)/R \quad .. (4.189)$$

$$A_{11} = -R_1/R \quad .. (4.190)$$

$$R_o = (D_p/L_p)(1 + br_p)^{1/2} \quad .. (4.191)$$

$$R = R_o + sL' \quad .. (4.192)$$

$$R_1 = R_o G_1/2 + sM_1 \quad .. (4.193)$$

$$J_o = s + R_o L' \quad .. (4.194)$$

$$J_1 = R_o H_1 \quad .. (4.195)$$

$$H_1 = M_1 + G_1 L'/2 \quad .. (4.196)$$

$$G_1 = 1 - u \quad .. (4.197)$$

$$M_1 = A_1(1 - S) - K_{11} L_o/2 \quad .. (4.198)$$

$$L_o = 1 - S_o + S_o^2 \quad .. (4.199)$$

$$A_o = 1 - 2S_o + 3S_o^2 - 4S_o^3 \quad .. (4.200)$$

$$A_1 = -K_{11} A_o/2 \quad .. (4.201)$$

$$U_1 = KK' X_{11} \quad .. (4.202)$$

$$X_{11} = (1 - M) \quad .. (4.203)$$

$$M = u \quad .. (4.204)$$

$$S = \exp(-KK') \quad .. (4.205)$$

$$K_{11} = -U_1 S_o \quad .. (4.206)$$

$$L' = L_o(1 - S_o) \quad .. (4.207)$$

Equation (4.91) for PVD is based on the assumptions that (i) the space charge layer effects are negligible (Moll et. al. 1962 and Jain 1981), (ii) the Boltazmann law is valid in the time dependent case also (Nosov 1969, Lindholm and Sah 1976, Neugroschel et. al. 1977, Lindholm et. al. 1977 and Neugroschel et. al. 1978) and (iii) the incident radiation is monochromatic.

In the following subsections the effect of relative dark saturation current of the diffused layer (J_o), absorption coefficient of light (α), surface generation coefficient (η), surface recombination velocity (s), relative excess minority carrier life time in the diffused layer (T) and thickness of the diffused layer (d) on PVD as calculated by using equation (4.91) will be analysed.

4.6.1 Effect of Relative Dark Saturation Current of the Diffused Layer on PVD

Effect of J_o on PVD as calculated by using equation

(4.91) is shown in figure 4.2. From this figure it is obvious that the presence of pn coupling causes a curvature in the beginning of the transient which increases as the value of J increases. Our this observation is in agreement with the theoretical observation of Tewary and Jain (1981) for the case of pn junction diode - the curvature of the FCVD plot increases with J and is attributed to the effect of band gap narrowing (discussed in chapter 1) caused by the heavy doping in the diffused layer. Experimental results of Neugroschel et. al. (1978) and Mahan et. al.(1979) on the decay of open circuit voltage also support this. Experimental results quoted by these authors show that PVD (or FCVD) curves are non-linear in the beginning of the transient.

4.6.2 Effect of Absorption Coefficient of Light on PVD

Effect of α on PVD is shown in figure 4.3. Corresponding points for the uncoupled case as obtained by using Jain's (1981) formulation (equation 2.48) have also been shown on this figure. The main observations of this figure are given below.

(i) an increase in the value of α enhances the decay rate.

(ii) for small values of time the coupled and uncoupled theories differ greatly but predict a common decay rate for large values of time

(iii) effect of pn coupling on PVD is more pronounced for larger values of α ($\geq 10^3$ cm^{-1}) than for its smaller values ($< 10^3$ cm^{-1}).

Our observation (i) is a well known case (Jain 1981 and Dhariwal and Vasu 1981). The faster decay of photo-voltage for larger α is caused by the increased slope of the excess minority carrier profile in steady-state. Another characteristic of the spectral dependence of PVD as mentioned in chapter 2 and also observed by Jain (1981) is that for $\alpha L_n << 1$ and $\alpha L_n >> 1$, the decay rate is independent of α. Consequently, the PVD curves for $\alpha = 0.1$ and 1 in figure 4.2 overlap.

Observation (ii) amounts to saying that the effect of pn coupling is substantial only in the initial stages of the decay. This is what Tewary and Jain (1981) remark regarding the effect of pn coupling on FCVD in a diode - effect of pn coupling is substantial for small values of time only. For large values of time decay is mainly controlled by the excess minority carrier life time in the base and consequently, both the coupled and uncoupled theories predict nearly the same decay rate which explains observation (ii).

To explain observation (iii) let us recall that the carrier concentration in the base (n(x)) increases with x

away from the junction for low values of α. Therefore as soon as light is switched off the junction loses carriers due to recombination, but also gains some carriers by diffusion from the nearby region which has a higher concentration of carriers. Thus the decay rate of voltage which depends upon the number of carriers at the junction, is slowed down by pn coupling. For large α, the carrier concentration falls as x increases from zero. In this case the junction loses carriers by recombination as well as by diffusion, which makes the voltage decay faster than that in the absence of pn coupling. In addition to this Shockley condition (equation 3.4) also requires that irrespective of the value of α some carriers on the base side must cross over the junction to the diffused layer side because $\tau_p \ll \tau_n$. This apparently increases the decay rate. The net decay rate in the presence of pn coupling is thus the resultant of these two processes (one due to α and other due to Shockley condition) and is greater than that in the uncoupled case. Effect of α on this is as follows:

(i) for small values of α, the recombination and crossing over of carriers to the diffused layer side contribute to it whereas diffusion (in the beginning of the transient) of carriers on the base side opposes it.

(ii) for large values of α, all the three factors namely

recombination, crossing over of carriers to the diffused layer side and diffusion contribute to it and will therefore be higher than that in case (i). This explains the observation.

4.6.3 Effect of Surface Generation Coefficient on PVD

Effect of surface generation coefficient (η) as introduced by Tewary and Jain (1980) in the surface boundary condition for solar cells is shown in figure 4.4. From this figure we notice that the effect of η on PVD is more pronounced for smaller values of α which is consistent with our observation regarding the effect of η on the decay rate A in section 4.4. (figure 4.1). A decreases with η for $\alpha < 10^2$ cm^{-1}. For $\alpha \geq 10^2$ cm^{-1} however, effect of η on PVD is independent of α which is also obvious in figure 4.1 (curves for $s = 10^4$ cms^{-1}) - A Vs α curves for different η meet at about $\alpha = 10^2$ cm^{-1} and overlap thereafter.

4.6.4 Effect of Surface Recombination Velocity on PVD

Effect of surface recombination velocity (s) on PVD is shown in figure 4.5. It is well known that an increase in the value of surface recombination velocity enhances the decay rate (see, for example, Nosov 1969, Choo and Masur 1970 and Bassett et. al. 1973) and may also be observed in figure 4.4. Another observation which emerges from figure 4.4 is that the effect of s on PVD is more pronounced for $\alpha = 10^3$ cm^{-1}

than for $\alpha = 10^2$ cm^{-1}. This is because as α increases, the absorption length of light ($= 1/\alpha$) decreases. Consequently, the effect of the diffused layer parameters and so of s on PVD increases. Similar effect of s on the steady-state open circuit photovoltage V_o may be observed in figure 3.2 (chapter 3): effect of s on V_o increases as α increases for $\alpha \geq 10$ cm^{-1} (curves for $\eta = 0$).

4.6.5 Effect of Relative Excess Minority Carrier Life Time in the Diffused Layer on PVD

Effect of relative excess minority carrier life time ($T \equiv \tau_p/\tau_n$) on PVD is shown in figure 4.6. From this figure we see that as T increases the decay rate decreases. This is physically understood because decay rate is governed by the life time of carriers and therefore as life time increases the decay rate decreases.

4.6.6. Effect of Diffused Layer Thickness on PVD

Effect of diffused layer thickness (d) on PVD is shown in figures4.7, 4.8 and 4.9 for $J = 0.1$, 5 and 10 respectively. The main observations of this figure are given below.

(i) effect of d on PVD is to enhance the decay rate and increases with J and

(ii) For a given value of J, effect of d on PVD increases as α increases.

These observations can be explained as follows. We know that as J increases the importance of the diffused layer increases and therefore effect of the diffused layer parameters and so of d on PVD increases. Since pn coupling increases the decay rate, so also will d. This explains our observation (i).

Regarding observation (ii), we know that as α increases the absorption length of light L_a ($= 1/\alpha$) decreases and therefore sensitivity of PVD to the diffused layer parameters increases. Now for a given value of J if we increase d, the decay rate for larger α will obviously be higher than that for low α.

From the foregoing analysis we conclude that the measurement of PVD in its initial stages would yield useful information about the excess minority carrier life time in the diffused layer and its surface properties.

It may be mentioned that theories exist (see, for example, McKelvey 1966 and Mallinson and Landeberg 1977a) which account for pn coupling in a solar cell in the steady-stage. The effect of diffused layer was, however, found to be negligible (see, for example, Neville 1978) which justifies the usual neglect of pn coupling in steady-stage in the absence of band gap narrowing. In the transient case, viz. PVD in a solar cell, pn coupling has not been included in any published calculations.

The effect of the transition region recombination has been theoretically analysed by Ellis and Moss (1970) and Mallinson and Landsberg (1977b) and is found to be important at low intensities. This and other contributions like those due to series resistance, bulk field etc. may be included in an elaborate design calculation by using the standard methods.

4.7 Convergence of the Series for Open Circuit Photovoltage Decay

The parameter b introduced in the last section has a powerful effect on the convergence of the series in equation (4.91). The best value of b that would lead to rapid convergence of the series is determined by the coefficients of the denominator of the transform. It has been found by Ward (1954) that the best value of b falls around the geometric mean of the roots of the transform. Should it result in slowly converging terms of like sign b should be made larger. On the other hand if it results in slow convergence with alternate signs, b should be made smaller.

The above guidelines for the choice of b help only when we are able to identify the roots of the transform, e.g. if our function is of the form $(S+c)^{-1}(S+d)^{-1}$ then $(cd)^{1/2}$ would be the best choice for the parameter b to start with. In our case, however, we come across the functions $(S+1/\tau_n)^{-1/2}$, $(S+1/\tau_p)^{-1/2}$, $(S+\frac{1-\alpha^2L_n^2}{\tau_n})^{-1}$ and $(S+\frac{1-\alpha^2L_p^2}{\tau_p})^{-1}$ and their

cross products. Moreover, all these coefficients viz. $1/\tau_n$, $1/\tau_p$, $(1-\alpha^2 L_n^2)/\tau_n$ and $(1-\alpha^2 L_p^2)/\tau_p$ appear in different combinations. All this mechanism makes it very difficult to relate the best value of b with these coefficients.

Regarding the choice of t, $t \sim 1/b$ would yield the best results. This is expected mathematically because for $\sigma = 0$ equation (4.87) reduces to

$$S = b \qquad .. (4.208)$$

The inverse Laplace transform of equation (4.208) yields $t = 1/b$.

To calculate PVD transient by this method, we started with $b = 0.2/\tau_n$ and increased it in small steps. For a given value of b we took $t = 0.95/b$ and thus calculated PVD by using equation (4.91). For a given value of b, the coefficients a_p and a_1 which show the convergence of the PVD series in equation (4.91) have been given in table 4.1.

As one check of the present theoretical formulae we neglected pn coupling by putting J and $L_p = 0$ and calculated PVD corresponding to the uncoupled case. These values when compared with the corresponding values obtained by using Jain's (1981) theory (equation 2.48) for uncoupled case showed a good agreement.

4.8 Conclusions

A detailed analysis of pn coupling in the transient state has been carried out. The theory is quite rigorous and is based upon the powerful mathematical technique of Laplace transform (Sneddon 1972). Importance and application of Tricomi Method (Sneddon 1972 and Ward 1954) for inverting the Laplace transform have been discussed.

It is shown that the leading term in the low time expansion of PVD is linear in time and is independent of the detailed nature of the excitation source (optical). The effect of various diffused layer parameters on PVD has been analysed. It is found that

(i) effect of pn coupling on PVD is substantial only at low values of time

(ii) pn coupling increases the curvature of the PVD curve in the initial stages of the transient

(iii) an increase in the value of the absorption coefficient of light increases the decay rate

(iv) effect of surface generation coefficient as introduced by Tewary and Jain (1980) in the surface boundary condition for solar cell is more pronounced at smaller values of α.

(v) surface absorption of carriers characterised by surface recombination velocity increases the decay rate

(vi) an increase in the value of the relative excess minority carrier life time in the diffused layer decreases the decay rate and

(vii) an increase in the thickness of the diffused layer increases the decay rate which is more pronounced for the larger values of the relative dark saturation current and the absorption coefficient of light.

It is concluded that the measurement of PVD in its initial stages should yield useful information about the excess minority carrier life time in the diffused layer and its surface properties.

References

1. Abromovitz M. and Stegun I.A. (1965) Ed. Handbook of Mathematical Functions (N.Y: Dover Publications).

2. Bassett R.J., Fulop W. and Hogarth C.A. (1973) Int. J. Electronics 35 177-92.

3. Choo S.C. and Mazur R.G. (1970) Solid State Electronics 13 553-64.

4. Courant R. and Hilbert D. (1931) Methoden der Mathematischen Physik I.

5. Dhariwal S.R., Kothari L.S. and Jain S.C. (1976) IEEE Trans. on Electron Devices ED-23 504-07.

6. Dhariwal S.R. and Vasu N.K. (1981) IEEE Electron Device Letters EDL-2 53-55.

7. Ellis B. and Moss T.S. (1970) Solid State Electronics 13 1-24.

8. Erdelyi A., Magnus W., Oberhettinger F. and Tricomi F.G. (1954) Tables of Integral Transform Vol I (N.Y.: Mc-Graw-Hill).

9. Jain S.C. (1981) Solid State Electronics 24 179-83.

10. Lindholm F.A. and Sah C.T. (1976) J.Appl. Phys. 47 4203-05.

11. Lindholm F.A., Neugroschel A., Sah C.T., Godlewski M.P. and Brandhorst Jr. H.W. (1977) IEEE Trans. on Electron Devices ED-24 402-10.

12. Mahan J.E., Ekstedt T.W., Frank R.I. and Kaplow R. (1979) IEEE Trans. Electron Devices ED-26 733-39.

13. Mallinson J.R. and Landsberg P.T. (1977a) Proc. Royal Soc. London A 355 115-30.

14. Mallinson J.R. and Landsberg P.T. (1977b) Proceedings of the International Photovoltaic Solar Energy Conversion held at Luxembourg; Published by D. Reidel Publishing Company Dordrecht, Holland.

15. McKelvey J.P. (1966) Solid State and Semiconductor Physics (N.Y: Harper and Row).

16. Moll J.L., Krakauer S. and Shen R. (1962) Proc. IRE 50 43-53.

17. Neugroschel A., Lindholm F.A. and Sah C.T. (1977) IEEE Trans. on Electron Devices ED-24 662-71.

18. Neugroschel A., Chen P.J., Pao S.C. and Lindholm F.A. (1978) IEEE Trans. on Electron Devices ED-25 485.

19. Neville Rechard C. (1978) Solar Energy Conversion: The Solar Cell (N.Y: Elsevier Scientific Publishing Company).

20. Nosov Y.R. (1969) Switching in Semiconductor Diodes (N.Y : plenum Press).

21. Sneddon I.N. (1972) The Use of Integral Transforms (N.Y : McGraw-Hill).

22. Tewary V.K. and Jain S.C. (1980) J. Phys. D: Appl. Phys. 13 835-37.

23. Tewary V.K. and Jain S.C. (1981) Technical Report Solid State Physics Laboratory Delhi, India.

24. Ward E.E. (1954) Proc. Cambridge Philosphical Soc. 50 49-59.

Table 4.1

Values of coefficients a_o and a_1 for $s = 10^3$ cms^{-1}, $\eta = 0$ and $J = 30$.

b \ α	10^2 cm^{-1}		10^3 cm^{-1}	
	a_o	a_1	a_o	a_1
0.97×10^5	-0.23	-0.10	-0.089	-0.012
0.15×10^6	-0.31	-0.12	-0.11	-0.024
0.19×10^6	-0.38	-0.13	-0.14	-0.033
0.24×10^6	-0.44	-0.12	-0.16	-0.039
0.29×10^6	-0.49	-0.11	-0.18	-0.044
0.34×10^6	-0.54	-0.096	-0.2	-0.047
0.39×10^6	-0.58	-0.078	-0.22	-0.048
0.44×10^6	-0.62	-0.058	-0.23	-0.049
0.48×10^6	-0.65	-0.038	-0.25	-0.049
0.53×10^6	-0.69	-0.017	-0.26	-0.048
0.58×10^6	-0.72	0.004	-0.28	-0.047
0.63×10^6	-0.75	0.026	-0.29	-0.046
0.68×10^6	-0.77	0.047	-0.31	-0.044
0.73×10^6	-0.8	0.068	-0.32	-0.041
0.78×10^6	-0.82	0.088	-0.33	-0.039
0.82×10^6	-0.85	0.11	-0.34	-0.036
0.87×10^6	-0.87	0.13	-0.35	-0.033
0.92×10^6	-0.91	0.15	-0.37	-0.030
0.97×10^6	-0.92	0.17	-0.38	-0.027
0.10×10^7	-0.94	0.19	-0.39	-0.024
0.11×10^7	-0.96	0.20	-0.40	-0.020
0.111×10^7	-0.99	0.22	-0.41	-0.017
0.121×10^7	-1.00	0.26	-0.43	-0.01
0.126×10^7	-1.02	0.27	-0.44	-0.006
0.131×10^7	-1.03	0.29	-0.45	-0.003

Captions for Figures

Figure 4.1: Variation of decay rate (A) of open circuit photovoltage at $t \approx 0$ as a function of absorption coefficient of light (α). For curves a, b and c, $s = 10^4$ cms^{-1} and $\eta = 0.1$, 0.01 and 0 respectively. For curves d, e and f, $s = 10^7$ cms^{-1} and $\eta = 0.1$, 0.01 and 0 respectively.

Figure 4.2: Effect of relative dark saturation current of diffused later (J) on PVD for $\alpha = 10^3$cm^{-1}, $s = 10^3$ cms^{-1}, $\eta = 0.01$, $T = 0.001$ and $d = 0.1\mu m$. Curves 1, 2 and 3 are for $J = 0.1$, 5 and 10 respectively.

Figure 4.3: Effect of absorption coefficient of light (α) on PVD for $s = 10^4$ cms^{-1}, $\eta = 0$, $T = 0.0003$, $J = 30$ and $d = 0.1$ μm. For curves 1, 2, 3 and 4; $\alpha = 1$, 10, 10^2 and 10^3 cm^{-1} respectively. Corresponding points for the uncoupled, case are shown by 0, X, Δ and □ respectively.

Figure 4.4: Effect of surface generation coefficient (η) on PVD for $s = 10^4$ cms^{-1}, $J = 30$, $T = 0.0003$ and $d = 0.1$ μm. Curves 1 and 2 are for $\eta = 0$ and 0.01 respectively. a, b and c denote the curves for $\alpha = 10$, 10^2 and 10^3 cm^{-1} respectively.

Figure 4.5: Effect of surface recombination velocity (s) on PVD for J = 30, T =0.0003, d = 0.1 μm and η = 0. Curves 1 and 2 are for α = 10^2 and 10^3 cm^{-1} respectively. a, b and c denote the curves for s = 10^2, 10^3 and 10^4 cms^{-1} respectively.

Figure 4.6: Effect of relative excess minority carrier life time in the diffused layer (T) on PVD for J = 0.1, s = 10^3 cms^{-1}, α = 10^3 cm^{-1} and d = 0.1 μm. Curves 1 and 2 are for T = 0.001 and 0.01 respectively.

Figure 4.7: Effect of diffused layer thickness (d) on PVD for J = 0.1, s = 10^3 cms^{-1}, η = 0.01, T = 0.001. For curve 1, α = 10 cm^{-1} and d = 0.1 μm (different values of d yield the same curve). For curves 2 and 3 d = 0.1 μm (or 0.3 μm) and 0.5 μm respectively and α = 10^2 cm^{-1}. For curves 4,5 and 6; d = 0.1, 0.3 and 0.5 μm respectively and α = 10^3 cm^{-1}.

Figure 4.8: Effect of diffused layer thickness (d) on PVD for J = 5, s = 10^3 cms^{-1}, η = 0.01 and T= 0.001. For curves 1,2 and 3; α = 10, 10^2 and 10^3 cm^{-1} respectively. a, b and c denote the curves for d = 0.1, 0.3 and 0.5 μm respectively.

Figure 4.9: Effect of diffused layer thickness (d) on PVD for $J = 10$, $s = 10^3$ cms^{-1}, $\eta = 0.01$ and $T = 0.001$. For curves 1, 2 and 3; $\alpha = 10$, 10^2 and 10^3 cm^{-1} respectively. a, b and c denote the curves for $d = 0.1$, 0.3 and 0.5 μm respectively.

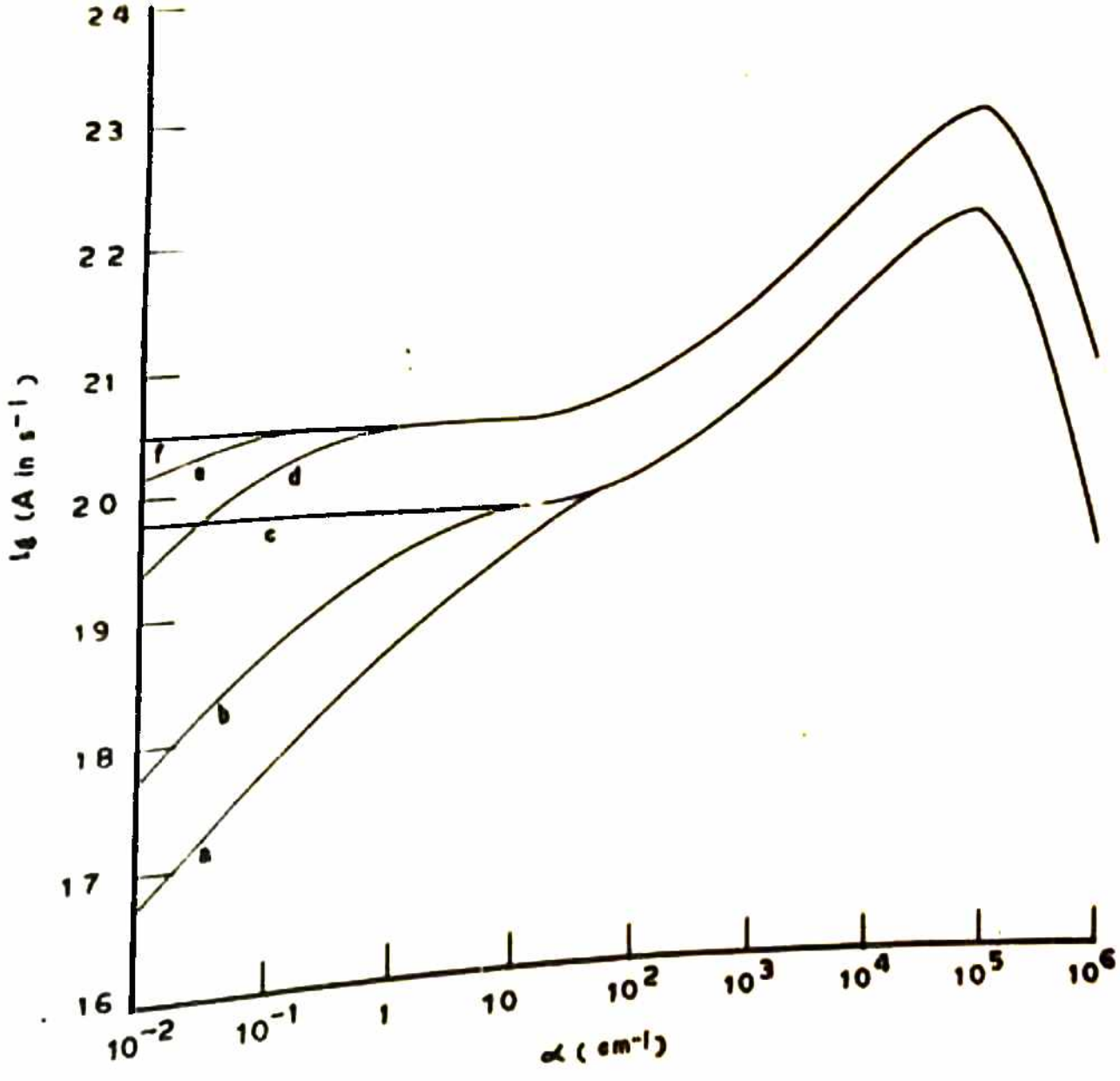
24
23
22
21
20
19
18
17
16
$\log (A \ln s^{-1})$
f
e
d
c
b
a
10^{-2}
10^{-1}
1
10
10^2
10^3
10^4
10^5
10^6
α (cm^{-1})

FIG. 4.1

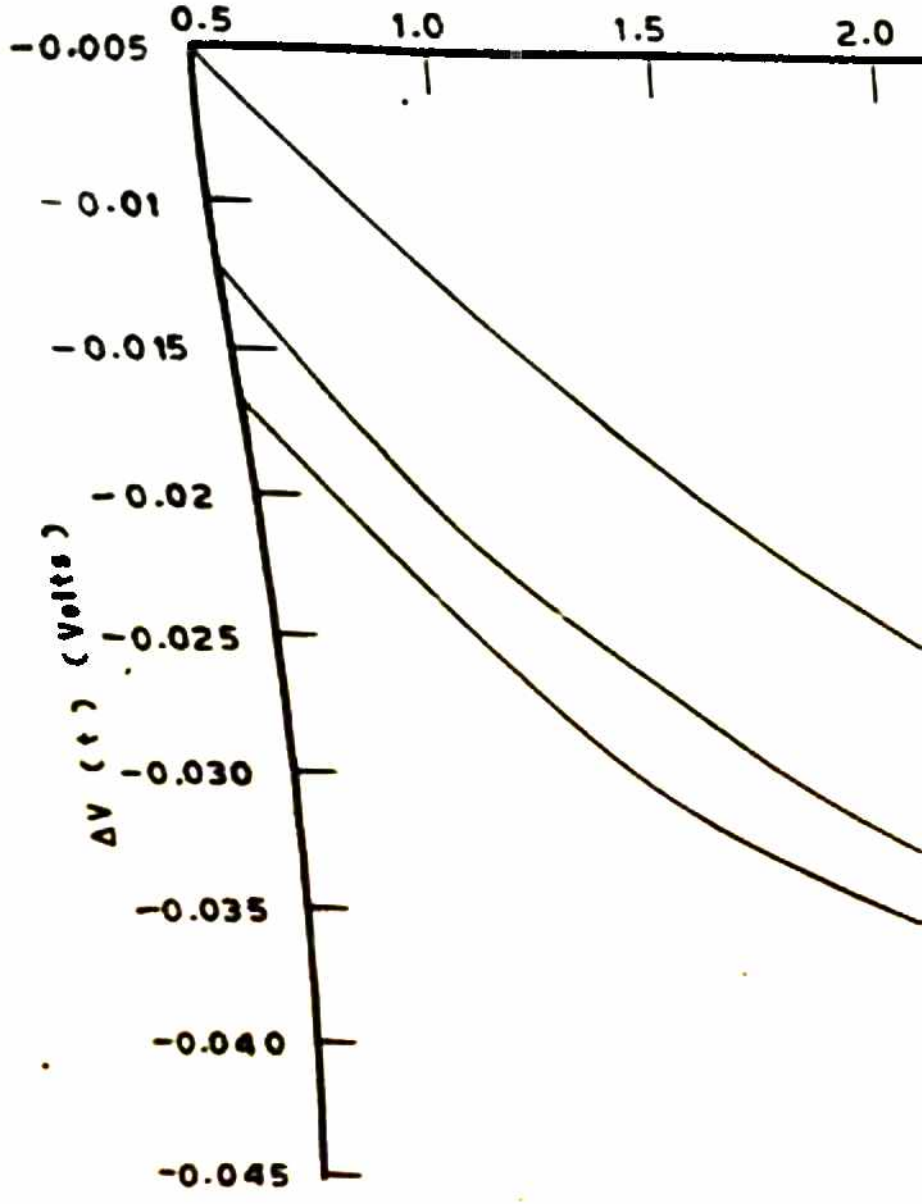
0.5
1.0
1.5
2.0
-0.005
-0.01
-0.015
-0.02
-0.025
-0.030
-0.035
-0.040
-0.045
ΔV (t) (Volts)

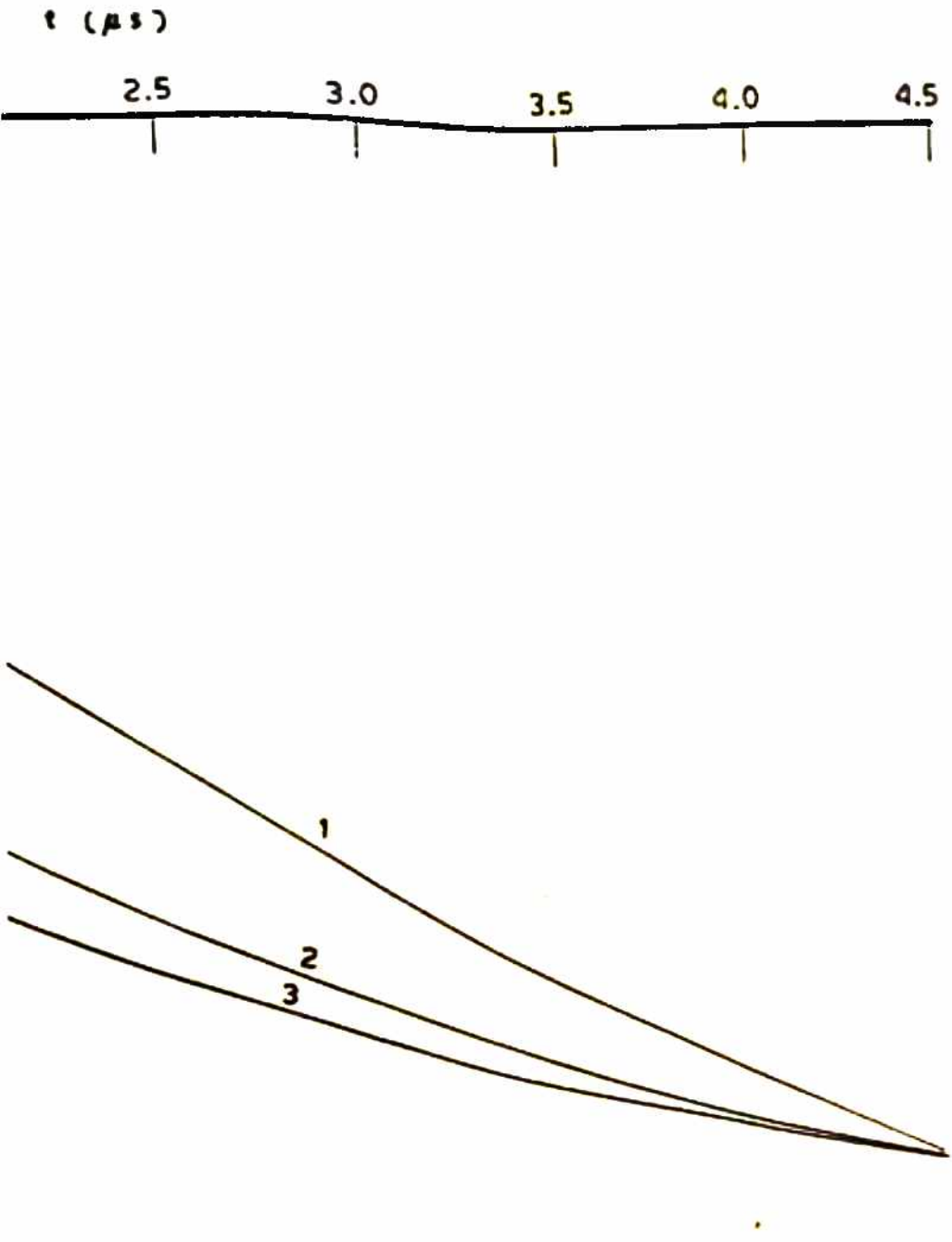

FIG. 4.2

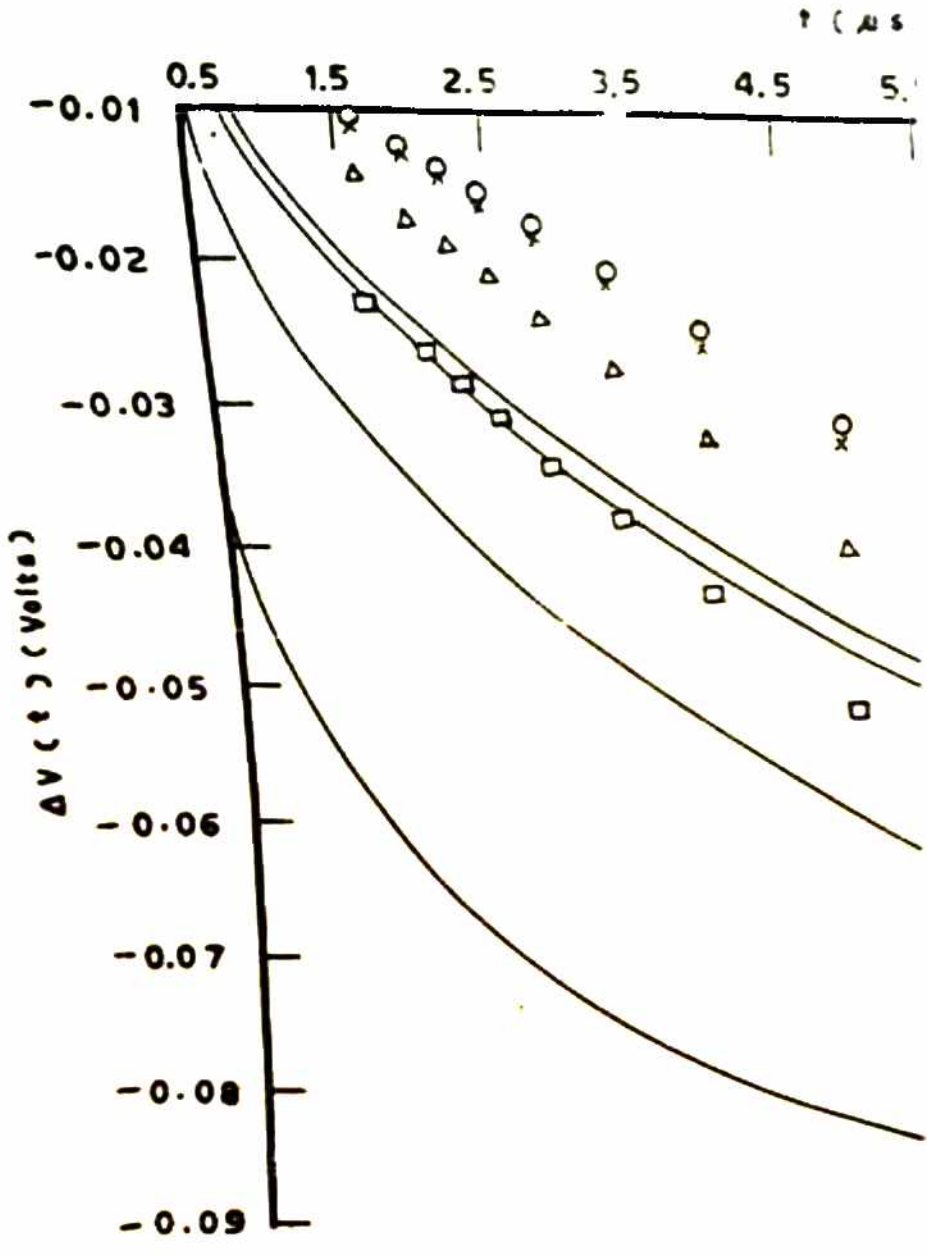
t (μs
0.5
1.5
2.5
3.5
4.5
5.
-0.01
-0.02
-0.03
-0.04
-0.05
-0.06
-0.07
-0.08
-0.09
ΔV (t) (Volts)

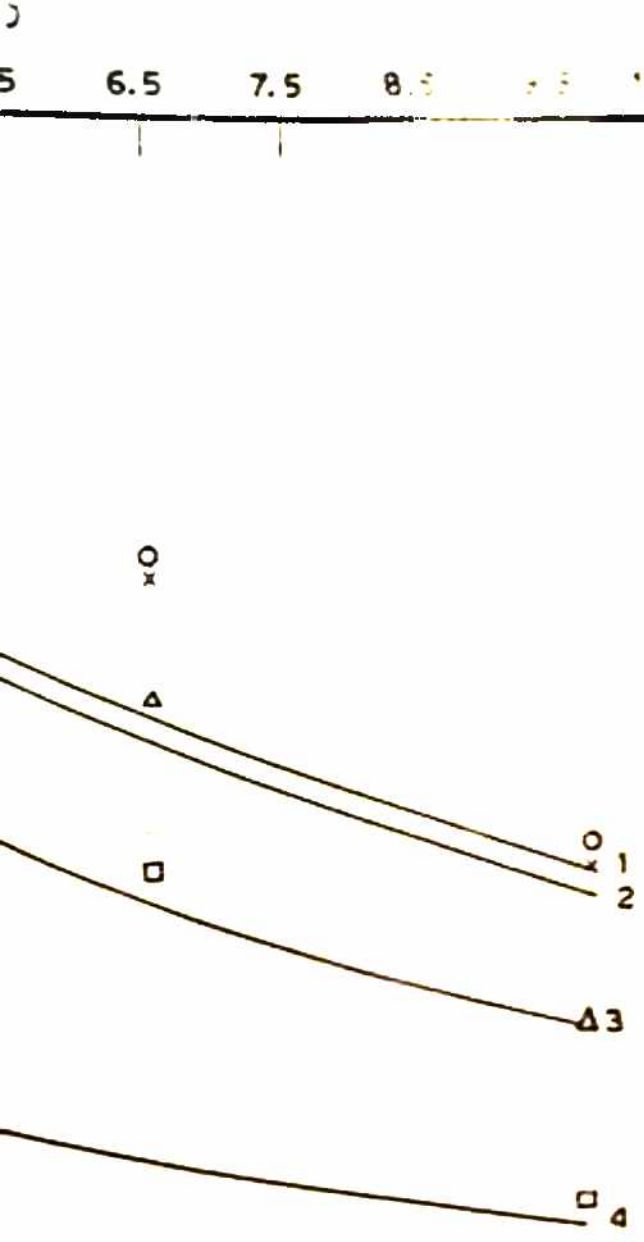

FIG. 4.3

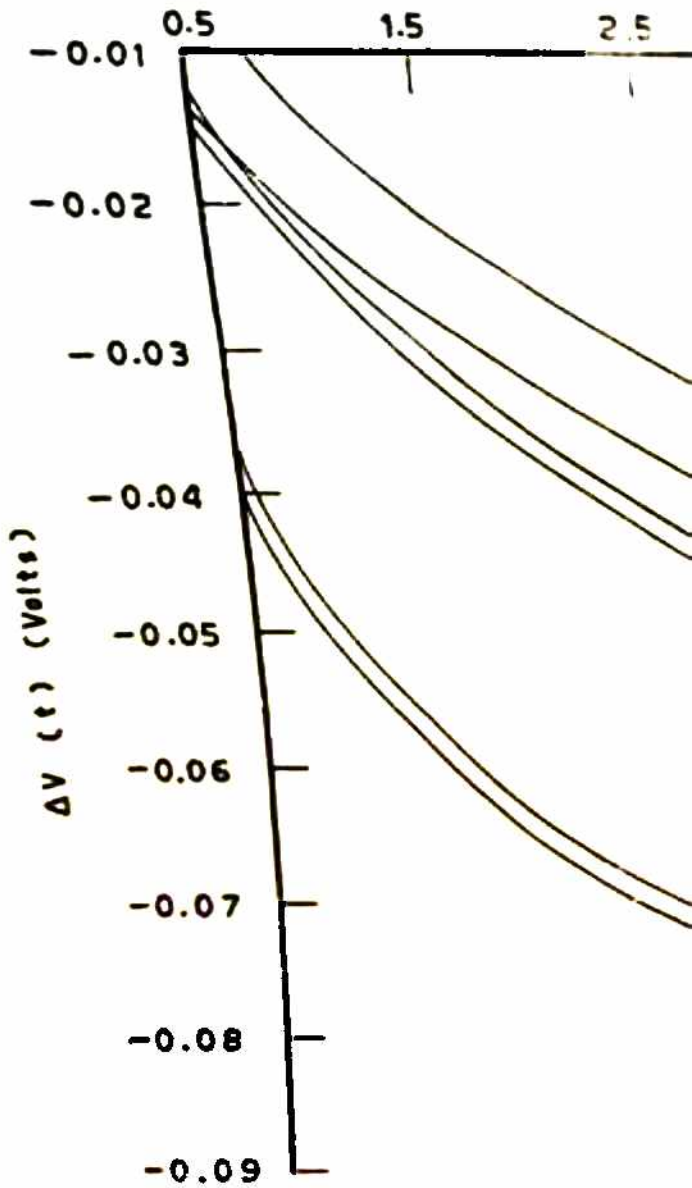
0.5
1.5
2.5
-0.01
-0.02
-0.03
-0.04
-0.05
-0.06
-0.07
-0.08
-0.09
ΔV (t) (Volts)

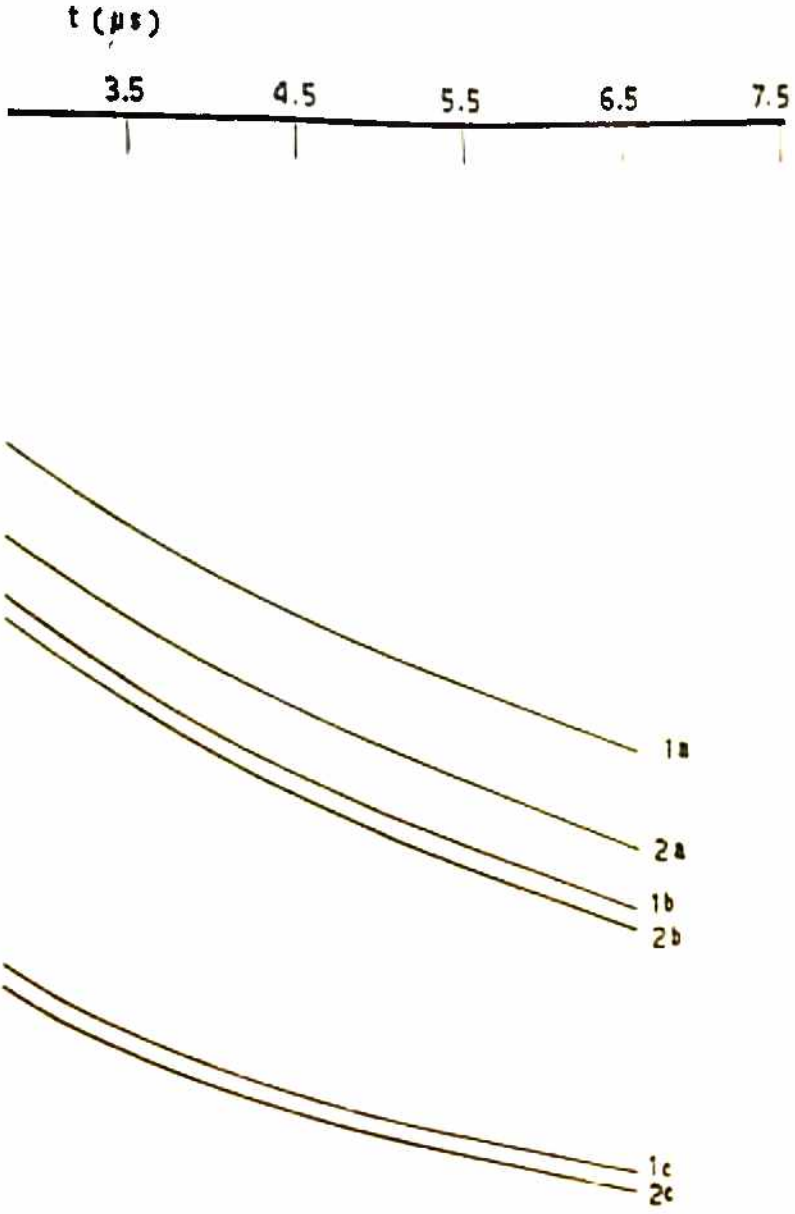

FIG. 4.4

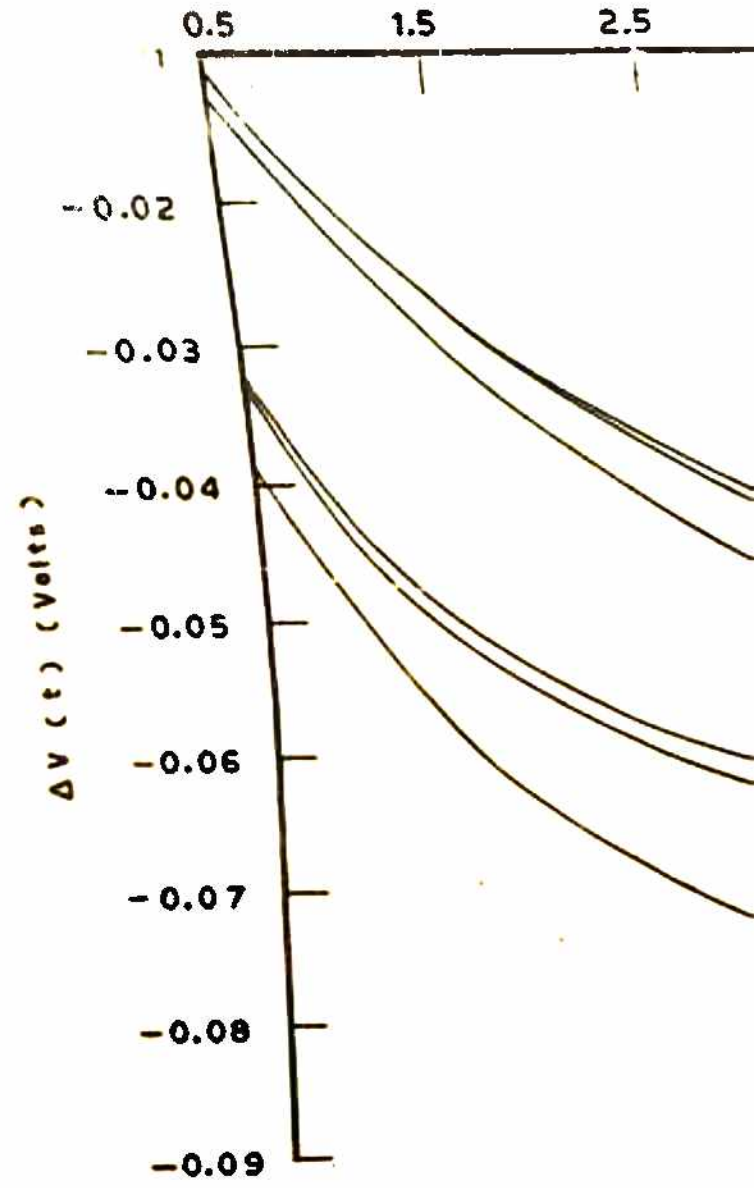
0.5
1.5
2.5
-0.02
-0.03
-0.04
-0.05
-0.06
-0.07
-0.08
-0.09
ΔV (t) (Volts)

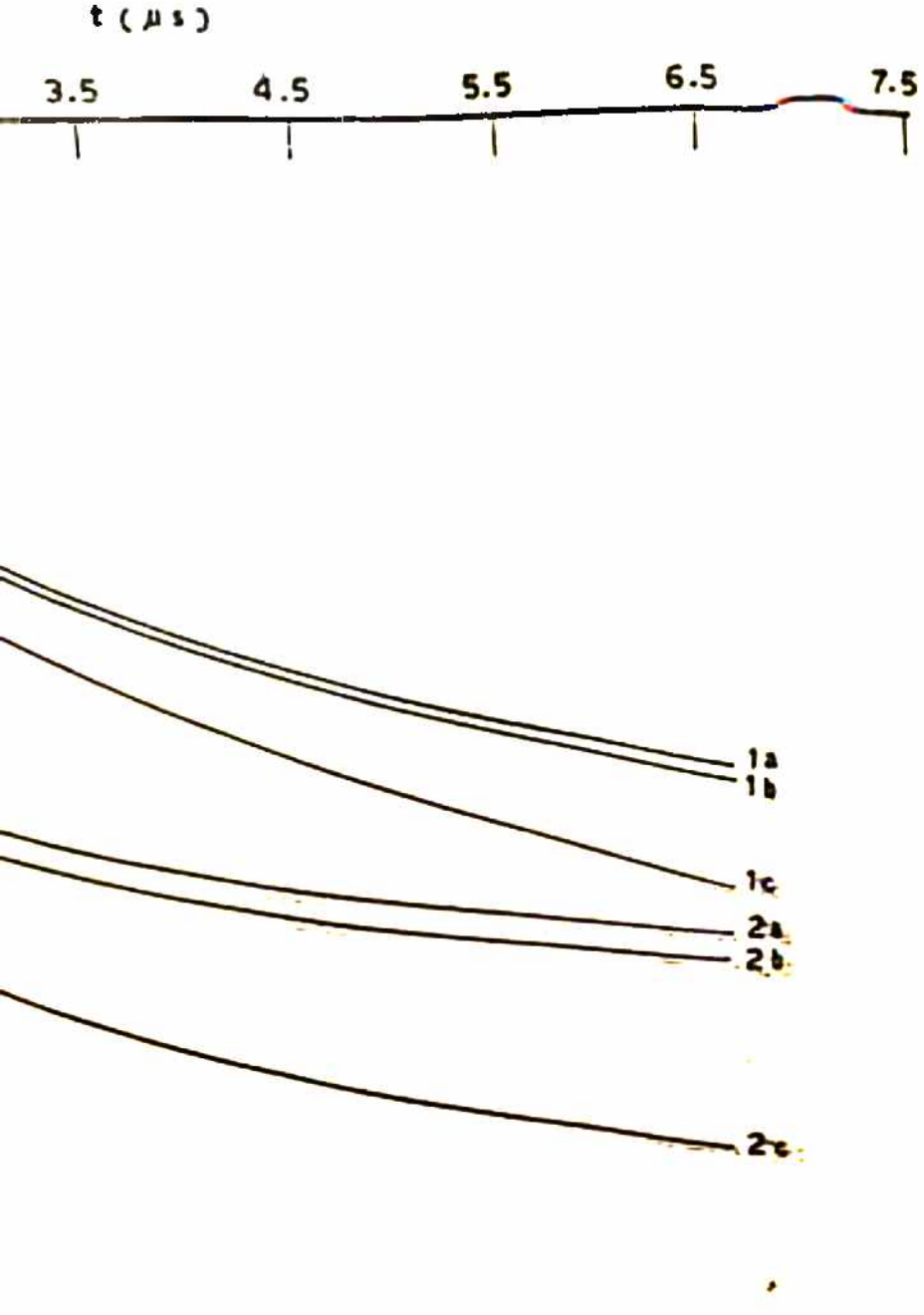

FIG. 4.5

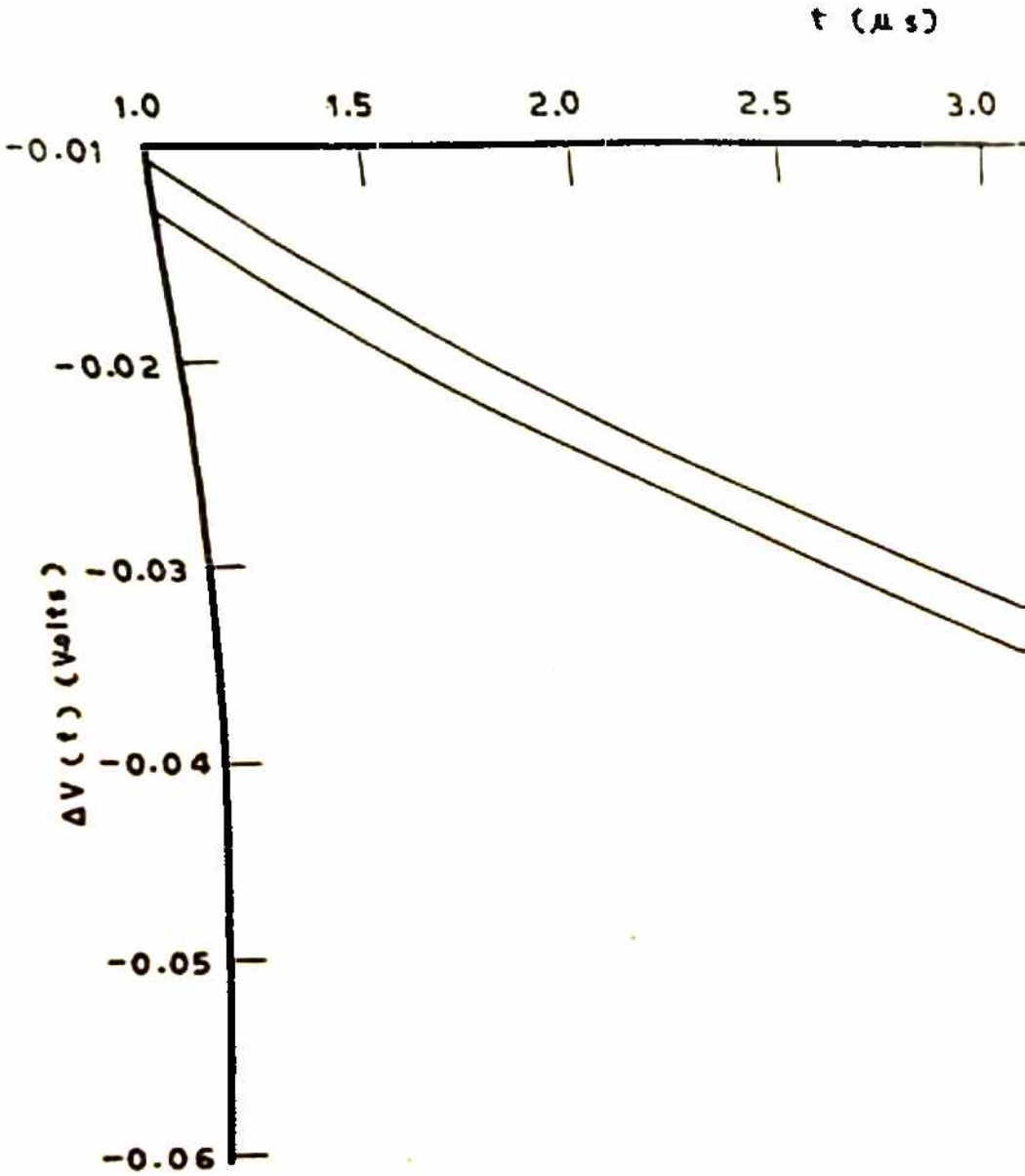

FIG. 4.6

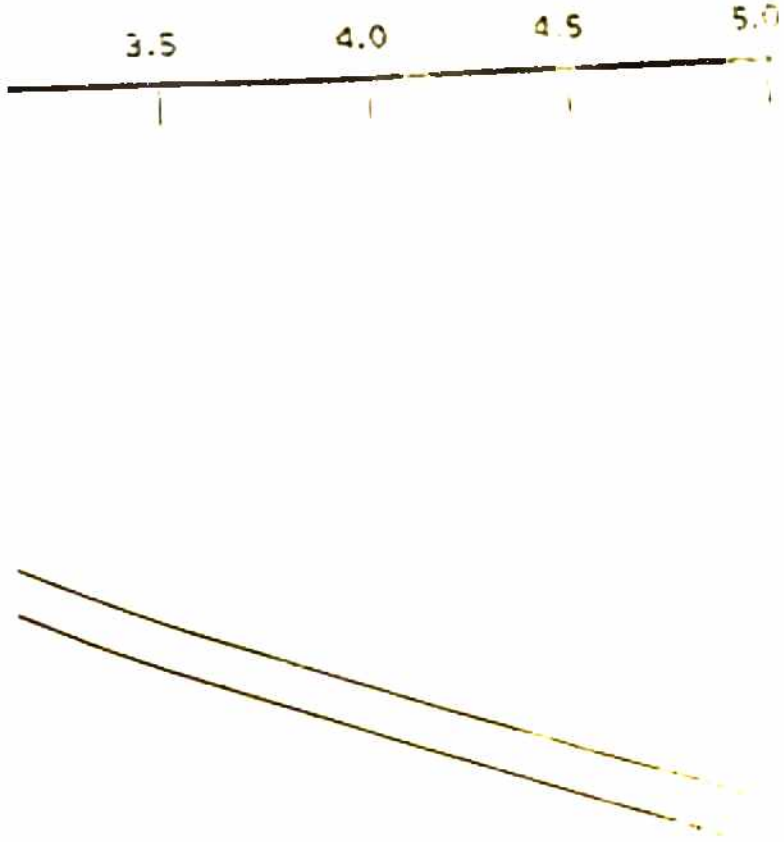
3.5
4.0
4.5
5.0

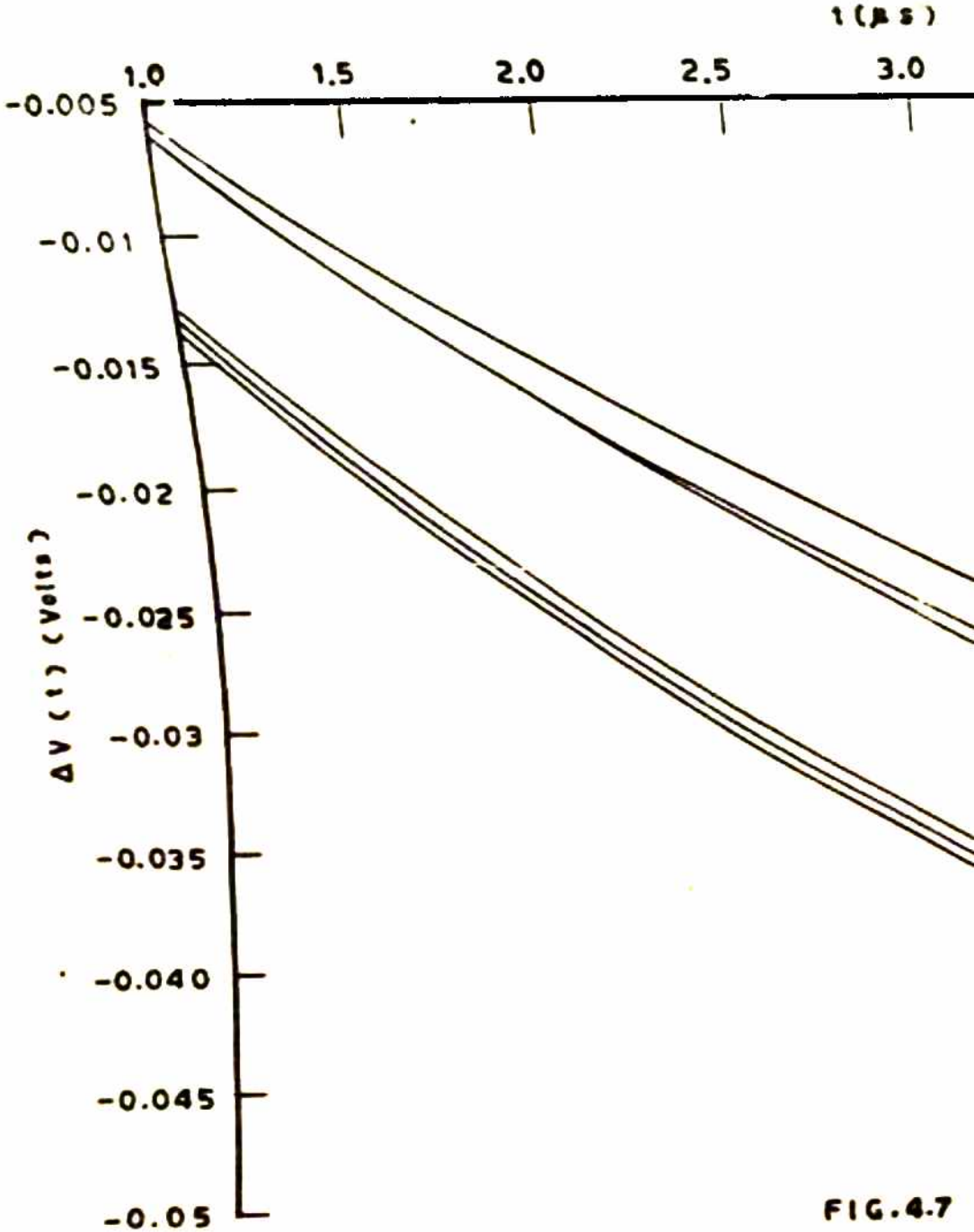
t (μs)
1.0
1.5
2.0
2.5
3.0
-0.005
-0.01
-0.015
-0.02
-0.025
-0.03
-0.035
-0.040
-0.045
-0.05
ΔV (t) (Volts)

FIG.4.7

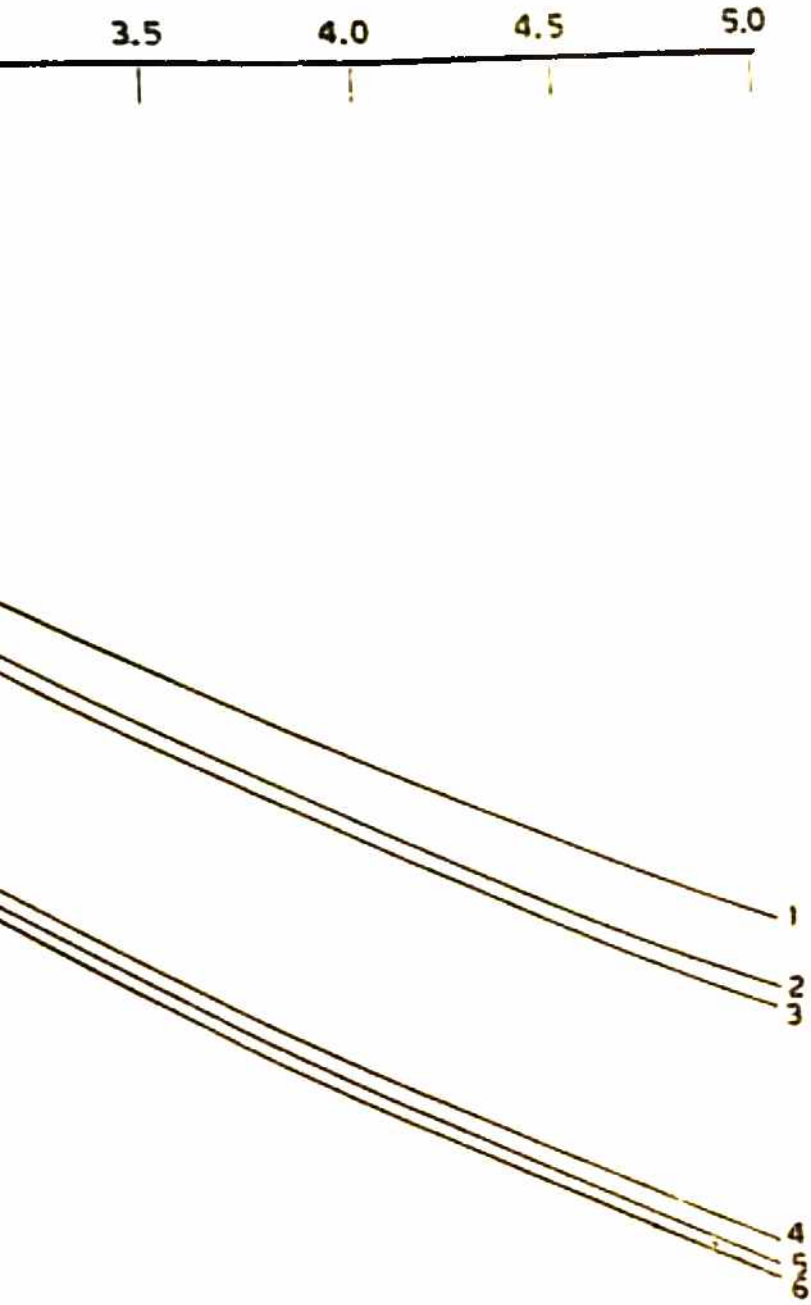
3.5
4.0
4.5
5.0
1
2
3
4
5
6

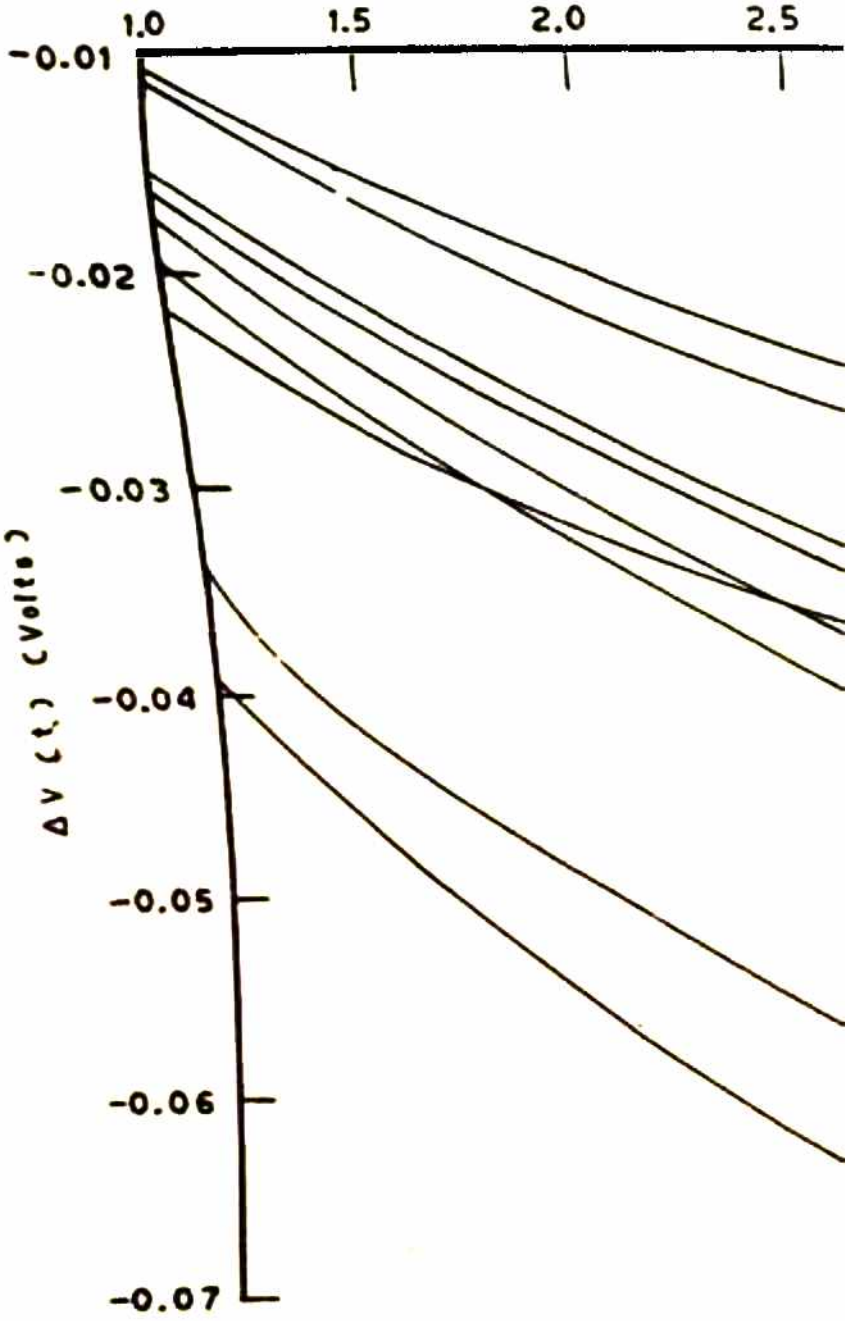
1.0
1.5
2.0
2.5
-0.01
-0.02
-0.03
-0.04
-0.05
-0.06
-0.07
ΔV (t) (Volts)

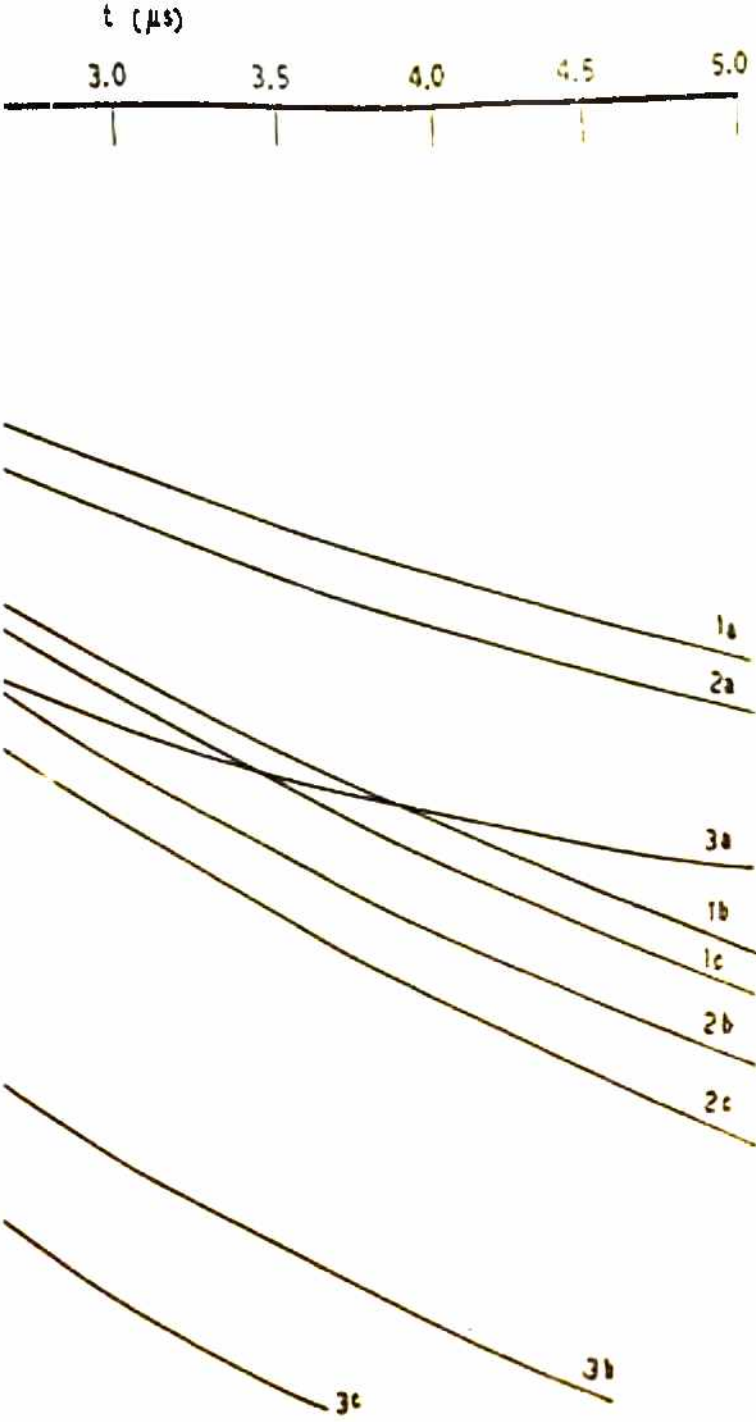

FIG. 4.8

5.0
4.5
3.5

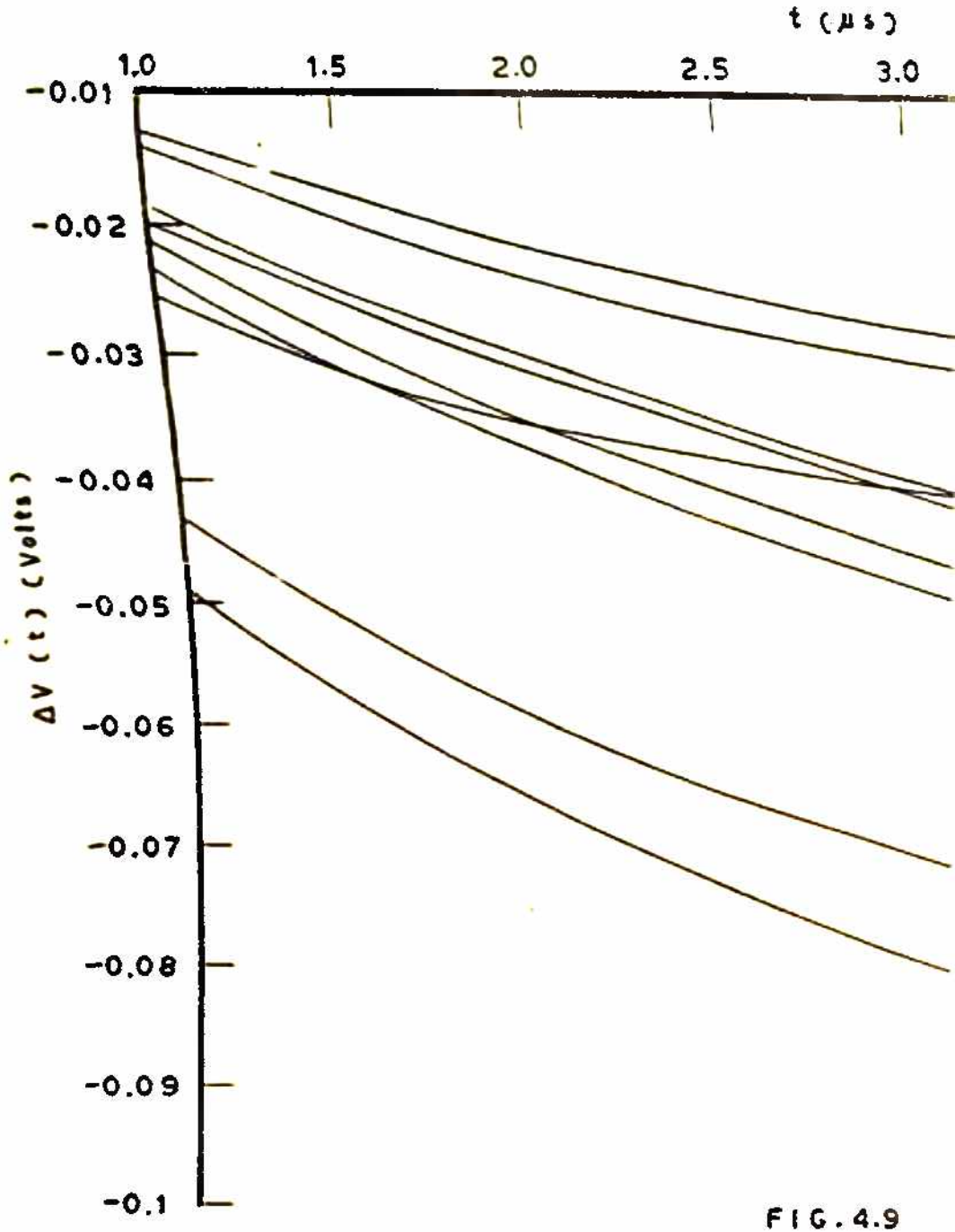
t (μs)
1.0
1.5
2.0
2.5
3.0
-0.01
-0.02
-0.03
-0.04
-0.05
-0.06
-0.07
-0.08
-0.09
-0.1
ΔV (t) (Volts)

FIG. 4.9